


The Alaska Volcano Observatory is a consortium between the U.S. Geological Survey, the University of Alaska Fairbanks Geophysical Institute, and the Alaska Division of Geological & Geophysical Surveys

2021 Volcanic Activity in Alaska and the Commonwealth of the Northern Mariana Islands—Summary of Events and Response of the Alaska Volcano Observatory



Scientific Investigations Report 2024–5014

Cover. Oblique aerial photograph of ash emanating from the north crater of Mount Young, on Semisopchnoi Island, Alaska, on May 30, 2021. Snow-covered Anvil Peak is in the background. U.S. Geological Survey photograph by H. Dieterich, May 30, 2021.

2021 Volcanic Activity in Alaska and the Commonwealth of the Northern Mariana Islands—Summary of Events and Response of the Alaska Volcano Observatory

By Tim R. Orr, Hannah R. Dietterich, David Fee, Tárсило Girona, Ronni Grapenthin, Matthew M. Haney, Matthew W. Loewen, John J. Lyons, John A. Power, Hans F. Schwaiger, David J. Schneider, Darren Tan, Liam Toney, Valerie K. Wasser, and Christopher F. Waythomas

The Alaska Volcano Observatory is a consortium between the U.S. Geological Survey, the University of Alaska Fairbanks Geophysical Institute, and the Alaska Division of Geological & Geophysical Surveys

Scientific Investigations Report 2024–5014

U.S. Department of the Interior
U.S. Geological Survey

U.S. Geological Survey, Reston, Virginia: 2024

For more information on the USGS—the Federal source for science about the Earth, its natural and living resources, natural hazards, and the environment—visit <https://www.usgs.gov> or call 1–888–392–8545.

For an overview of USGS information products, including maps, imagery, and publications, visit <https://store.usgs.gov/> or contact the store at 1–888–275–8747.

Any use of trade, firm, or product names is for descriptive purposes only and does not imply endorsement by the U.S. Government.

Although this information product, for the most part, is in the public domain, it also may contain copyrighted materials as noted in the text. Permission to reproduce [copyrighted items](#) must be secured from the copyright owner.

Suggested citation:

Orr, T.R., Dietterich, H.R., Fee D., Girona, T., Grapenthin, R., Haney, M.M., Loewen, M.W., Lyons, J.J., Power, J.A., Schwaiger, H.F., Schneider, D.J., Tan, D., Toney, L., Wasser, V.K., Waythomas, C.F., 2024, 2021 Volcanic activity in Alaska and the Commonwealth of the Northern Mariana Islands—Summary of events and response of the Alaska Volcano Observatory: U.S. Geological Survey Scientific Investigations Report 2024–5014, 64 p., <https://doi.org/10.3133/sir20245014>.

ISSN 2328-0328 (online)

Acknowledgments

This report represents the work of the entire Alaska Volcano Observatory staff, colleagues from other U.S. Geological Survey (USGS) volcano observatories, and cooperating State and Federal agencies. We thank those members of the public who shared observations and photographs. Technical reviews by Jordan Lubbers, Aaron Wech, and Michelle Coombs improved the content and consistency of this report. The Alaska Volcano Observatory is funded by the USGS Hazards Program and the State of Alaska.

Contents

Acknowledgments	iii
Abstract	1
Introduction	1
Volcanic Activity in Alaska and the Commonwealth of the Northern Mariana Islands.....	6
Shrub Mud Volcano	6
Mount Spurr	9
Iliamna Volcano.....	12
Mount Katmai (Novarupta).....	14
Aniakchak Crater	15
Mount Veniaminof.....	16
Pavlof Volcano.....	21
Mount Okmok.....	26
Mount Cleveland	28
Atka Volcanic Complex	30
Great Sitkin Volcano	31
2016–2021 Precursory Unrest	32
May 25 Explosion	34
Characterization of the May 25 Eruption	35
2021 Effusive Phase	37
Mount Gareloi.....	39
Semisopochnoi Island (Mount Young).....	41
Davidof Volcano	46
Mount Pagan	48
References Cited.....	51
Glossary of Selected Terms and Acronyms	58

Figures

1. Maps of Alaskan volcanoes highlighted in this summary and their monitoring statuses and of Guam and the Commonwealth of the Northern Mariana Islands	2
2. Annotated satellite image of the Copper River Basin in Alaska, showing the location of Shrub, Upper Klawasi, and Lower Klawasi mud volcanoes in relation to Mount Drum and the community of Glennallen.....	7
3. Annotated satellite image of Shrub mud volcano, Alaska, showing mud flows emplaced since its rejuvenation of activity in 1996	7
4. Oblique aerial photograph, looking south, of the vents at the north base of Shrub mud volcano, Alaska	8
5. Oblique aerial photograph of the summit of Shrub mud volcano, Alaska, showing the approximate locations of new active springs and the extent of new mud deposits.....	8
6. Photograph of the summit pit at Shrub mud volcano, Alaska, in 2021.....	9
7. Oblique aerial photograph of Mount Spurr, Alaska	10
8. Map of Cook Inlet, Alaska, showing Mount Spurr and Iliamna Volcano.....	10

9.	Time-series plot showing high-frequency vertical-component seismic signals generated by the mass movement of April 7, 2021, at Mount Spurr, Alaska	11
10.	Time-series plots showing array processing results for infrasound generated by the Mount Spurr mass movement of April 7, 2021, as recorded at the KENI infrasound array near the City of Kenai, Alaska	11
11.	Oblique aerial photograph (looking west) at Iliamna Volcano, Alaska, on August 14, 2021.....	12
12.	Time-series plot showing high-frequency vertical-component seismic signals generated by the ice and rock avalanche of August 5, 2021, at Iliamna Volcano, Alaska.....	13
13.	Time-series plots showing array processing results for infrasound generated by the Iliamna Volcano ice and rock avalanche of August 5, 2021, as recorded at the KENI infrasound array near the City of Kenai, Alaska.....	13
14.	Oblique, processed satellite image showing a resuspended ash plume from the Mount Katmai area extending across the Shelikof Strait to Kodiak Island, Alaska	14
15.	True-color visible satellite image showing a resuspended ash plume drifting from valleys on the north side of Shelikof Strait toward Kodiak Island, Alaska.....	15
16.	Satellite imagery of resuspended ash and its source area at Aniakchak Crater, Alaska	16
17.	Map of Mount Veniaminof, Alaska, showing locations of cones A and B in the summit caldera and the approximate final extent of ash deposits identifiable in satellite imagery	17
18.	Timeline of observed activity at Mount Veniaminof in 2021, showing changes in Aviation Color Code; days when webcam and satellite imagery recorded ash, steam plumes, and (or) sulfur dioxide; days with tremor and (or) explosions large enough to be detected by regional infrasound sensors; days with elevated surface temperatures; and magnification of parts <i>A–D</i> for the period spanning March 1 through May 1, 2021	17
19.	Images of the eruption of Mount Veniaminof, Alaska, in March 2021	18
20.	Photographs of eruptive activity at Mount Veniaminof, Alaska, in 2021	19
21.	Visible satellite image of Mount Veniaminof, Alaska, after the end of its eruption in 2021	20
22.	Backscattered electron images of polished tephra samples from the 2021 eruption of Mount Veniaminof, Alaska.....	20
23.	Photograph of Pavlof Volcano from the Dolgoi Island webcam on August 5, 2021, at 08:34 Alaska daylight time	21
24.	Timeline of outward indications of volcanic unrest at Pavlof Volcano, Alaska, and time-series plot of real-time seismic amplitude for seismic station PVV, August 5–December 31, 2021.....	22
25.	Mid-infrared satellite image showing elevated surface temperatures at Pavlof Volcano, Alaska	22
26.	Time-series plot of volcanic radiative power versus time for the period of 2021 when satellite detections of elevated surface temperatures indicated lava at the surface of Pavlof Volcano, Alaska	23
27.	Annotated short-wave infrared satellite image of features and deposits observed at Pavlof Volcano, Alaska, in November 2021.....	23
28.	Annotated map of features and deposits on the southeast flank of Pavlof Volcano, Alaska.....	24
29.	Annotated map of features and deposits on the southeast flank of Pavlof Volcano, Alaska.....	25

30.	Oblique aerial photograph of Mount Okmok on April 28, 2021, looking southwest	26
31.	Global Positioning System velocity map and displacement time series with 68 percent confidence levels showing movement of monitoring station OKCE from September 2008 through December 2021 at Mount Okmok, Alaska	27
32.	Global Positioning System velocity map and displacement time series with 68 percent confidence levels showing movement of monitoring station OKCE from January through December 2021 at Mount Okmok, Alaska	27
33.	Sentinel-2 satellite image of Mount Cleveland, within the Islands of Four Mountains group, which also includes Carlisle volcano, Herbert volcano, and Tanax̄ Angunaŋ̄ volcano	28
34.	Time-series plots and graph of activity at Mount Cleveland, Alaska, in 2021	28
35.	Satellite and oblique aerial images of Mount Cleveland, Alaska, in 2021	29
36.	Map showing hypocenters located at Atka volcanic complex, Alaska, during August 10–12, 2021	30
37.	Helicorder plot of seismic data from station KOKV during August 10–11, 2021, showing an earthquake swarm beneath Atka volcanic complex, Alaska	31
38.	Map showing the extent of active lava flow on Great Sitkin Island, Alaska, as of January 1, 2022.....	32
39.	Photograph and Interferometric Synthetic Aperture Radar image of the summit of Great Sitkin Volcano, Alaska.....	32
40.	Chronology of the volcanic unrest and eruption at Great Sitkin Volcano, Alaska, in 2021	33
41.	Helicorder plot of seismic data from station GSSP, on the west side of Great Sitkin Island, Alaska, showing the swarm of long-period events that immediately preceded a small explosion that took place on May 26, 2021, at 05:04 coordinated universal time	34
42.	Photographs of the May 25, 2021, explosion of Great Sitkin Volcano, Alaska, taken at 20:04 Hawaii-Aleutian daylight time and 20:06 HADT from aboard the passing research vessel Tiglax, operated by the U.S. Fish and Wildlife Service	34
43.	Time-series plot showing infrasound bracketing the explosion of Great Sitkin Volcano, Alaska, on May 25, 2021, as recorded at station GSMY	35
44.	Images of deposits associated with the May 25, 2021, explosion at Great Sitkin Volcano, Alaska.....	35
45.	Example of a juvenile breadcrust bomb collected from deposits of the May 26, 2021, explosion at Great Sitkin Volcano, Alaska.....	36
46.	Backscatter electron images of polished breadcrust bomb samples from the May 25, 2021, explosion of Great Sitkin Volcano, Alaska.....	36
47.	Orthoimages of Great Sitkin Volcano, Alaska, on June 11, 2021	37
48.	High-resolution satellite synthetic aperture radar amplitude spotlight imagery of the summit of Great Sitkin Volcano, Alaska, on July 23, 2021, at 5:32 coordinated universal time	38
49.	Growth over time of the lava flow at Great Sitkin Volcano, Alaska	38
50.	Map showing earthquake hypocenters located at Great Sitkin Volcano, Alaska, during 2021	39

51. Photographs of Mount Gareloi, Alaska.....	40
52. Time-series graph showing the amplitude of long-period events automatically recorded during the 2021 episode of unrest at Mount Gareloi, Alaska.....	40
53. Map of Semisopochnoi Island, Alaska, showing the active north cone of Mount Young and other important geographic features	41
54. Images of gas emissions from Mount Young, Alaska, in 2021.....	42
55. Timeline of Aviation Color Code changes and time-series plots of infrasound detections at Semisopochnoi Island, Alaska, in 2021.....	43
56. Timeline of Aviation Color Code changes and time-series plot of real-time seismic amplitude measurement values at station CERB, on Semisopochnoi Island, Alaska.....	44
57. Satellite imagery of ash and sulfur emissions from Semisopochnoi Island, Alaska, in September 2021	44
58. Timeline of Aviation color codes and remote sensing observations at Semisopochnoi Island, Alaska, in 2021	45
59. Backscatter electron images of samples collected from Mount Young, Alaska, on May 30 and June 1, 2021	45
60. Map of Davidof volcano, an informal name for a volcanic system comprising Davidof Island, Khvostof Island, and Pyramid Island, Alaska	46
61. Photographs of Davidof volcano, Alaska.....	46
62. Photograph of thick pyroclastic flow and fall deposits on Davidof Island, Alaska	47
63. Map and cross-sectional plot of the hypocenters from the earthquake swarm near Davidof volcano, Alaska, during December 1–31, 2021	47
64. Annotated satellite image of Pagan Island showing Mount Pagan and South Pagan volcano.....	48
65. Screenshot from a video showing ash emissions from Mount Pagan on July 29, 2021	49
66. TROPOMI satellite images showing sulfur dioxide gas extending from Mount Pagan, Alaska	49
67. True-color satellite image showing a sinuous ash cloud extending more than 500 kilometers westward from Mount Pagan at an altitude of 3 kilometers above sea level	50

Tables

1. Summary of monitoring highlights at volcanoes in Alaska and the Commonwealth of the Northern Mariana Islands in 2021, including but not limited to confirmed eruptions, increases in seismic activity, and other notable events.....	3
2. Aviation Color Code and Volcano Alert Level changes in 2021 at Alaska volcanoes discussed in this report	3
3. Definitions of the Aviation Color Codes used by United States volcano observatories ..	5
4. Definitions of the Volcano Alert Levels used by United States volcano observatories....	5
5. Summary of activity and observations at Mount Young, Alaska, in 2021	43

Conversion Factors

U.S. customary units to International System of Units

Multiply	By	To obtain
Length		
foot (ft)	0.3048	meter (m)
foot (ft)	0.0003048	kilometer (km)

International System of Units to U.S. customary units

Multiply	By	To obtain
Length		
centimeter (cm)	0.3937	inch (in.)
meter (m)	3.281	foot (ft)
meter (m)	1.094	yard (yd)
kilometer (km)	0.6214	mile (mi)
kilometer (km)	0.5400	mile, nautical (nmi)
Area		
square meter (m ²)	0.0002471	acre
square meter (m ²)	10.76	square foot (ft ²)
Volume		
cubic meter (m ³)	35.31	cubic foot (ft ³)
cubic meter (m ³)	1.308	cubic yard (yd ³)
cubic kilometer (km ³)	0.2399	cubic mile (mi ³)
Flow rate		
meter per second (m/s)	3.281	foot per second (ft/s)
cubic meter per second (m ³ /s)	35.31	cubic foot per second (ft ³ /s)

Temperature in degrees Celsius (°C) may be converted to degrees Fahrenheit (°F) as follows:

$$^{\circ}\text{F} = (1.8 \times ^{\circ}\text{C}) + 32.$$

Datum

Altitude, as used in this report, refers to distance above sea level of a location in the air.

Elevation, as used in this report, refers to distance above sea level of a location on the land surface.

Depth, as used in this report, refers to distance below sea level.

Locations in latitude and longitude are presented in decimal degrees referenced to the World Geodetic System 1984 (WGS84) datum, unless otherwise noted.

Vertical coordinate information for earthquakes is referenced to the World Geodetic System 1984 (WGS84), and elevations of volcanoes are referenced to the North American Vertical Datum of 1988 (NAVD88), unless otherwise noted.

Abbreviations

#	number
AAWU	Alaska Aviation Weather Unit
AKDT	Alaska daylight time; UTC–8 hours
AKST	Alaska standard time; UTC–9 hours
ASL	above sea level
AVO	Alaska Volcano Observatory
ChST	Chamorro standard time; UTC +10 hours
CNMI	Commonwealth of the Northern Mariana Islands
GNSS	Global Navigation Satellite System
GVP	Smithsonian Institution Global Volcanism Program
HADT	Hawaii-Aleutian daylight time; UTC –9 hours
HAST	Hawaii-Aleutian standard time; UTC –10 hours
Hz	hertz
InSAR	interferometric synthetic aperture radar
LP	long-period
NOAA	National Oceanic and Atmospheric Administration
NWS	National Weather Service
OMI	Ozone Mapping Instrument
OMPS	Ozone Mapping and Profile Suite
ppmv	parts per million volume
RSAM	real-time seismic amplitude measurement
SAR	synthetic aperture radar
SIGMET	significant meteorological information statement
SO ₂	sulfur dioxide
Suomi-NPP	Suomi National Polar-Orbiting Partnership satellite
SWIR	short-wave infrared
TROPOMI	the TROPospheric Monitoring Instrument
UAFGI	University of Alaska Fairbanks Geophysical Institute
USFWS	U.S. Fish and Wildlife Service
USGS	U.S. Geological Survey
UTC	coordinated universal time; same as Greenwich mean time
VEI	volcanic explosivity index

2021 Volcanic Activity in Alaska and the Commonwealth of the Northern Mariana Islands—Summary of Events and Response of the Alaska Volcano Observatory

By Tim R. Orr,¹ Hannah R. Dietterich,¹ David Fee,² Társilo Girona,² Ronni Grapenthin,² Matthew M. Haney,¹ Matthew W. Loewen,¹ John J. Lyons,¹ John A. Power,¹ Hans F. Schwaiger,¹ David J. Schneider,¹ Darren Tan,² Liam Toney,² Valerie K. Wasser,² and Christopher F. Waythomas¹

Abstract

In 2021, the Alaska Volcano Observatory responded to eruptions, volcanic unrest or suspected unrest, increased seismicity, and other significant activity at 15 volcanic centers in Alaska and the Commonwealth of the Northern Mariana Islands. Eruptive activity in Alaska consisted of repeated small, ash-producing, phreatomagmatic explosions from Mount Young on Semisopochnoi Island; an explosion at Great Sitkin Volcano followed by the eruption of a thick lava flow that filled and overflowed the summit crater; weak explosive activity and the eruption of small, channelized flows at Pavlof Volcano; and a short-lived eruption at Mount Veniaminof that produced ash emissions from an intracaldera cone, as well as lava flows confined to a melt pit in the ice mantling the cone's flank. Mount Cleveland had a period of unrest, but no eruptive activity took place there. Anomalous seismicity was also detected at Atka volcanic complex, Mount Gareloi, and Davidof volcano. New warm springs opened and deposited mud at the summit and north base of Shrub mud volcano. Other activity of note in Alaska consisted of large ice and rock avalanches at Iliamna Volcano and Mount Spurr, ash resuspension events at Mount Katmai and Aniakchak Crater, and anomalous deformation at Mount Okmok that was consistent with a shallow intrusion of magma. In the Commonwealth of the Northern Marianas Islands, a brief, ash-producing eruption occurred at Mount Pagan.

Introduction

The Alaska Volcano Observatory (AVO) is a joint program of the U.S. Geological Survey (USGS), the University of Alaska Fairbanks Geophysical Institute, and the Alaska Division of Geological & Geophysical Surveys. AVO was formed in 1988 and uses Federal, State, and university resources to (1) monitor and study Alaska's hazardous volcanoes (fig. 1) in order to assess the nature, timing, and likelihood of volcanic activity; (2) assess volcanic hazards

associated with anticipated activity, including the kinds of events, their effects, and areas at risk; and (3) provide timely and accurate information on volcanic hazards, and warnings of impending dangerous activity, to officials (local, State, and Federal) and the public. The USGS branch of AVO also monitors the volcanoes in the Commonwealth of the Northern Mariana Islands (CNMI) (fig. 1).

This report summarizes notable unrest and other kinds of activity associated with volcanoes in Alaska and the CNMI during 2021 (tables 1, 2) and briefly describes AVO's response. It contains information about all identified volcanic unrest, even if no formal public notification was issued at the time. Observations, images, and information that are typically not published elsewhere are included in this report. Similar summaries of volcanic unrest and AVO's response have been published annually since 1992.

The AVO volcano monitoring program involves daily analyses of satellite and webcam imagery, seismicity, and infrasound detections; occasional overflights and ground visits; airborne and ground-based gas measurements; and the compilation of visual observations taken from observatory personnel members, residents, mariners, and pilot weather reports (PIREP; reports of meteorological phenomena encountered by aircraft in flight). AVO also receives real-time ground deformation data from permanent Global Navigation Satellite System (GNSS) stations at eight Alaskan volcanoes: Akutan Peak, Augustine Volcano, Makushin Volcano, Mount Okmok, Redoubt Volcano, Shishaldin Volcano, Mount Spurr, and Westdahl volcano (an ice-clad edifice with no formal name that occupies the west end of Unimak Island). These deformation data are supplemented with Interferometric Synthetic Aperture Radar (InSAR) imagery (for example, Lee and others, 2010).

Observations from these multiple sources inherently relate data to several different datums. Ash altitudes are commonly from PIREPs or, for ash resuspension events from the National Weather Service, are based on analysis of satellite imagery, and the altitudes given herein can be somewhat imprecise. Earthquake depths are modeled in relation to the World Geodetic System of 1984 (WGS 1984), and the accuracy of depth given directly relates to how many stations were used to record the event (that is, accuracy of depth

¹ U.S. Geological Survey.

² University of Alaska Fairbanks.

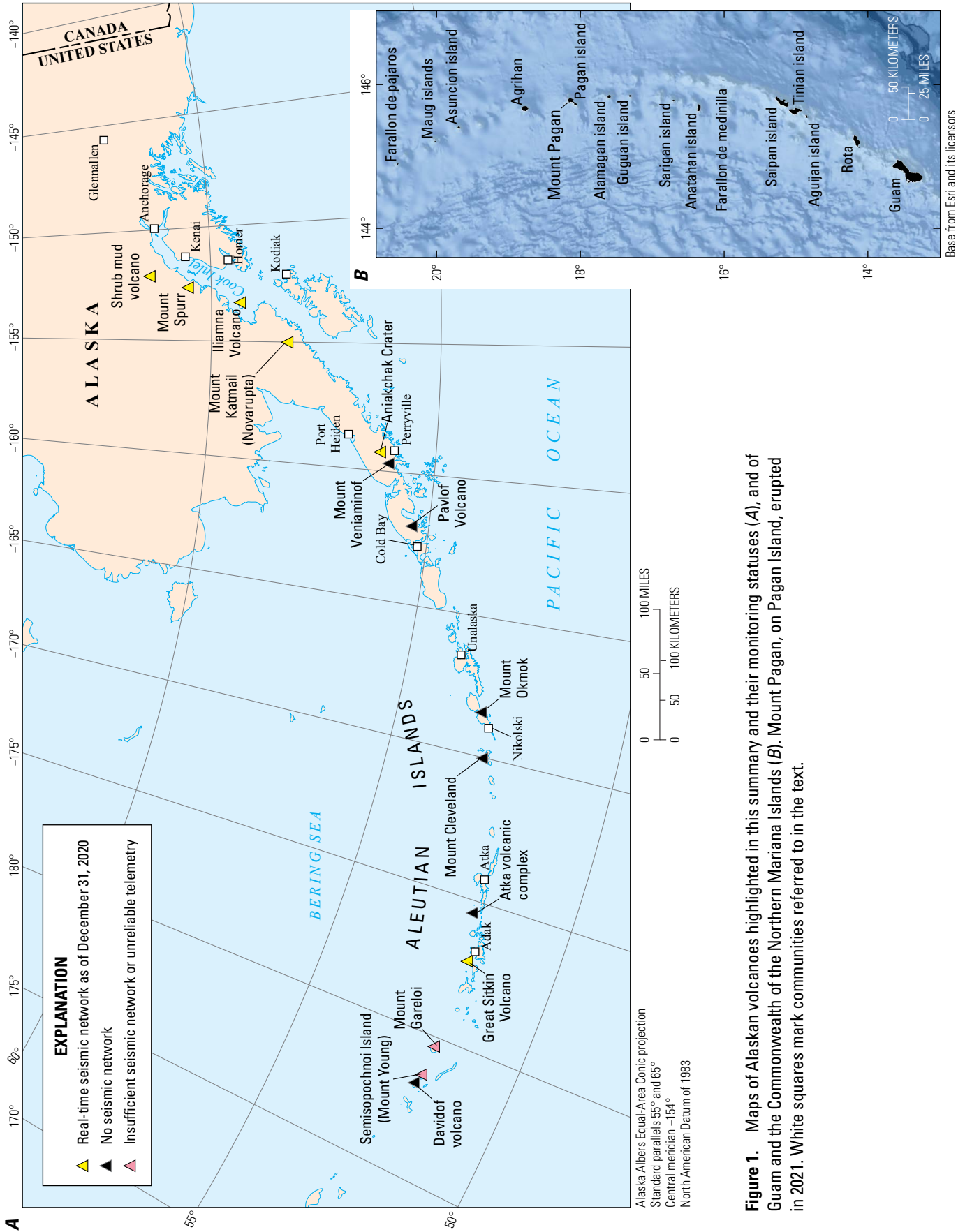


Figure 1. Maps of Alaskan volcanoes highlighted in this summary and their monitoring statuses (A), and of Guam and the Commonwealth of the Northern Mariana Islands (B). Mount Pagan, on Pagan Island, erupted in 2021. White squares mark communities referred to in the text.

Table 1. Summary of monitoring highlights at volcanoes in Alaska and the Commonwealth of the Northern Mariana Islands in 2021, including but not limited to confirmed eruptions, increases in seismic activity, and other notable events.[Volcano locations shown in [figure 1](#).]

Volcano	Type of activity
Shrub mud volcano ¹	New mud springs
Mount Spurr	Ice and rock avalanche
Iliamna Volcano	Ice and rock avalanche
Mount Katmai (Novarupta)	Resuspension of 1912 ash
Aniakchak Crater	Resuspension of ash
Mount Veniaminof	Eruption with ash emissions and lava flows
Pavlof Volcano	Eruption with ash emissions; fountaining; lava flows and lahars
Mount Okmok	Continued long-term inflation with pulse during October–November
Mount Cleveland	Elevated surface temperatures and gas emissions
Atka volcanic complex ¹	Earthquake swarm
Great Sitkin Volcano	Explosive eruption and lava flow
Mount Gareloi	Elevated seismicity
Semisopochnoi Island (Mount Young)	Phreatomagmatic explosions with ash emissions
Davidof volcano ¹	Earthquake swarm
Mount Pagan	Explosive eruption with ash emissions

¹Informal name.**Table 2.** Aviation Color Code and Volcano Alert Level changes in 2021 at Alaska volcanoes discussed in this report.[See [tables 3](#) and [4](#) for definitions of Aviation Color Codes and Volcano Alert Levels. Dates shown as month/day/year. Times shown as HH:MM in coordinated universal time (UTC)]

Aviation Color Code/ Volcano Alert Level	Date and time of change (UTC)	Aviation Color Code/ Volcano Alert Level	Date and time of change (UTC)
Shrub mud volcano		Pavlof Volcano	
UNASSIGNED	No change for entire year	GREEN/NORMAL	Beginning of year
Mount Katmai (Novarupta)		YELLOW/ADVISORY	07/09/2021 (19:40)
GREEN/NORMAL	No change for entire year	ORANGE/WATCH	08/05/2021 (17:55)
Mount Veniaminof		Mount Cleveland	
GREEN/NORMAL	Beginning of year	UNASSIGNED	Beginning of year
UNASSIGNED	01/15/2021 (21:33)	YELLOW/ADVISORY	03/20/2021 (21:44)
ORANGE/WATCH	03/04/2021 (18:04)	UNASSIGNED	10/20/2021 (23:04)
YELLOW/ADVISORY	04/02/2021 (17:33)	Atka volcanic complex	
ORANGE/WATCH	04/05/2021 (20:23)	GREEN/NORMAL	Beginning of year
YELLOW/ADVISORY	04/21/2021 (18:54)	YELLOW/ADVISORY	08/11/2021 (22:22)
UNASSIGNED	05/12/2021 (21:13)	GREEN/NORMAL	08/27/2021 (17:24)
GREEN/NORMAL	07/08/2021 (18:38)		

4 2021 Volcanic Activity in Alaska—Summary of Events and Response of the Alaska Volcano Observatory

Table 2. Aviation Color Code and Volcano Alert Level changes in 2021 at Alaska volcanoes discussed in this report.—Continued

Aviation Color Code/ Volcano Alert Level	Date and time of change (UTC)	Aviation Color Code/ Volcano Alert Level	Date and time of change (UTC)
Great Sitkin Volcano			
GREEN/NORMAL	Beginning of year	RED/WARNING	04/16/2021 (03:15)
YELLOW/ADVISORY	05/13/2021 (00:57)	ORANGE/WATCH	04/17/2021 (20:49)
ORANGE/WATCH	05/26/2021 (03:43)	YELLOW/ADVISORY	05/07/2021 (19:16)
RED/WARNING	05/26/2021 (05:30)	ORANGE/WATCH	05/19/2021 (05:18)
ORANGE/WATCH	05/26/2021 (16:31)	YELLOW/ADVISORY	06/16/2021 (21:59)
YELLOW/ADVISORY	05/27/2021 (20:58)	ORANGE/WATCH	07/13/2021 (00:14)
ORANGE/WATCH	07/23/2021 (22:25)	YELLOW/ADVISORY	07/22/2021 (00:28)
Mount Gareloi			
GREEN/NORMAL	Beginning of year	ORANGE/WATCH	07/31/2021 (18:19)
UNASSIGNED	03/31/2021 (18:21)	RED/WARNING	09/20/2021 (05:58)
GREEN/NORMAL	05/27/2021 (20:13)	ORANGE/WATCH	09/21/2021 (04:12)
YELLOW/ADVISORY	06/08/2021 (17:43)	Davidof volcano	
GREEN/NORMAL	07/28/2021 (19:33)	UNASSIGNED	Beginning of year
Semisopochnoi Island (Mount Young)			
UNASSIGNED	Beginning of year	YELLOW/ADVISORY	12/10/2021 (21:38)
YELLOW/ADVISORY	02/07/2021 (04:51)	UNASSIGNED	12/29/2021 (21:11)
ORANGE/WATCH	02/08/2021 (23:11)	Mount Pagan	
YELLOW/ADVISORY	02/19/2021 (18:28)	UNASSIGNED	Beginning of year
ORANGE/WATCH	03/19/2021 (13:46)	YELLOW/ADVISORY	07/29/2021 (09:12)
		ORANGE/WATCH	09/01/2021 (18:44)
		YELLOW/ADVISORY	09/10/2021 (18:15)
		UNASSIGNED	09/24/2021 (22:00)

decreases with less recording stations). The summit elevations of the volcanoes are derived from the 2019 Interferometric Synthetic Aperture Radar data. These elevations may differ from past AVO annual summaries, which were taken directly from the AVO database (<https://avo.alaska.edu/>).

With this information, AVO assigns each monitored volcano an Aviation Color Code and Volcano Alert Level, which indicate its current activity status (Gardner and Guffanti, 2006). No assignment is given to unmonitored volcanoes at background level. The Aviation Color Code addresses the hazards to aviation posed by a volcano, whereas the Volcano Alert Level addresses the hazards on the ground. Although the Aviation Color Code and Volcano Alert Level

are usually changed upward or downward together, certain situations may dictate that they are changed independently. For instance, a volcano may produce lava flows that are dangerous on the ground and merit a Volcano Alert Level of **WARNING**, but the hazard to aviation is minimal and merits an Aviation Color Code of **ORANGE**. Where possible, Volcano Alert Level announcements contain additional explanations of volcanic activity and expected hazards. [Tables 3 and 4](#) define each Aviation Color Code and Volcano Alert Level.

Duty scientists are responsible for compiling all monitoring data to provide scheduled and event-driven public notices, as appropriate. AVO scientists participate in

Table 3. Definitions of the Aviation Color Codes used by United States volcano observatories.

Aviation Color Code	Definition
GREEN	Volcano is in typical background, noneruptive state or, after a change from a higher level, volcanic activity has ceased, and volcano has returned to noneruptive background state.
YELLOW	Volcano is exhibiting signs of elevated unrest above known background level or, after a change from a higher level, volcanic activity has decreased significantly but continues to be closely monitored for possible renewed increase.
ORANGE	Volcano is exhibiting heightened or escalating unrest with increased potential of eruption, timeframe uncertain, or eruption is underway with no or minor volcanic-ash emissions [ash-plume height specified, if possible].
RED	Eruption is imminent with significant emission of volcanic ash into the atmosphere likely, or eruption is underway or suspected with significant emission of volcanic ash into the atmosphere [ash-plume height specified, if possible].
UNASSIGNED	Ground-based instrumentation is insufficient to establish that volcano is at typical background level (GREEN/NORMAL). When activity at such a volcano increases to the point of being detected by remote sensing instruments, distant seismic networks, or eyewitness reports, an alert level and color code are assigned accordingly. When activity decreases, volcano goes back to UNASSIGNED without going through GREEN/NORMAL .

Table 4. Definitions of the Volcano Alert Levels used by United States volcano observatories.

Volcano Alert Level	Definition
NORMAL	Volcano is in typical background, noneruptive state or, after a change from a higher level, volcanic activity has ceased, and volcano has returned to noneruptive background state.
ADVISORY	Volcano is exhibiting signs of elevated unrest above known background level or, after a change from a higher level, volcanic activity has decreased significantly but continues to be closely monitored for possible renewed increase.
WATCH	Volcano is exhibiting heightened or escalating unrest with increased potential of eruption, timeframe uncertain, or eruption is underway but poses limited hazards.
WARNING	Highly hazardous eruption is imminent, underway, or suspected.
UNASSIGNED	Ground-based instrumentation is insufficient to establish that volcano is at typical background level (GREEN/NORMAL). When activity at such a volcano increases to the point of being detected by remote sensing instruments, distant seismic networks, or eyewitness reports, an alert level and color code are assigned accordingly. When activity decreases, volcano goes back to UNASSIGNED without going through GREEN/NORMAL .

a weekly remote sensing rotation, during which time they produce daily reports summarizing satellite and webcam observations at volcanoes with elevated Aviation Color Codes and Volcano Alert Levels. The reports also describe any notable observations at the other volcanoes AVO monitors. All observations are archived in a relational database. A second cadre of scientists from AVO and the USGS National Earthquake Information Center monitors volcano seismicity and infrasound using local and regional sensors. This team compiles three separate seismic reports daily, spaced ~8 hours apart. Like the daily remote sensing reports, the seismic reports are also catalogued in a relational database.

As of December 31, 2019, 33 of the historically active volcanoes and volcanic fields in Alaska were instrumented with seismometers and other instrumentation operated by AVO. Included in this list are those volcanoes that have insufficient seismic instrumentation to calculate reliable earthquake hypocenters and magnitudes, or those whose

real-time telemetry was not reliable enough to produce a complete record of earthquake activity in 2021. Specifically, Bogoslof volcano (an informally named, mostly submarine volcano near and under Bogoslof Island) was monitored by only one seismograph station and Mount Cleveland was monitored by only two local seismograph stations, so both lacked the minimum number of stations to locate earthquakes. Little Sitkin Island and Semisopochnoi Island were also considered unmonitored because the telemetry for each of their subnetworks was unreliable.

The volcanoes in this report are presented in geographic order from east to west along the Aleutian Arc, followed by the CNMI. Each entry has a title block containing information about that volcano: its identifier number (#) assigned by the Smithsonian Institution Global Volcanism Program (GVP); its latitude, longitude, and summit elevation; the name of its geographic region; and an abbreviated summary of its 2021 activity. The title block is followed by a description of the



What is a “Historically Active Volcano”?

AVO defines an active volcano as a volcanic center that has had a historical eruption (see “[What is an ‘eruption’](#)”) or a historical period of intense deformation, seismic activity, or fumarolic activity, which are inferred to reflect the presence of magma at shallow levels beneath the volcano. AVO considers the historical period in Alaska to be since 1741, when written records of volcanic activity began. On the basis of a rigorous reanalysis of all volcanic activity accounts in Alaska (from many sources), Cameron and others (2018) concluded that 54 Alaskan volcanoes fit these criteria. In this report, we modify the number of historically active volcanoes to 52 because we consider (1) Korovin Volcano and Mount Kliuchef to be subfeatures of Atka volcanic complex and (2) Novarupta to be a subfeature of Mount Katmai. As geologic understanding of Alaskan volcanoes improves through additional fieldwork and modern radiometric dating techniques, our list of active volcanoes will continue to evolve.



What is an “Eruption”?

The specific use of the term “eruption” varies from scientist to scientist and has no universally agreed-upon definition. Here, we adopt the usage of Siebert and others (2010, p. 17), who define eruptions as “* * * events that involve the explosive ejection of fragmental material, the effusion of liquid lava, or both”. The critical elements of this definition are the nouns “ejection” and “effusion,” which refer to dynamic surface processes that pose some level of hazard. The presence or absence of “juvenile material,” or newly erupted rock, which can sometimes be ambiguous, is not relevant to this use of the term eruption, particularly when communicating a potential hazard. This definition does not, however, include passive volcanic degassing or hydrothermal fluid discharge.

volcano and a summary of its past activity, then a detailed account of its activity in 2021, often with accompanying tables, images, figures, or all three. This information is derived from formal public AVO information products, internal online electronic logs compiled by AVO staff, and published material (such as Miller and others [1998]).

AVO uses informal names for some volcanoes for clarity; the names provided by the U.S. Board on Geographic Names (through the Geographic Names Information System) may match poorly with the volcanoes themselves. For example, Bogoslof volcano comprises more islands than Bogoslof Island. Alaska also has volcanoes without official place names, such as Takawangha volcano, which require the use of informal names.

In this report, volcano locations (in decimal degrees latitude and longitude) are taken from AVO’s database of Alaskan volcanoes (Cameron and others, 2022). Measurements are presented in the International System of Units, except for altitudes, which are reported in feet (ft) above sea level (ASL), in line with Federal aviation standards, followed by meters (m). General date references are given in local time unless specified otherwise. Most volcanoes in Alaska are in the Alaska standard time (AKST) or Alaska daylight time (AKDT) zones, but all Aleutian volcanoes west of Umnak Island (see the community of Nikolski, Alaska, on [figure 1](#)) are in the Hawaii-Aleutian standard time (HAST) or Hawaii-Aleutian daylight time (HADT) zones. Mount Pagan falls within the Chamorro standard time (ChST) zone. During 2021, daylight saving time ran from March 14 to November 7.

Volcanic Activity in Alaska and the Commonwealth of the Northern Mariana Islands

Shrub Mud Volcano

Not listed in GVP database
62.149°, -145.021°
900 m

Klawasi group mud volcano, Copper River Basin



NEW MUD SPRINGS

Shrub mud volcano, the northernmost of the three Klawasi group mud volcanoes in the Copper River Basin of south-central Alaska, is located ~25 kilometers (km) east of the community of Glennallen, Alaska, and ~280 km northeast of the City of Anchorage, Alaska ([figs. 1, 2](#)). It sits near the west slope of Mount Drum, a Pleistocene volcano in Wrangell-St. Elias National Park and Preserve, and is located on land administered by Ahtna, Incorporated, an Alaska Native regional corporation. Shrub mud volcano is 104 m tall and, although classified as a mud volcano, is shrouded in glacial debris. Note that because the name “Klawasi group” and its constituent mud volcanoes are not included in the U.S. Geographic Names Information System, these names are considered informal.

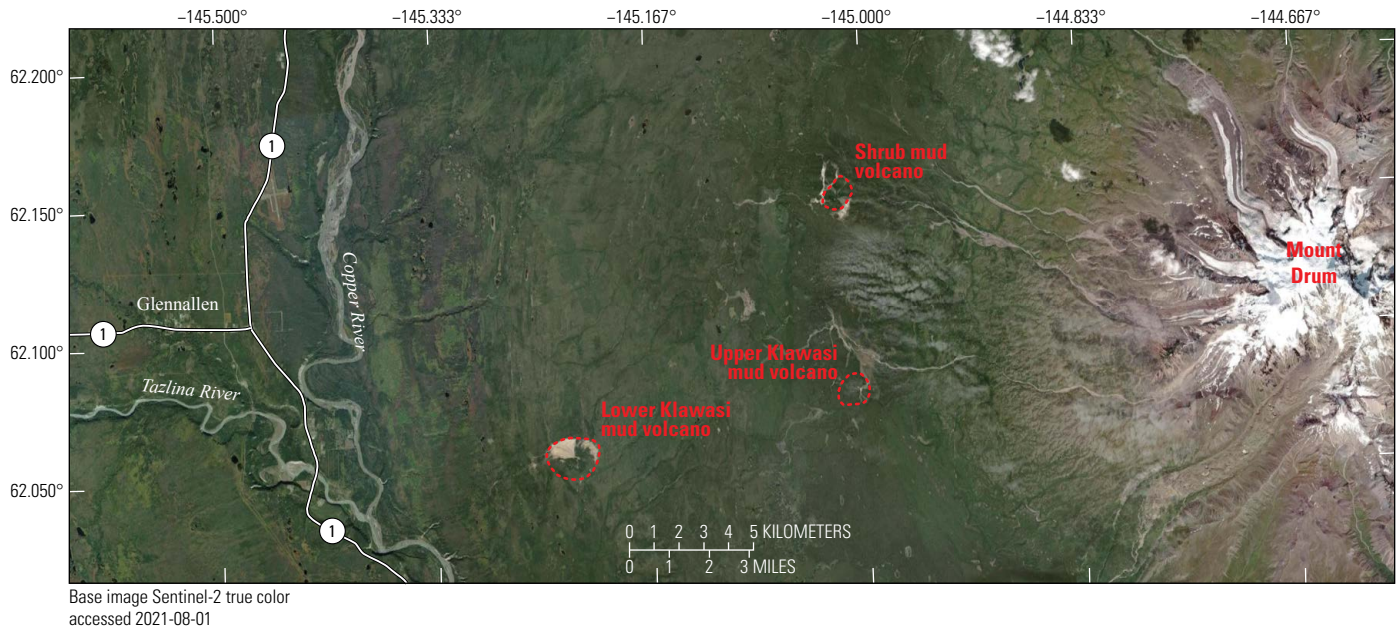


Figure 2. Annotated satellite image of the Copper River Basin in Alaska, showing the location of Shrub, Upper Klawasi, and Lower Klawasi mud volcanoes in relation to Mount Drum and the community of Glennallen.

Shrub mud volcano was barely active for decades, with only extremely weak activity observed in the mid-1950s (Nichols and Yehle, 1961). By comparison, the other Klawasi group mud volcanoes, Upper Klawasi and Lower Klawasi mud volcanoes, have historically produced minor mud discharge and weak gas emissions almost constantly. During the summer of 1996, Shrub mud volcano began to vigorously erupt carbon dioxide-rich gas and warm, saline mud (Richter and others, 1998a), producing mud flows that traveled down the flanks of its edifice and extended out from its base (fig. 3). This activity waned over the following few years, eventually evolving into a bubbling pond of muddy water ~40 m in diameter within a shallow pit near the summit. This pond made Shrub mud volcano more like Upper and Lower Klawasi mud volcanoes, which both have similar features. The summit pond has remained active since it formed, showing little change in behavior or appearance until 2021.

Activity at Shrub mud volcano changed in 2017, when new springs opened on its east flank and erupted mud for several months (fig. 3) (Cameron and others, 2023). These events were followed in 2019 by the extrusion of mud from a line of new springs that opened at the base of the north flank (fig. 3) (Orr and others, 2023), in the same general area as the activity that first marked the mud volcano’s rejuvenation in 1996. This area still hosted activity when visited by AVO workers in 2021 (figs. 3, 4), although the arrangement of the springs had changed: new springs had opened and many of the older springs were no longer active. The line of springs

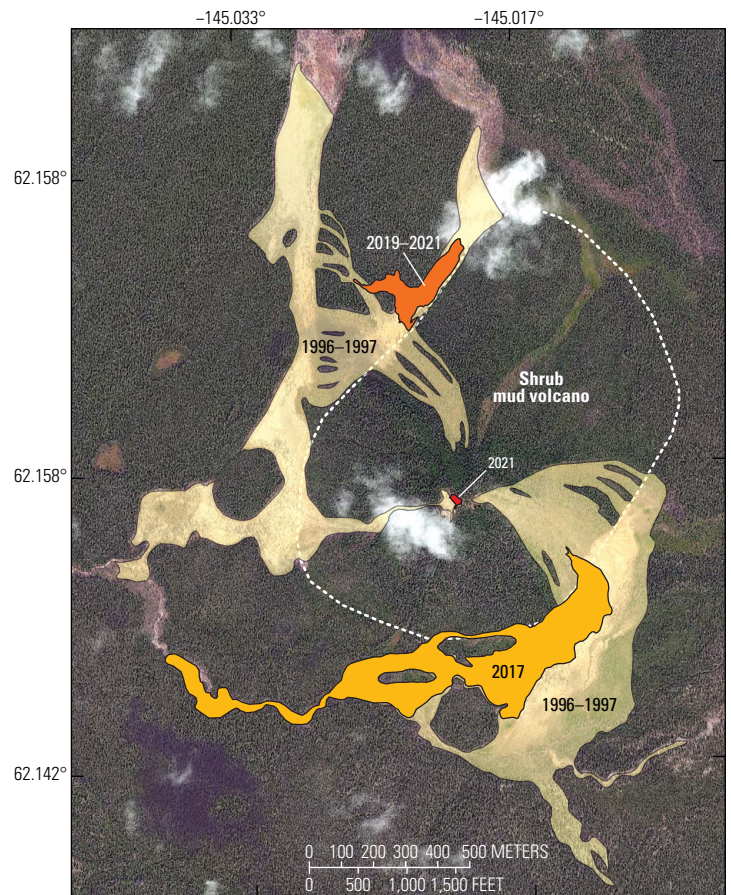


Figure 3. Annotated satellite image of Shrub mud volcano, Alaska, showing mud flows emplaced since its rejuvenation of activity in 1996. Dashed line shows margins of the mud volcano.

EXPLANATION	
■	2021 mud flow
■	2019–2021 mud flow
■	2017 mud flow
■	1996–1997 mud flow

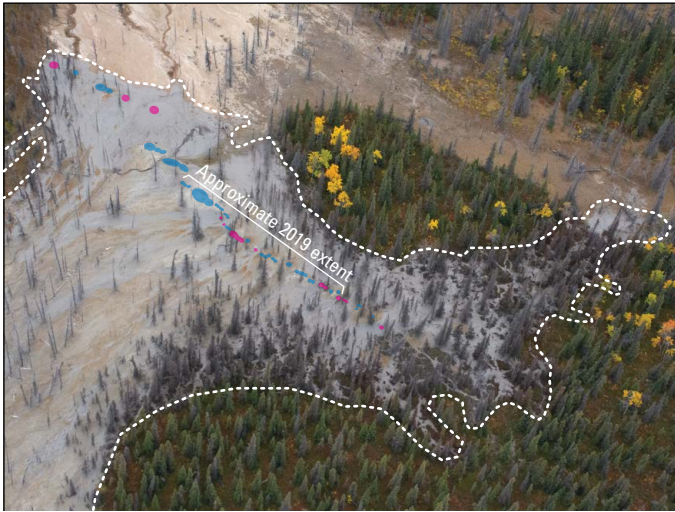


Figure 4. Oblique aerial photograph, looking south, of the vents at the north base of Shrub mud volcano, Alaska. Active (or recently active) vents are highlighted in magenta and inactive vents in blue. The extent of vents identified in 2019 is marked. The dotted line shows the margins of mud flows emplaced since 2019. Photograph by T. Orr, U.S. Geological Survey, September 16, 2021.

had also clearly lengthened to both the northwest and the southeast. However, the principal change to the area, and the site with the most discharge, was a new line of springs oriented en echelon to the 2019 springs and offset ~20 m to their southwest (fig. 4).

New activity was also discovered at Shrub mud volcano's summit when visited in 2021 (fig. 3), made apparent by both a fresh tree-kill area upslope from (east of) the summit pit and new mud deposits that coated the pit's east wall (figs. 5, 6). The source of this mud was a string of recently opened springs (fig. 5) that actively discharged hot, muddy water. This line of springs started at the north wall of the pit, extended southeastward and uphill to just below the summit, then stretched back down to the south wall of the pit. The most active of these new springs was a small, sputtering geyser ~20 centimeters (cm) high with a temperature of ~54 degrees Celsius (°C) (fig. 5). This temperature is the highest measured at Shrub mud volcano since 2000, before the summit pond formed. A few of the new springs were inactive, such as those on the barren slope above the south wall of the pit.

The muddy water that filled the summit pit during previous field visits had been mostly replaced with more solid mud by the time of the 2021 field visit (fig. 6), probably owing

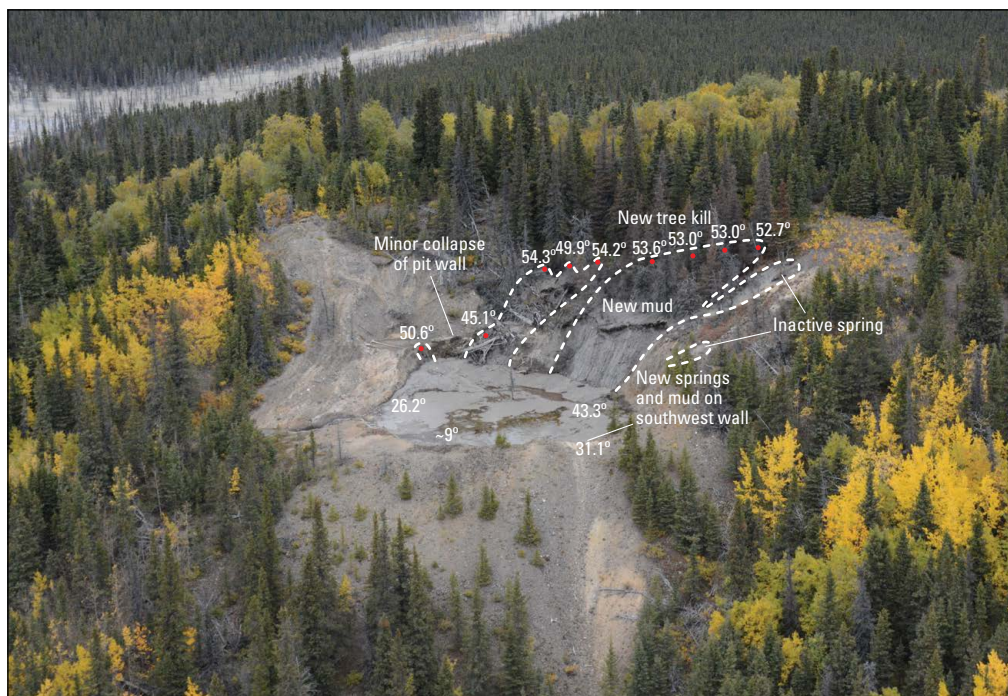


Figure 5. Oblique aerial photograph of the summit of Shrub mud volcano, Alaska, showing the approximate locations of new active springs (dots) and the extent of new mud deposits (dashed lines). Additional small springs, not visible in the photo, are present on the southwest wall of the pit. Also shown are water temperatures in degrees Celsius, as measured by thermocouple and forward-looking infrared. Photograph by T. Orr, U.S. Geological Survey, September 16, 2021.



Figure 6. Photograph of the summit pit at Shrub mud volcano, Alaska, in 2021. Fresh mud, fed from new hot springs upslope, coats the east wall. Since prior field observations in 2019, most water in the summit pond has disappeared, the pit has filled substantially with mud, and all vigorous upwelling has ceased. The main upwelling area in 2019 was just behind the tree roots protruding from the mud; this tree rolled about 120° clockwise and became more submerged from 2019 to 2021. Photograph by T. Girona, University of Alaska Fairbanks Geophysical Institute, September 16, 2021.

to an influx of mud from the new springs on the slope above. Small, bubbling springs were distributed across this mud floor, but no dominant upwelling area existed in the remaining pond. This differs from previous visits, when workers observed a main upwelling area at the north end of the pond—in 2021, that area was covered in mud crossed by rivulets of warm water fed from upslope (fig. 6). The outflow stream discharge was also estimated to have increased by 3–4 times since the field visit in 2019.

Mount Spurr

GVP# 313040

61.299°, -152.254°

3,376 m

Cook Inlet

ICE AND ROCK AVALANCHE



Mount Spurr is a 3,376-meter-high, ice- and snow-covered stratovolcano located ~125 km west of Anchorage (fig. 1). Its largely ice-covered summit cone might be a lava dome complex (Nye and Turner, 1990), although its last known eruption, calculated by correlating tephra deposits, took place ~5,200 years ago (Riehle, 1985). More recently, in 2004–2006, Mount Spurr experienced a period of unrest interpreted to be the result of new magma injecting to a shallow level beneath the volcano (Power, 2004; Power and others, 2004). This unrest was marked by elevated seismicity, magmatic gas emissions, the generation of debris flows, and increased heat flux, the last of which formed a water-filled ice cauldron at the volcano's summit (Neal and others, 2005; Coombs and others, 2006; McGimsey and others, 2007; Neal and others, 2009). Although the summit of Mount Spurr has not erupted recently, a satellite vent 3.5 km south of the summit, named Crater Peak (fig. 7), produced explosive eruptions in 1953 and 1992 (Keith, 1995, and references therein). Both eruptions led to ashfalls that impacted populated areas in south-central Alaska.



Figure 7. Oblique aerial photograph of Mount Spurr, Alaska. Photograph by T. Orr, U.S. Geological Survey, October 9, 2021.

Although no eruptive activity or unrest took place at Mount Spurr in 2021, one notable ice and rock avalanche was large enough to be recorded by regional geophysical sensors. This mass movement signal was recorded on Mount Spurr’s local seismic network (fig. 8) on April 7 at 05:22 AKDT (13:22 UTC). The event’s seismic waveforms indicated that it had a duration of ~2 minutes (fig. 9). Acoustic waves were likewise detected at station SPCP (on Mount Spurr) and at KENI infrasound array (near the City of Kenai, Alaska) (figs. 8, 10); these waves also had a coherent signal duration of ~2 minutes. No clear satellite views were available for this event, precluding AVO from identifying a precise source or deposit area and estimating the avalanche volume. However, the peak period of the long-period (LP) seismic energy was ~15 seconds, indicating that the event was smaller than the widely recorded Mount Spurr ice and rock avalanche of July 15, 2019 (Orr and others, 2023).



Figure 8. Map of Cook Inlet, Alaska, showing Mount Spurr and Iliamna Volcano. Blue dot indicates the location of monitoring stations mentioned in the text.

Base from Esri and its licensors

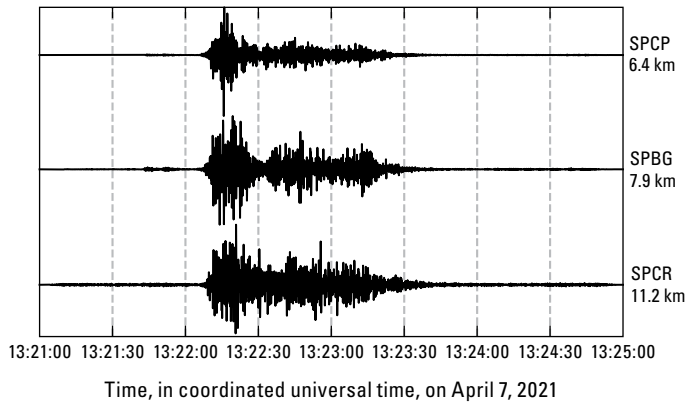


Figure 9. Time-series plot showing high-frequency vertical-component seismic signals generated by the mass movement of April 7, 2021, at Mount Spurr, Alaska. Signals are filtered in the 1–5 hertz band and normalized to their maximum amplitudes. Approximate distances in kilometers (km), listed below each station code, are measured from the summit of Mount Spurr.

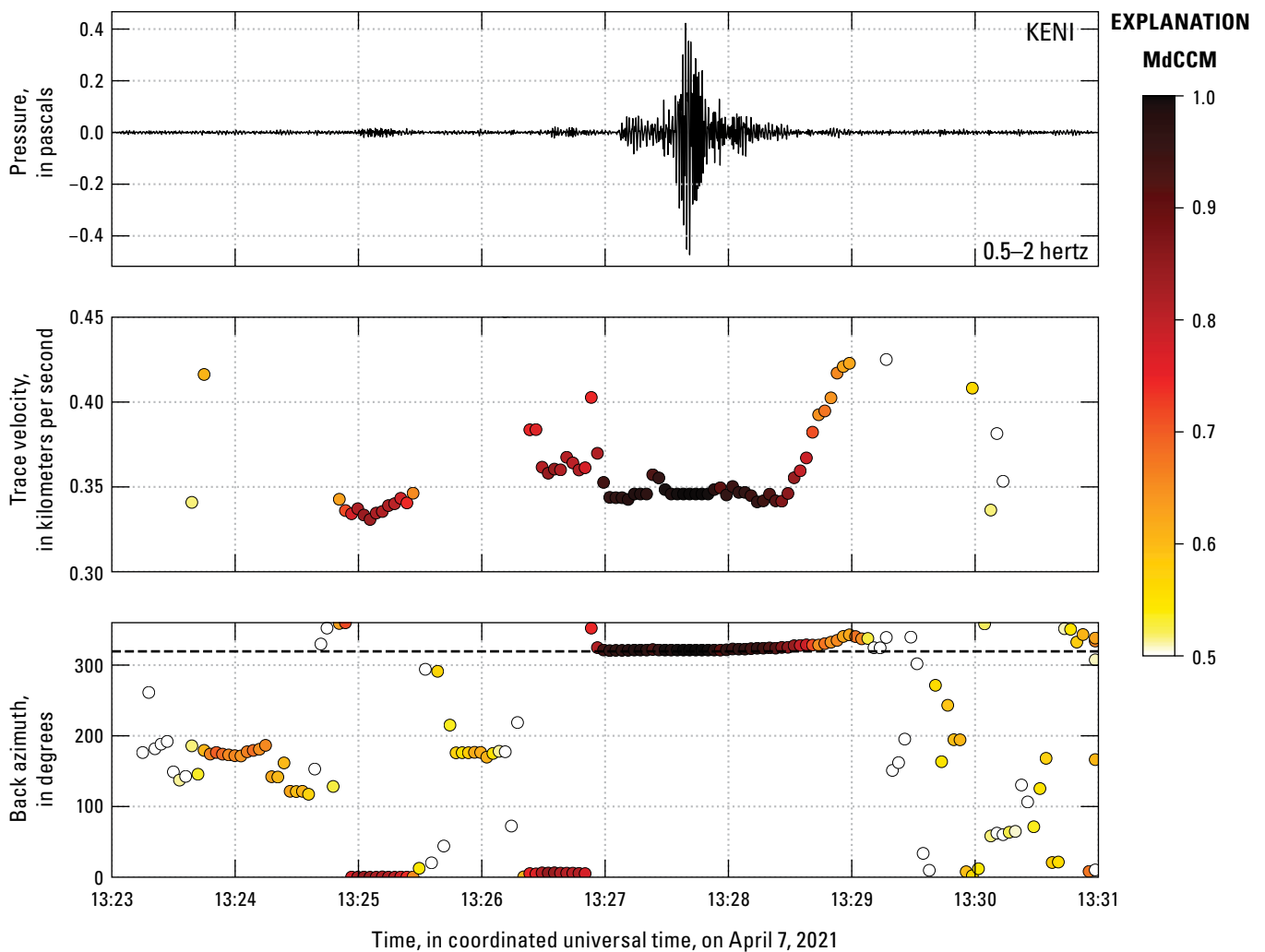


Figure 10. Time-series plots showing array processing results for infrasound generated by the Mount Spurr mass movement of April 7, 2021, as recorded at the KENI infrasound array near the City of Kenai, Alaska. The graphs show variations in pressure (A), median cross-correlation maxima (MdCCM) (B), trace velocity (C), and back azimuth (D). MdCCM measure the coherency of acoustic waves traversing the array. Note the consistent back azimuth toward Mount Spurr (dashed horizontal line in part D) during the period of high MdCCM.

Iliamna Volcano

GVP# 313020
 60.032°, -153.092°
 3,046 m
 Cook Inlet

**ICE AND ROCK AVALANCHE**

Iliamna Volcano is a glacier-carved stratovolcano on the southwest coast of Cook Inlet, ~215 km southwest of Anchorage (figs. 1 and 8). Although Iliamna Volcano has no known historical eruptions, past geologic studies there document evidence of late Holocene explosive activity and repeated, extensive mass wasting of its steep, hydrothermally altered edifice (Waythomas and Miller, 1999). Fumaroles at an elevation of ~2,740 m on the east flank of the volcano almost continuously produce plumes of steam condensate and volcanic gas (Werner and others, 2011). In the past three decades, researchers have documented two magmatic intrusions beneath Iliamna Volcano (Roman and others, 2004; Prejean and others, 2012).

A large ice and rock avalanche took place on the east flank of Iliamna Volcano on August 5, 2021, at 07:21 AKDT (15:21 UTC). Afterward, satellite imagery and oblique aerial photographs showed a dark-colored flow deposit on Iliamna Volcano's east-facing Red Glacier (fig. 11). This avalanche initiated less than 1 km from the volcano's summit and traveled at least 4 km almost due east, generating seismic and acoustic signals recorded locally and regionally. High-frequency signals were clearly recorded on Iliamna Volcano's seismic network (fig. 12). Farther away, the KENI infrasound array at Kenai (figs. 8, 13), and the HOM infrasound station in the City of Homer, Alaska, detected acoustic waves from the event.

Red Glacier has hosted many avalanches historically and prehistorically (Waythomas and others, 2000); the most recent ice and rock avalanche of comparable size to this event occurred in June 2019 (Toney and others, 2021; Orr and others, 2023). These mass flows are generally composed of mostly ice and snow with smaller amounts of rock (involved through entrainment or as part of the original failure region). Avalanches on Red Glacier are highly mobile, traveling at mean speeds of ~50 meters per second (m/s) (Caplan-Auerbach and Huggel, 2007) and peak speeds, estimated via numerical modeling and seismic force inversion, of greater than (>) 70 m/s (Schneider and others, 2010; Toney and others, 2021). Judging by the size of the deposit and the



Figure 11. Oblique aerial photograph (looking west) at Iliamna Volcano, Alaska, on August 14, 2021. Red dashed line marks approximate outline of August 5 avalanche. Photograph by B.D. Jacob, ACE Air Cargo.

amplitudes of the seismic and infrasound signals, the August 2021 event appears to be smaller than the June 2019 ice and rock avalanche.

Figure 12. Time-series plot showing high-frequency vertical-component seismic signals generated by the ice and rock avalanche of August 5, 2021, at Iliamna Volcano, Alaska. Signals are filtered in the 1–5 hertz band and normalized to their maximum amplitudes. Distances in kilometers (km), listed below each station code, are measured from the crown of the avalanche as estimated from satellite imagery.

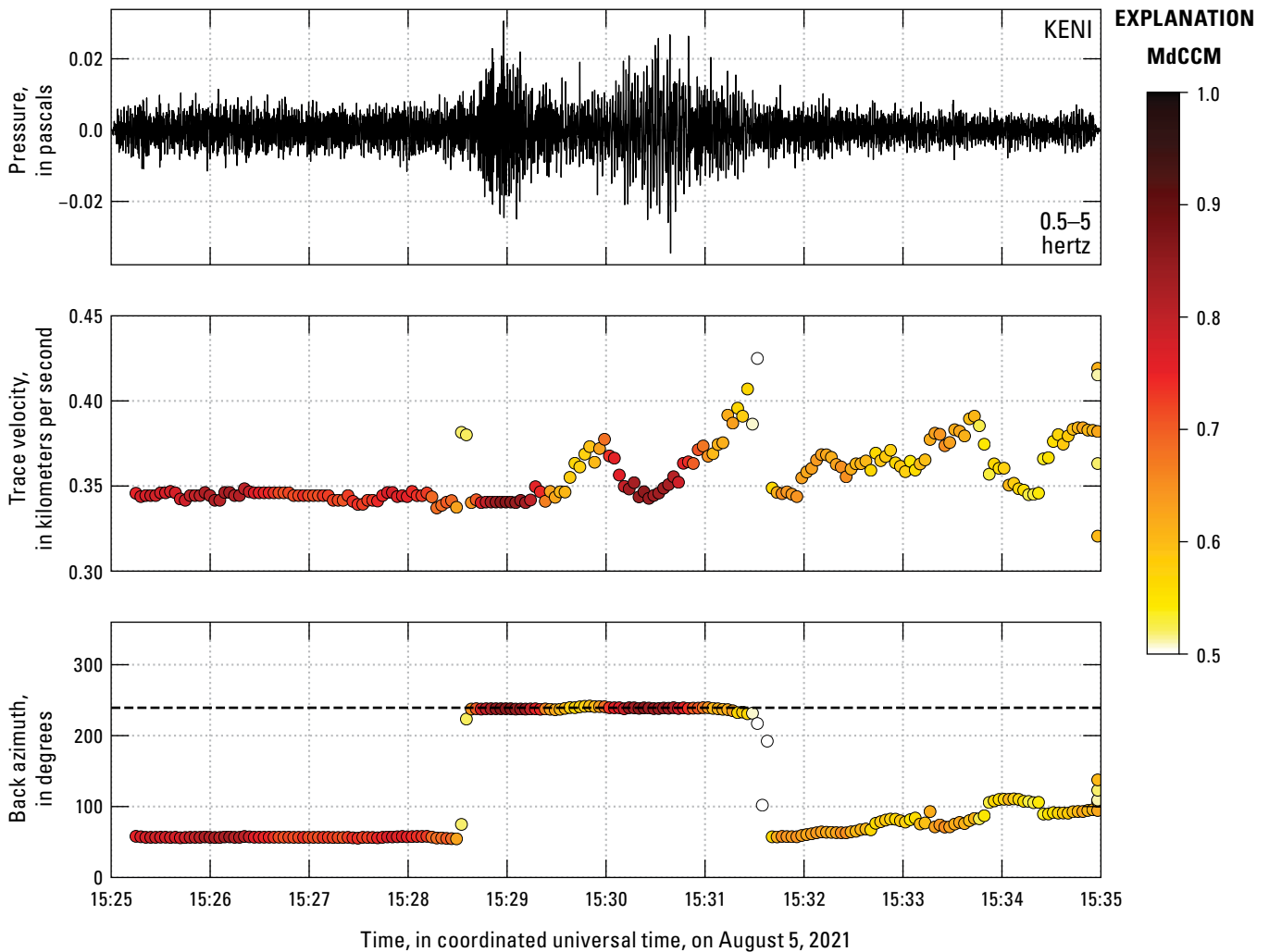
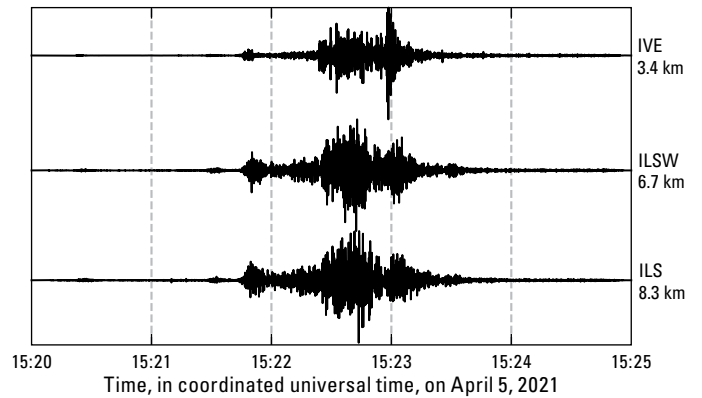


Figure 13. Time-series plots showing array processing results for infrasound generated by the Iliamna Volcano ice and rock avalanche of August 5, 2021, as recorded at the KENI infrasound array near the City of Kenai, Alaska. The graphs show variations in pressure (A), trace velocity (B), and back azimuth (C). Median cross-correlation maxima (MdCCM) measure the coherency of acoustic waves traversing the array. Note the consistent back azimuth toward Iliamna Volcano (dashed horizontal line) during the period of high MdCCM.

**Mount Katmai
(Novarupta)**

GVP# 312170
 58.279°, -154.953°
 2,057 m
 Alaska Peninsula

RESUSPENSION OF 1912 ASH



Mount Katmai and its satellite vent Novarupta, the latter which is thought to have been fed by a shallow sill from a magma body beneath the former (Hildreth and Fierstein, 2000), are located on the Alaska Peninsula, ~440 km southwest of Anchorage, Alaska (fig. 1). The 1912 Novarupta-Katmai eruption—the largest eruption of the 20th century—produced ~17 cubic kilometers (km³) of fall deposits and 11 km³ of pyroclastic material that filled nearby valleys around the volcano (Hildreth and Fierstein, 2012). The pyroclastic deposit in these valleys is as much as 200 m thick, and some areas remain almost entirely devoid of vegetation more than a century after the eruption. When the landscape is snow-free, and particularly when the ground has little moisture content, strong winds can pick up this ash and create large ash clouds. The wind can then transport the resuspended ash, most often southeastward across Shelikof Strait, Kodiak Island, and the Gulf of Alaska. These ash clouds are often seen by individuals downwind and are recorded in satellite imagery,

where they commonly appear to originate from a broad area rather than a specific volcanic source. Although they look identical to dispersing volcanic ash clouds in satellite imagery, they are not the result of volcanic activity. This resuspension phenomenon has been observed and documented many times over the last several decades (Hadley and others, 2004; Wallace and Schwaiger, 2019), including seven times in 2021. The events observed in 2021 did not warrant a change in the Aviation Color Code and Volcano Alert Level, which remained **GREEN** and **NORMAL** throughout the year.

On August 28, 2021, strong winds picked up loose volcanic ash from the Mount Katmai (Novarupta) region and carried it southeastward toward Kodiak Island. The National Weather Service (NWS) had forecasted this event a few days prior, and when it occurred, the NWS Alaska Aviation Weather Unit (AAWU) reported cloud heights as much as ~6,000 ft (~1,800 m) ASL, issuing a significant meteorological information statement (SIGMET) for aviators. AVO also issued an Information Statement.

The following month, strong winds again generated a cloud of resuspended ash that drifted over Kodiak Island. This event, like the one a month prior, was anticipated by the NWS a few days in advance. The drifting ash cloud appeared clearly in satellite data (fig. 14) for ~24 hours, starting in the afternoon of September 20. AAWU issued a SIGMET reporting ash at altitudes as high as ~8,000 ft (~2,400 m) ASL; AVO correspondingly issued an Information Statement. Trace ash fall was reported in the City of Kodiak, Alaska, and owing to the forecast of this event, a local observer was able to sample the ash fall and send it to AVO.

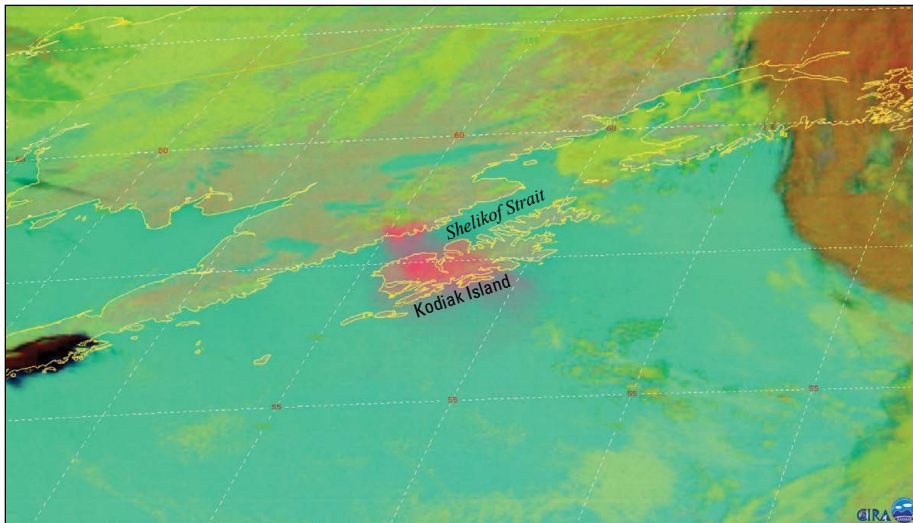
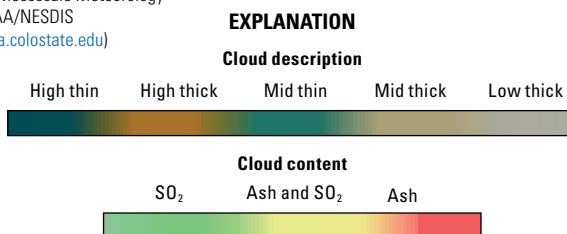


Figure 14. Oblique, processed satellite image showing a resuspended ash plume (in red) from the Mount Katmai (Novarupta) area extending across the Shelikof Strait to Kodiak Island, Alaska. Red numbers denote degrees latitude; green numbers denote degrees longitude. Image acquired by GOES-17 on September 21, 2021, at 00:20 Alaska standard time (08:20 coordinated universal time).

Base from Regional and Mesoscale Meteorology Branch (RAMMB) of NOAA/NESDIS (<https://rammb-slider.cira.colostate.edu>)



The ash resuspension had ceased for only two days when, beginning late in the afternoon on September 23, winds again picked up loose ash. This ash cloud drifted east across northern Kodiak Island at an apparently lower altitude (~5,000 ft [~1,500 m] ASL), though no ashfall was reported. This resuspension event also lasted ~24 hours, during which time AAWU issued a SIGMET and AVO issued an Information Statement.

AVO observed the next minor cloud of resuspended ash in satellite views on September 26. This cloud drifted southeastward toward the middle of Shelikof Strait, never reaching Kodiak Island. No Information Statements were issued for this minor event.

Before dawn on October 2, strong winds near Mount Katmai once again picked up loose volcanic ash and carried it southeastward toward Kodiak Island. As with most previous resuspension events at Mount Katmai in 2021, the NWS had forecasted the event a few days prior. AAWU issued a SIGMET and the NWS Forecast Office issued a Marine Weather Statement. AVO issued an Information Statement reporting ash clouds that reached altitudes of ~6,000 ft (~1,800 m) ASL. Meteorological clouds obscured satellite observations the next day, but the SIGMET remained in place for ~24 hours owing to the likelihood of continued ash resuspension.

Starting on the morning of November 17, another cloud of resuspended ash appeared clearly in satellite data. Most of the typical source region for resuspended ash at Mount Katmai was covered in snow at the time, so this event's ash source was apparently confined to valleys on the north side of Shelikof Strait, in the vicinity of Mount Katmai (fig. 15). AAWU issued a SIGMET reporting a cloud altitude as high as ~7,000 ft (~2,100 m) ASL; AVO correspondingly issued an Information Statement. Resuspended ash was visible in satellite data until about midnight, although reports of resuspended ash from the

City of Kodiak continued into the following day. Residents in Kodiak collected trace ashfall.

The last resuspension event in the Mount Katmai region in 2021 occurred on November 25. AAWU issued a SIGMET reporting a cloud that drifted over Kodiak Island at an altitude as high as ~5,000 ft (~1,500 m) ASL. The NWS Forecast Office issued a Marine Weather Statement and AVO issued an Information Statement.

Aniakchak Crater

GVP# 312090
56.906°, -158.209°
1,298 m
Alaska Peninsula



RESUSPENSION OF ASH

Aniakchak Crater is a circular caldera 10 km in diameter and 1 km deep, located on the Alaska Peninsula, ~25 km east-southeast of the City of Port Heiden, Alaska, and ~665 km southwest of Anchorage (fig. 1). The crater formed ~3,400 years ago during a catastrophic event that erupted 75 km³ of material (Miller and Smith, 1987; Dreher and others, 2005; Bacon and others, 2014). Many lava domes, lava flows, and scoria cones occupy the caldera interior (Neal and others, 2000); the largest intracaldera cone is Vent Mountain, which is 2.5 km in diameter and stands 430 m above the floor of the caldera. The only historical eruption at Aniakchak Crater was a powerful explosive event in 1931 that covered a large part of the eastern Alaska Peninsula with ash (Nicholson and others, 2011).

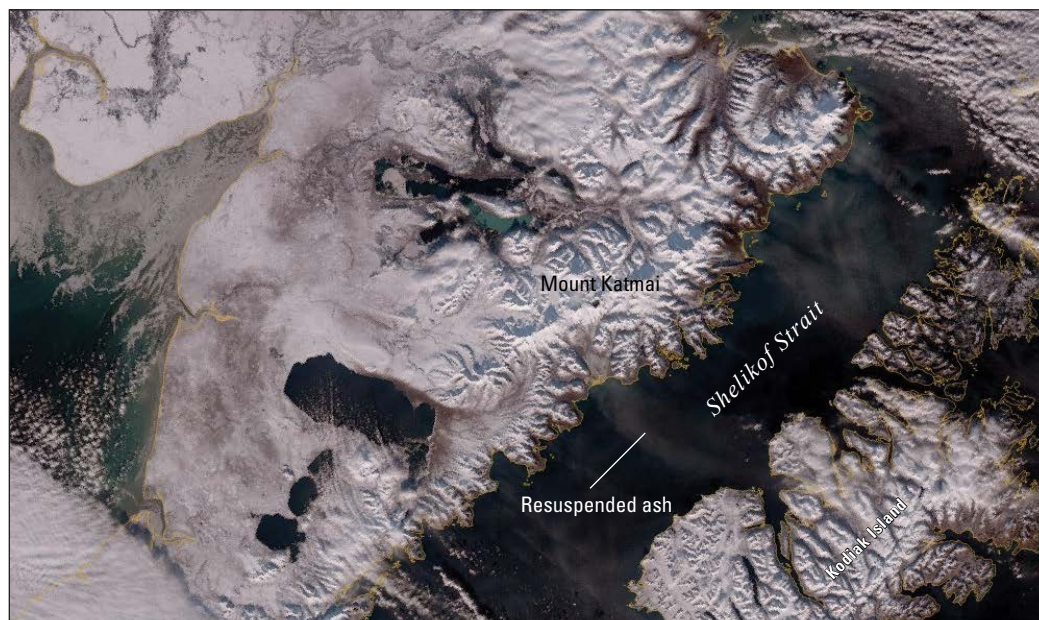


Figure 15. True-color visible satellite image showing a resuspended ash plume drifting from valleys on the north side of Shelikof Strait toward Kodiak Island, Alaska. Image acquired by the Visible Infrared Imaging Radiometer Suite instrument on November 17, 2021, at 14:03 Alaska daylight time (22:03 coordinated universal time).

When the landscape near Aniakchak Crater is snow-free, and particularly when the ground has little moisture content, strong winds can pick up ash and create large ash clouds. The wind can then transport this resuspended ash, which can pose a hazard to aviation. On August 1–2, 2021, strong southerly winds entrained and resuspended ash from the region north of Aniakchak Crater and east of Port Heiden before carrying it ~200 km northward over Bristol Bay. High-resolution satellite views indicated that the event's source region was north of the caldera at the sparse surface exposures of pyroclastic-flow deposits from the caldera-forming eruption (fig. 16A). The drifting ash cloud appeared in imagery from the Geostationary

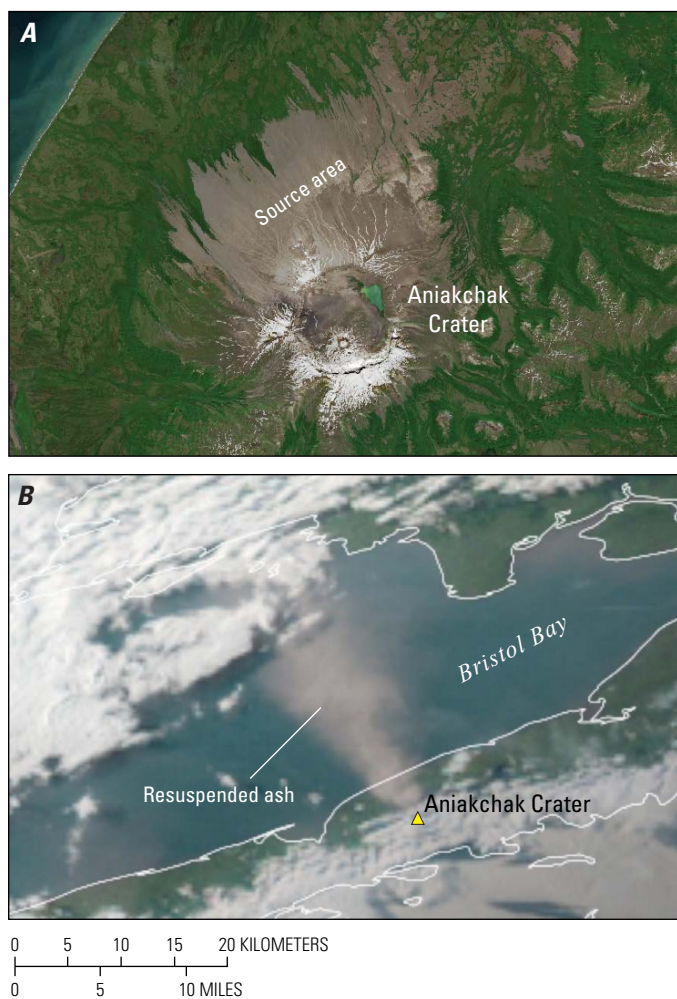


Figure 16. Satellite imagery of resuspended ash and its source area at Aniakchak Crater, Alaska. *A*, Satellite image acquired by Sentinel-2 on July 3, 2019, showing the source area for resuspended ash north of Aniakchak Crater. *B*, Oblique true-color satellite image acquired by the Geostationary Operational Environmental Satellite on August 1, 2021, at 20:50 Alaska daylight time (August 2 at 04:50 coordinated universal time), showing a resuspended ash plume drifting northward over Bristol Bay from the area north of Aniakchak Crater. Coastline shown in white.

Operational Environmental Satellite for ~18 hours beginning late in the morning on August 1 (fig. 16B). Ground-level webcam views from Port Heiden also recorded this resuspended ash. In response, AAWU issued a SIGMET for aviators and AVO issued an Information Statement. AVO received no reports of ashfall at Port Heiden. The Aviation Color Code and Volcano Alert Level remained **GREEN** and **NORMAL** for Aniakchak Crater during 2021.

Mount Veniaminof

GVP# 312070
56.198°, -159.393°
2,511 m
Alaska Peninsula

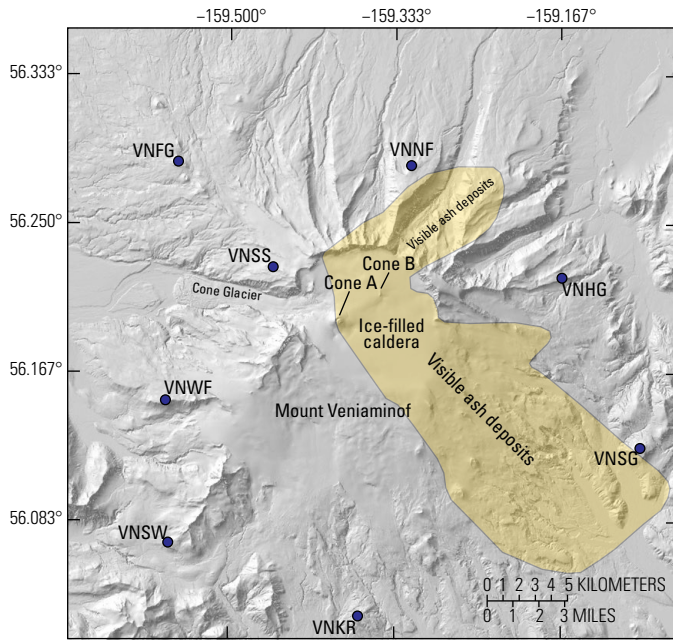


ERUPTION WITH ASH EMISSIONS AND LAVA FLOWS

Mount Veniaminof is an ice-clad andesite and dacite stratovolcano on the Alaska Peninsula, ~35 km north of the community of Perryville, Alaska, and ~775 km southwest of Anchorage (fig. 1). The volcano has a total volume of ~350 km³, making it one of the largest of the Aleutian Arc (Miller and others, 1998; Bacon and others, 2009). Extensive pyroclastic-flow deposits around Mount Veniaminof record the occurrence of two Holocene caldera-forming eruptions (Miller and Smith, 1987), but Mount Veniaminof is also one of the most active volcanoes in Alaska; it has erupted at least 20 times since 1830, including in 2021 (as described herein). All aforementioned historical eruptions were likely from cone A, the informal name for a prominent, 300-m-high cinder cone within the volcano's 10-km-wide, ice-filled caldera (fig. 17). The last eruption of Mount Veniaminof prior to 2021 was in 2018 (Cameron and others, 2023; Waythomas, 2021).

Mount Veniaminof showed no indication of activity at the start of 2021. In response to a prolonged local seismic network outage that started in December 2020, AVO changed the volcano's Aviation Color Code and Volcano Alert Level from **GREEN** and **NORMAL** to **UNASSIGNED** on January 15, 2021, reflecting the observatory's limited ability to detect volcanic activity there.

On March 1, the TROPospheric Monitoring Instrument (TROPOMI) onboard the Copernicus Sentinel-5 Precursor satellite identified unrest at Mount Veniaminof in the form of elevated sulfur dioxide (SO₂) emissions. The TROPOMI sensor measures variations in the wavelength-dependent absorption of ultraviolet energy due to the presence of gases (such as ozone and SO₂) and retrieves the amount of gas present in the total atmosphere to account for the observed absorption. On March 2, satellite imagery again showed SO₂. Elevated surface temperatures began to appear in



Base from U.S. Geological Survey 5-meter Alaska Digital Elevation models, 2017—USGS National Map 3DEP Downloadable Data Collection: U.S. Geological Survey data release, accessed December 12, 2021, at <https://elevation.alaska.gov/>. [Also available at <https://www.sciencebase.gov/catalog/item/530f4226e4b0e7e46bd2c315>.]

Figure 17. Map of Mount Veniaminof, Alaska, showing locations of cones A and B in the summit caldera and the approximate final extent of ash deposits identifiable in satellite imagery. Blue dot indicates seismic monitoring stations.

satellite imagery early on March 4, and then a few hours later, at 05:13 AKST (14:13 UTC), regional infrasound instruments detected an explosion. Satellite imagery recorded a corresponding ash plume shortly thereafter. An ashy plume from cone A was seen in webcam imagery after sunrise, confirming that an eruption was underway. AVO responded later that morning by increasing the Aviation Color Code and Volcano Alert Level to **ORANGE** and **WATCH**. A retrospective analysis of high-resolution satellite imagery identified ash deposition near cone A and melting of glacial ice ~1 km to its east on February 28, but no signs of activity on February 25, suggesting that the eruption began between those two dates. **Figure 18** shows a timeline of the activity observed at Mount Veniaminof in 2021.

The eruption reached its climax on March 4–10, producing moderately to strongly elevated surface temperatures, ash emissions, and frequent explosions detected by infrasound. Several explosions on March 6 were heard and even felt in Perryville, ~35 km away. Webcam and satellite data from this period showed ash emissions from cone A and a steam plume from the growing melt pit east of the cone (**fig. 19**). Between March 6 and March 10, the ash plumes reached as high as ~15,000 ft (~4,600 m) ASL and traveled as far as 220 km from the volcano. Owing to the height and extent of these ash plumes, local flight restrictions were set

in place on March 9. Tephra deposits from the ash plumes were mostly confined to the caldera, but some ash fell outside the caldera on March 8, reaching as far as 22 km from the vent. The ash during this interval was blown predominantly southeastward (**figs. 17, 19B, 20**).

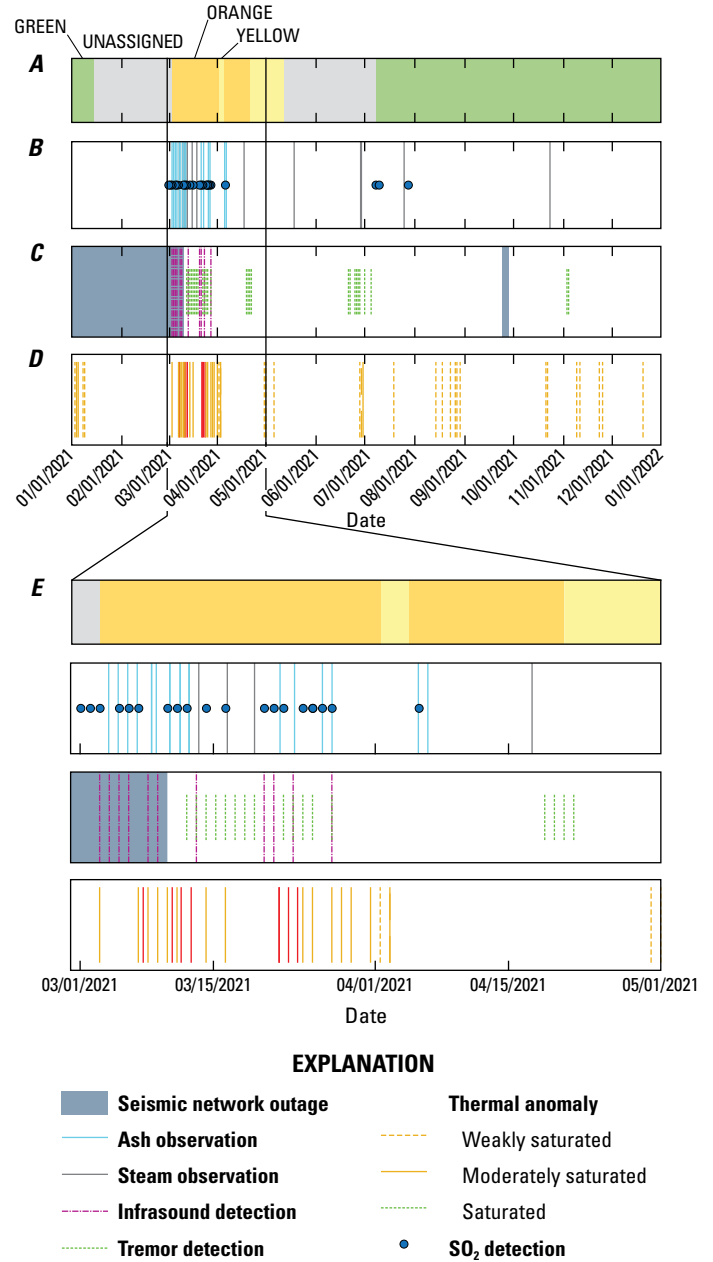


Figure 18. Timeline of observed activity at Mount Veniaminof in 2021, showing changes in Aviation Color Code (A); days when webcam and satellite imagery recorded ash, steam plumes, and (or) sulfur dioxide (SO₂) (B); days with tremor and (or) explosions large enough to be detected by regional infrasound sensors (C); days with elevated surface temperatures (and their subjective strength) (D); and magnification of parts A–D for the period spanning March 1 through May 1, 2021 (E). Dates shown as month/day/year.

Lava effusion from vents within the glacial melt pit on the east flank of cone A first appeared in satellite imagery on March 7. The sub-circular melt pit continued to widen as the lava spread away from the flank vents and encompassed an area of nearly 700,000 square meters (m²) by late March (figs. 20, 21).

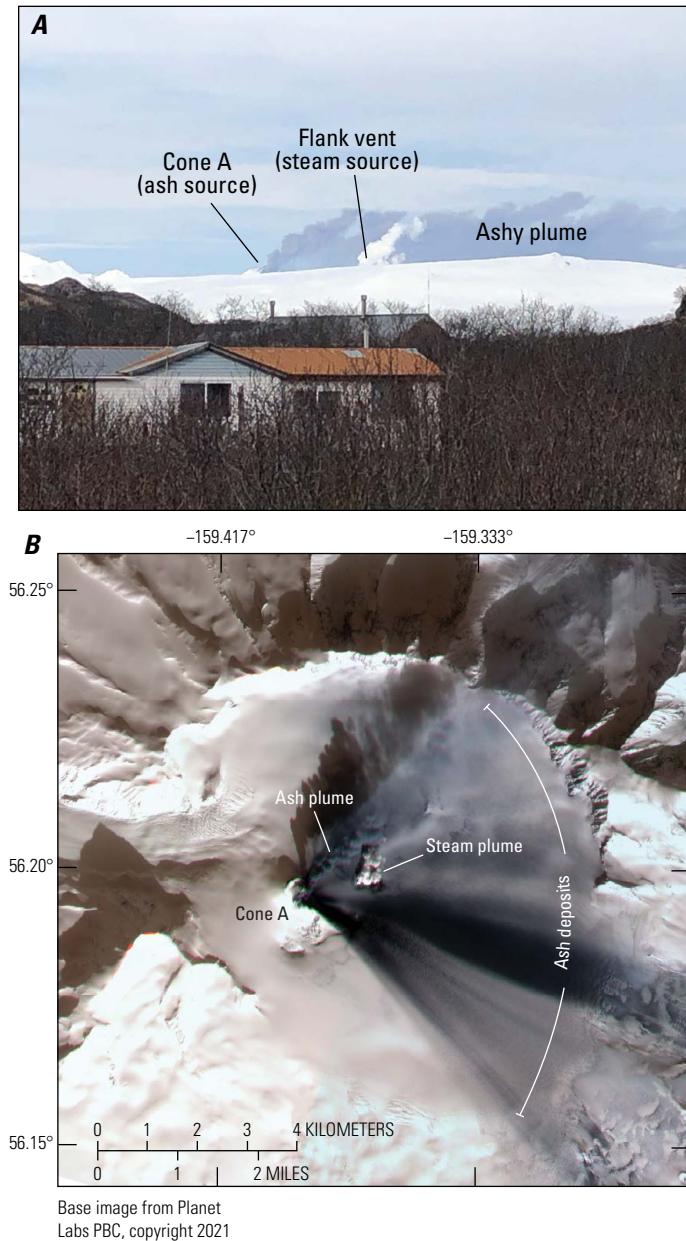


Figure 19. Images of the eruption of Mount Veniaminof, Alaska, in March 2021. *A*, Photograph showing the eruption of Mount Veniaminof as viewed from the City of Perryville, Alaska, on March 9, 2021. A gray, ashy plume emits from cone A and drifts northeastward (to the right). A white steam plume, presumably from a lava flow melting glacial ice around the flank vent, appears in the image center. Copyrighted by A. Shangin, (2021); used with permission. *B*, Satellite image acquired on March 7, 2021, showing an ashy plume erupting from Cone A and a small, white steam plume emanating from a melt pit northeast of the cone.

Less intense activity characterized the second half of March at Mount Veniaminof. Two seismic stations at the volcano came back online on March 12, allowing AVO geophysicists to detect tremor and LP earthquakes once again. Tremor was detected daily, whereas explosions and ash plumes were detected less frequently. Thermal anomalies from lava effusion were weaker in the second half of the month than in the first half. Lava effusion and minor ash emissions likely continued within the caldera throughout much of this time, although observations were limited to those on clear weather days. Ash plume altitudes remained lower than ~10,000 ft (~3,000 m) ASL. Although not reported, webcam imagery suggested that trace amounts of ash fell in Perryville on March 27, making it the only day during the eruption when a community may have been impacted by ash.

On April 1, the eruption paused and the volcano showed only slightly elevated surface temperatures, which were probably related to cooling lava flows. The Aviation Color Code and Volcano Alert Level were lowered to **YELLOW** and **ADVISORY** on April 2 in response to this decreased activity. However, an ash plume on April 5 prompted AVO to raise the Aviation Color Code and Volcano Alert Level back to **ORANGE** and **WATCH**. A second ash plume was observed on April 6. No eruptive activity was observed thereafter, so the Aviation Color Code and Volcano Alert Level were lowered to **YELLOW** and **ADVISORY** on April 21, then back to **UNASSIGNED** on May 12. Elevated surface temperatures detected in the weeks after the pause were most likely related to a warm summit cone and cooling lava flows (fig. 21). Altogether, the three lava flows that erupted within the glacial melt pit covered a combined area of ~2.7×10⁴ m² (Waythomas, 2021).

AVO workers fully restored the Mount Veniaminof local seismic network during a field campaign in late June and early July. The Aviation Color Code and Volcano Alert Level were consequently changed to **GREEN** and **NORMAL** on July 8. Tremor, steam plumes, SO₂ emissions, and thermal anomalies were detected in geophysical and remote sensing data shortly before and during the field campaign, which ran from June 28 to July 5. However, the field crew itself observed no noteworthy activity (fig. 21). No further unrest took place at Mount Veniaminof for the remainder of 2021.

Tephra samples were collected from a snow pit ~2 km east of cone A, adjacent to the melt pit (fig. 21), during the field campaign. Four distinct tephra layers were sampled; each consisted of black and red-oxidized grains intermixed with loose plagioclase crystals. Each layer had a modal grain size of 0.25–0.5 millimeter (mm) and a maximum grain size of 2 mm. One layer also had apparent accretionary lapilli. Petrographic analysis of the samples showed that the phenocrysts, like those sampled from the 2018 eruption (Loewen and others 2021), comprised normally zoned plagioclase (fig. 22A, B), olivine (fig. 22C), and rare clinopyroxene. The groundmass was a mixture of microlitic sideromelane (fig. 22D), tachylyte, and lithic components. The glass composition was similar to that erupted in 2018, although with slightly lower silica concentrations (like the 2013 eruption glass).

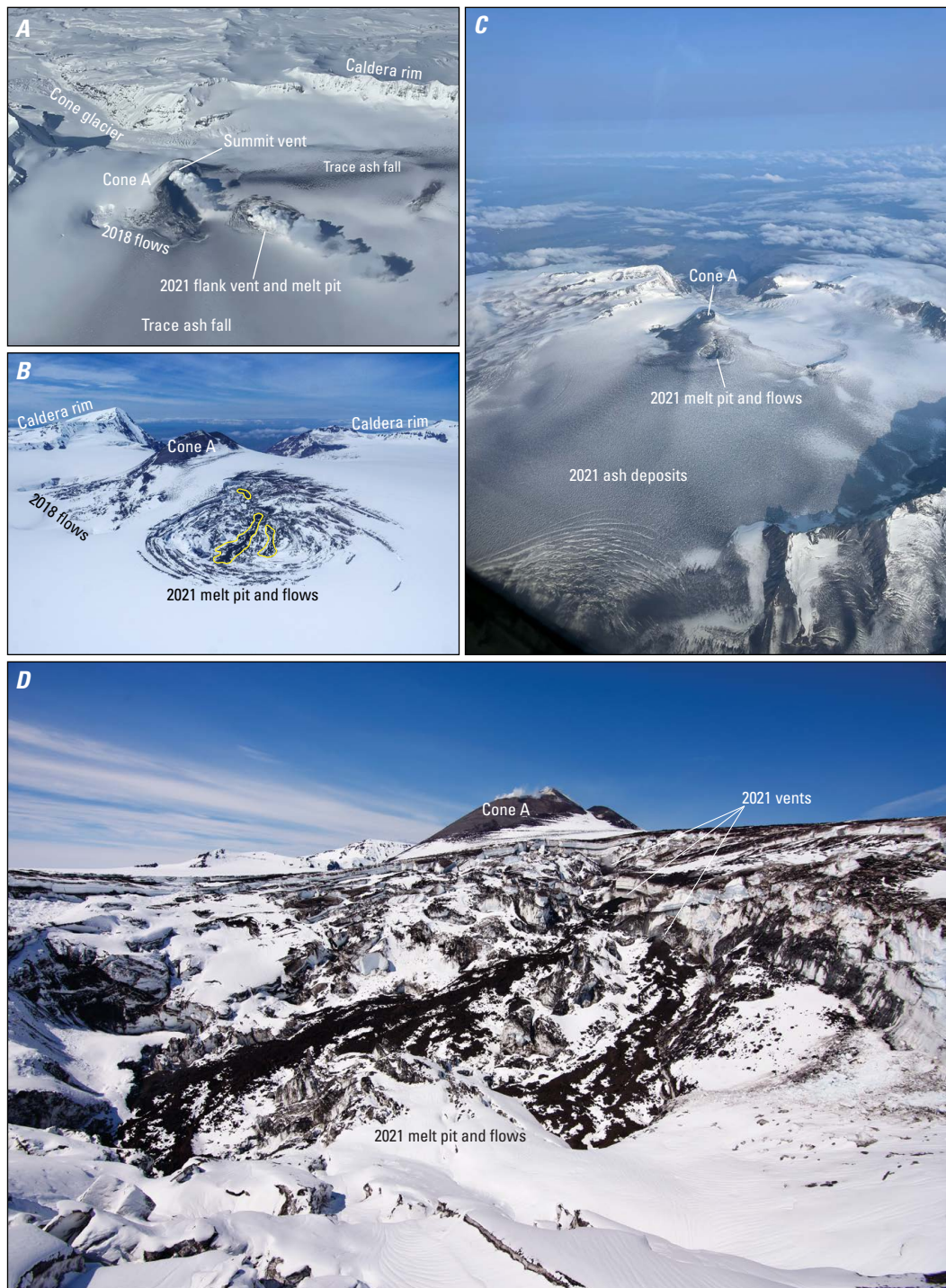


Figure 20. Photographs of eruptive activity at Mount Veniaminof, Alaska, in 2021. *A*, Oblique aerial photograph (looking northwest) showing activity at the volcano. Steam plumes emanate from the cone A summit and from its flank vents. Trace ash deposits extend northeastward and southeastward from cone A. Photograph by B.D. Jacob, ACE Air Cargo, March 11, 2021. *B*, Oblique aerial photograph (looking west) showing a melt pit and the lava flows (outlined) produced by flank vent activity. Photograph by V. Wasser, University of Alaska Fairbanks Geophysical Institute, June 29, 2021. *C*, Oblique aerial photograph (looking west) showing new ash deposits within the caldera. Photograph by B.D. Jacob, ACE Air Cargo, August 14, 2021. *D*, Photograph (looking west) of the vents and lava flows active in 2021 within the melt pit of the caldera glacier. Cone A, in the background, is still warm enough to be snow-free. Parts of the lava flow are hot enough to be steaming. Photograph by C. Read, U.S. Geological Survey, June 29, 2021.

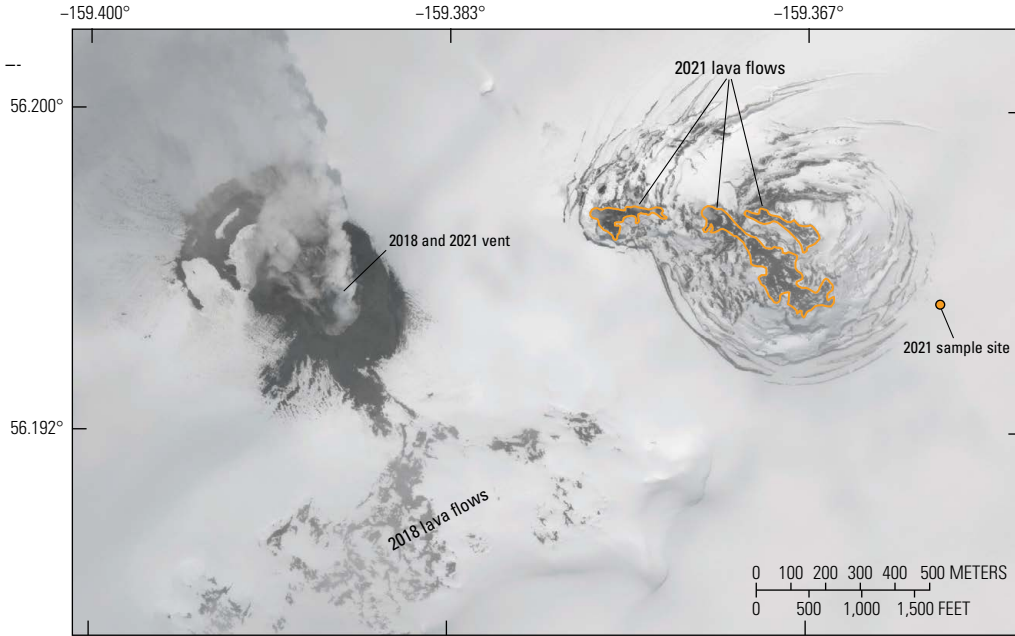


Figure 21. Visible satellite image of Mount Veniaminof, Alaska, after the end of its eruption in 2021. Steam emissions obscure the vent of cone A that was active in 2018 and 2021. Snow partially covers the 2018 lava flow field. A melt pit east of the summit cone contains lava flows (approximate extents outlined) from the 2021 flank vent. The 2021 tephra sample site is highlighted. Image acquired by WorldView-3 on June 7, 2021.

Base image from Digital

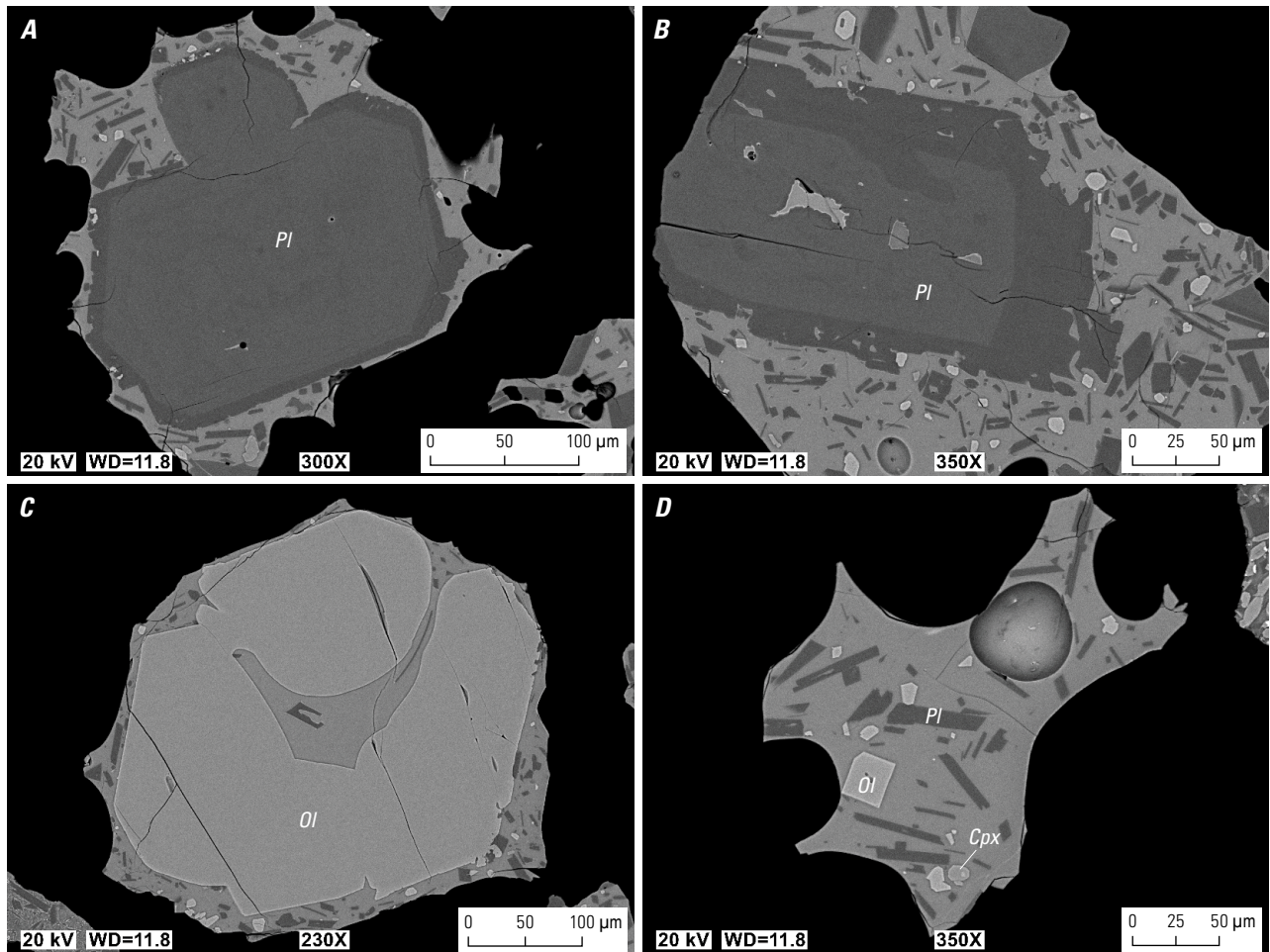



Figure 22. Backscattered electron images of polished tephra samples from the 2021 eruption of Mount Veniaminof, Alaska. *A, B*, Normally zoned plagioclase (Pl) phenocrysts. *C*, Normally zoned olivine (Ol) with a melt embayment. *D*, Typical microlitic sideromelane groundmass on a vesicular grain; microlites are plagioclase (Pl), olivine (Ol), and clinopyroxene (Cpx). Images taken with a JEOL 6510LV scanning electron microscope. kV, kilovolt; WD, working distance, µm, micrometer.

Pavlof Volcano

GVP# 312030
 55.417°, -161.894°
 2,526 m
 Alaska Peninsula

ERUPTION WITH ASH EMISSIONS, FOUNTAINING, LAVA FLOWS, AND LAHARS



Pavlof Volcano is a cone-shaped stratovolcano composed of basaltic andesite lava flows and pyroclastic rock. The volcano is located on the Alaska Peninsula, east of the City of Cold Bay, Alaska, and with 38 documented eruptions since 1817, it is considered one of the most active volcanoes in North America. The most recent eruption began in 2021 and is described herein. Eruptions at Pavlof Volcano have ranged in style from Strombolian to Vulcanian (Waythomas and others, 2006), and as a dominantly open-vent system, many of the volcano’s eruptions occur with little precursory seismic activity or ground deformation observed in InSAR (Lu and Dzurisin, 2014; Pesicek and others, 2018). Prior to 2021, the last eruption at Pavlof Volcano took place in 2016 and was characterized by continuous seismic tremor, infrasound

detections, and lightning accompanying ash emissions that rose to an altitude of ~20,000 ft (~6,100 m) ASL (Fee and others, 2017; Cameron and others, 2020).

After a 9-month quiescent period that started in late 2020, seismic activity at Pavlof Volcano increased on July 9, 2021, in a distinct change from its background levels. Tremor periods observed on that date prompted AVO to increase the Aviation Color Code and Volcano Alert Level from **GREEN** and **NORMAL** to **YELLOW** and **ADVISORY**. From July 9 to August 5, seismic activity at the volcano was characterized by more volcanic tremor periods and occasional low-frequency events, but no outward signs of eruptive activity were observed.

On August 5, 2021, clear webcam views of Pavlof Volcano showed episodic, low-level ash emissions (fig. 23). These intermittent ash bursts came from a new vent on the upper southeast flank of the volcano, which produced diffuse ash clouds that rose just above the summit and drifted roughly 10–15 km southeastward before dissipating. Seismic and infrasound data associated this activity with occasional small explosions and tremor. The ash emissions clearly indicated that an active eruption was in progress, so AVO raised the Aviation Color Code and Volcano Alert Level to **ORANGE** and **WATCH** later that day.

Seismic and infrasound sensors regularly recorded small explosions through the rest of the year, and when viewing conditions permitted, minor ash emissions appeared in

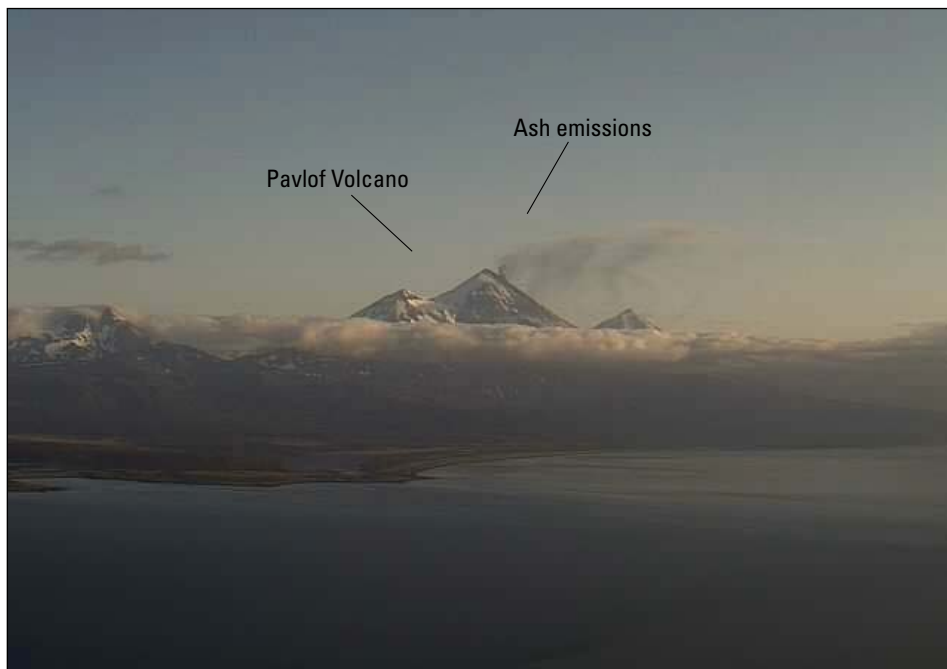


Figure 23. Photograph of Pavlof Volcano (looking northeast) from the Dolgoi Island webcam on August 5, 2021, at 08:34 Alaska daylight time (16:34 coordinated universal time). Diffuse ash emissions originate from a vent on the upper southeast flank and extend a short distance southward from the volcano.

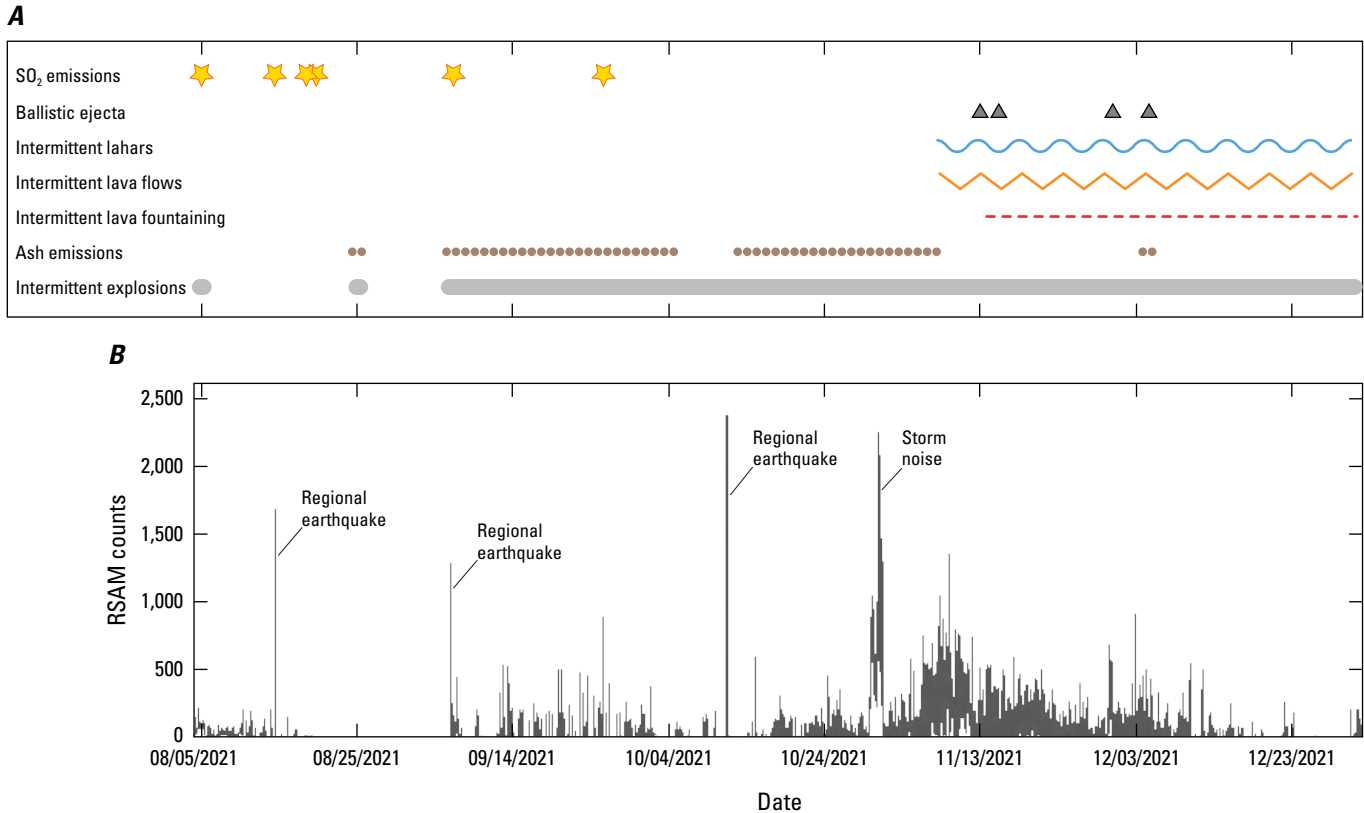


Figure 24. Timeline of outward indications of volcanic unrest at Pavlof Volcano, Alaska (A), and time-series plot of real-time seismic amplitude (RSAM) for seismic station PVV (B), August 5–December 31, 2021. Location of station PVV shown on figure 25. SO₂, sulfur dioxide.

webcam views and were observed by pilots (fig. 24). Diffuse ash clouds intermittently rose as high as ~12,000 ft (~3,700 m) ASL and were visible in satellite data as far as 10–15 km beyond the vent. Ash fallout during this period settled mainly on the upper south-southeast flank of the volcano, within 2–3 km of the vent. Occasional stronger ash bursts and farther-traveling ash clouds may have produced trace amounts (less than 1/32 inch or 0.8 mm) of ash fall as far as 10–15 km southeast of the vent, but this amount of ash is difficult to observe in satellite data and so could not be confirmed.

On August 25 and 26, mid-infrared satellite images showed slightly elevated surface temperatures at the summit of the volcano for the first time (fig. 25). The detection of elevated surface temperatures in satellite data usually indicates that lava is at or near the surface; however, lava flows at Pavlof Volcano were not confirmed until November 8, when the thermal output at the vent increased considerably (fig. 26). The presence of shallow subsurface magma and hot gases may have contributed to the slightly elevated thermal signals observed between late August and early November.

Satellite images acquired on November 11 showed an active lava flow or spatter accumulation, about 200 m in length, and associated lahar deposits (extending ~2 km beyond the vent) on the upper southeast flank of the volcano (fig. 27). Many

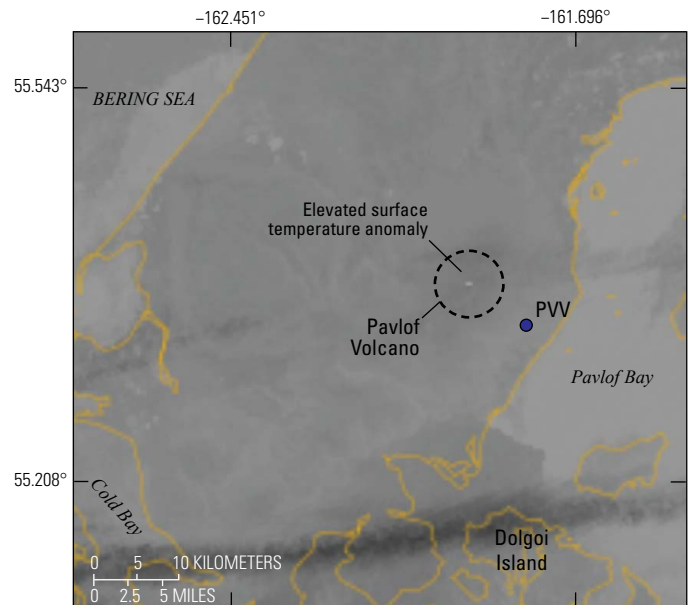


Figure 25. Mid-infrared satellite image showing elevated surface temperatures at Pavlof Volcano, Alaska. Blue dot shows location of station PVV (fig. 24). Image acquired by the NOAA-20 Visible Infrared Imaging Radiometer Suite, August 26, 2021.

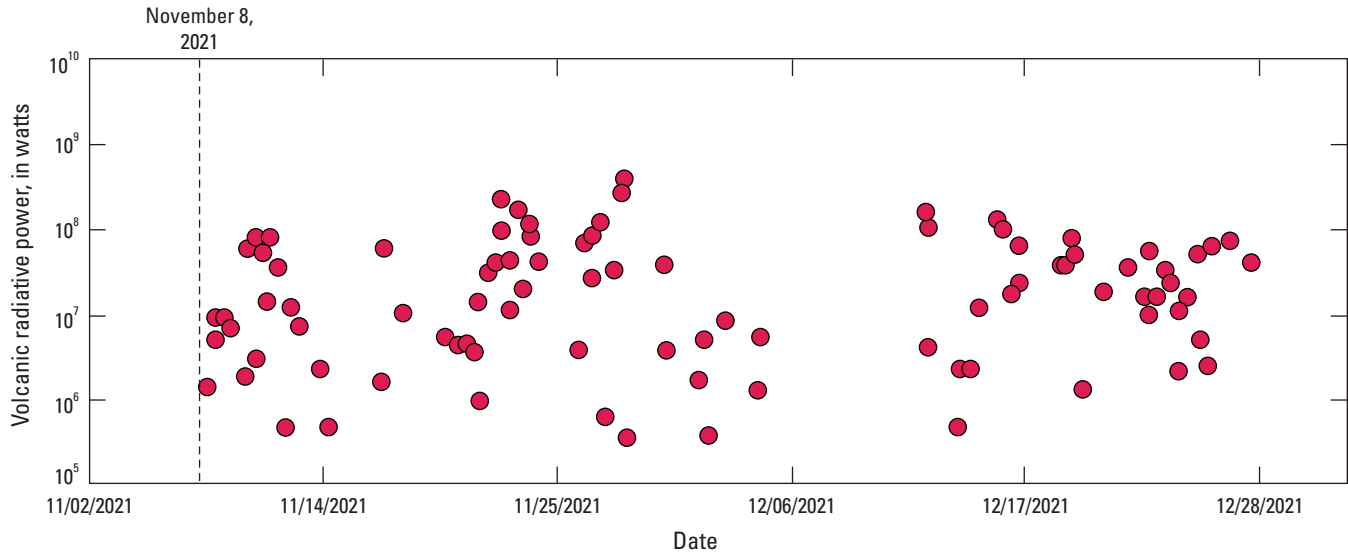
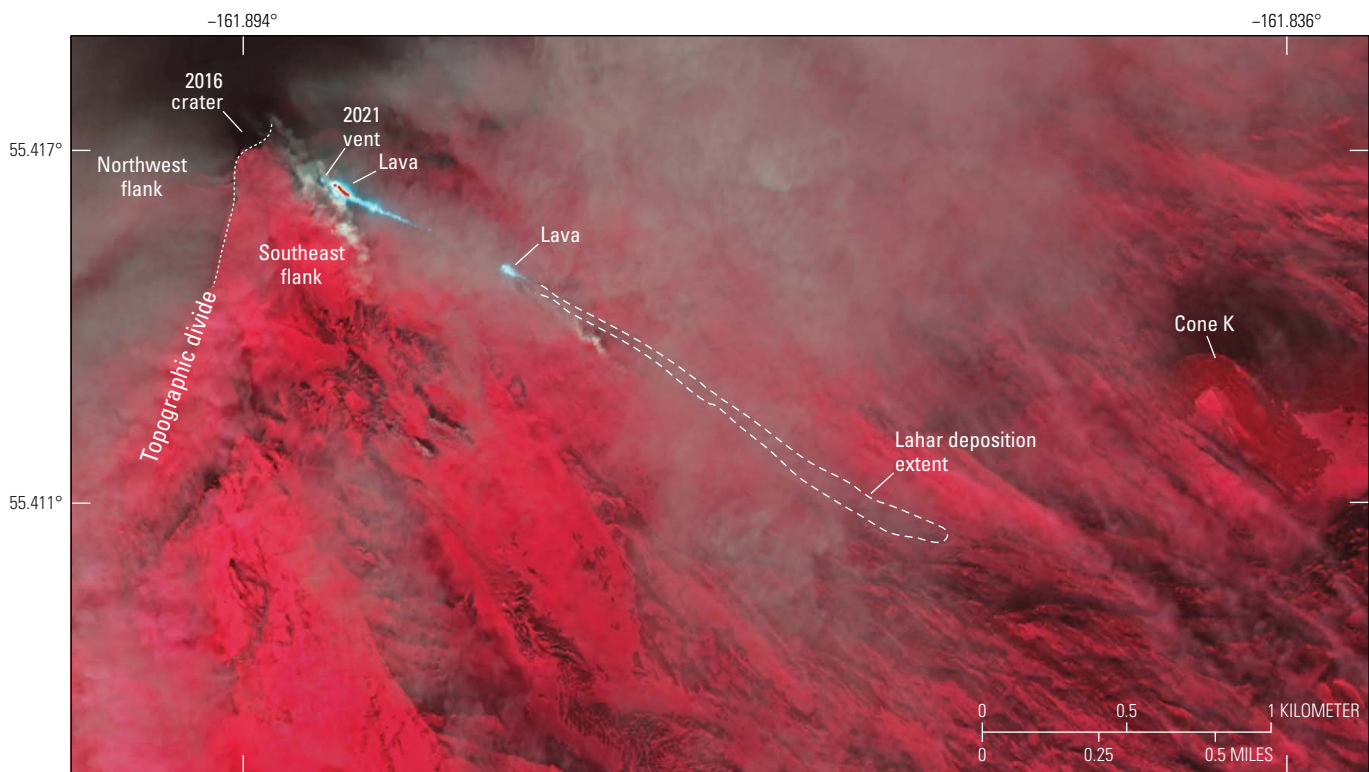


Figure 26. Time-series plot of volcanic radiative power versus time for the period of 2021 when satellite detections of elevated surface temperatures indicated lava at the surface of Pavlof Volcano, Alaska. Lava effusion began on November 8, 2021. Data from University of Turin and University of Florence (2022), derived from Sentinel-2 thermal imagery (Massimetti and others, 2020). Dates shown as month/day/year.



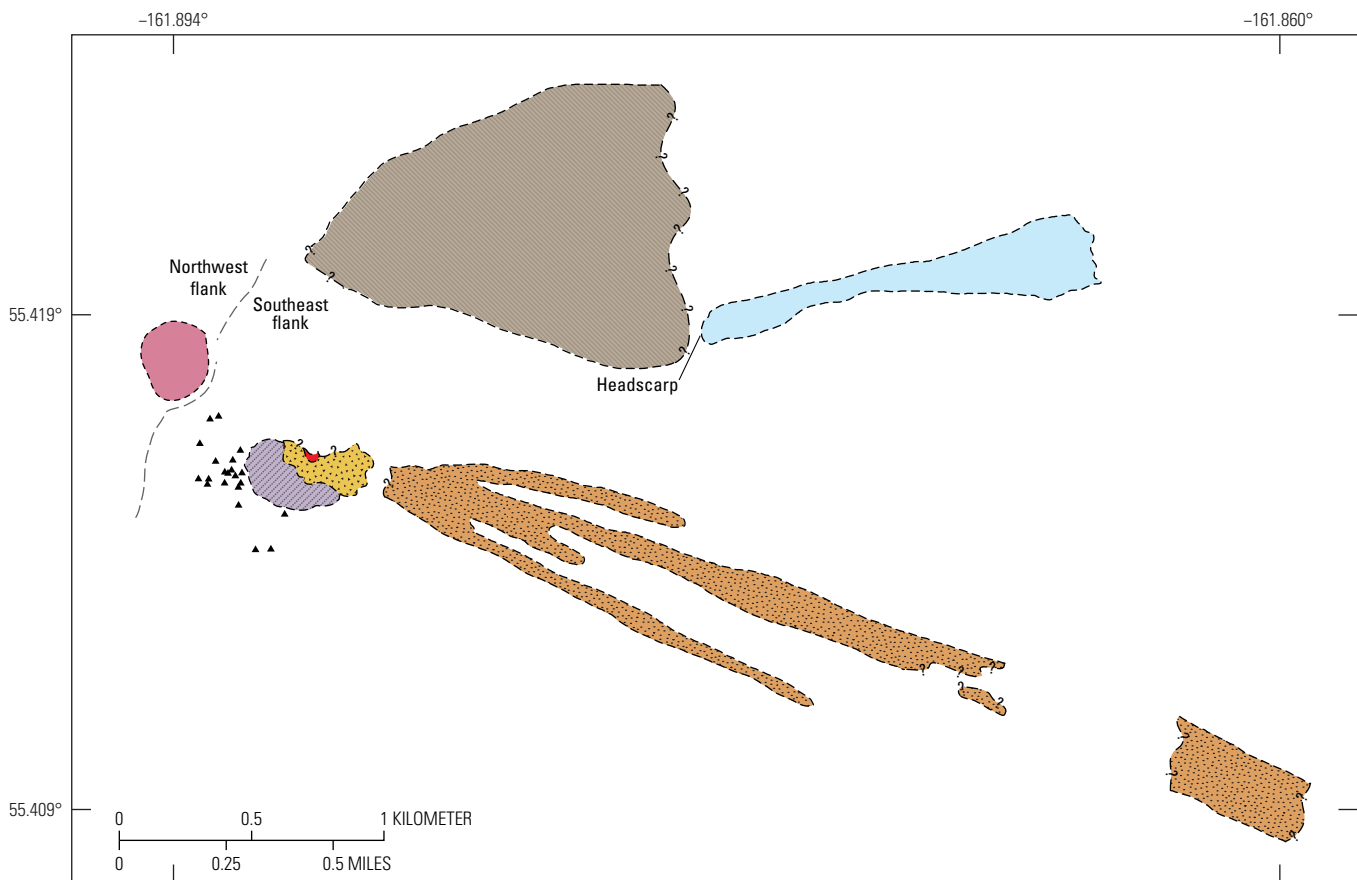
Base image from DigitalGlobe
NextView License, copyright 2021

Figure 27. Annotated short-wave infrared satellite image of features and deposits observed at Pavlof Volcano, Alaska, in November 2021. Lava flows render as bright blue and red in contrast to the magenta color of the surrounding snow-covered landscape. Image acquired by WorldView-3, November 11, 2021

historical eruptions of Pavlof Volcano have been characterized by lava fountaining or jetting that result in the accumulation of spatter around the vent. Occasionally, these growing spatter piles become unstable and collapse, forming hot particulate flows that are capable of eroding and melting glacier ice and snow on the volcano. The formation of meltwater by this process is a primary mechanism for lahar generation at Pavlof Volcano (Waythomas and others, 2017). The eruptive activity in early November may have been characterized by such periods of lava fountaining, spatter accumulation, and the extrusion of hot, granular flows that produced the lahar deposits observed in satellite imagery (fig. 27). A Sentinel-2

short-wave infrared (SWIR) image from November 12 showed a circular area of hot material around the active vent, consistent with the notion that spatter accumulation had been occurring. However, none of the webcam views or occasional pilot reports from November and December confirmed incandescence or lava fountaining at the south flank vent.

On November 17, satellite observations indicated both the presence of ballistic clasts around the vent (some located as far as 2.5 km away) and continued lahar development that was likely associated with ongoing lava-ice-snow interaction. The ballistic clasts were ejected during energetic explosions that were recorded in seismic and infrasound data during the



Base from Digital Globe, WorldView-3 satellite image acquired December 1, 2021

EXPLANATION

- 2016 Crater
- Trace ash-fall deposits
- Snow-avalanche deposits
- 2021 vent
- Spatter, ash, and debris deposits
- Diffuse field of small ballistic particles
- Lahar deposits
- Approximate boundary
- Topographic divide
- Unknown or uncertain boundary
- Individual ballistic particle

Figure 28. Annotated map of features and deposits on the southeast flank of Pavlof Volcano, Alaska. Annotations drawn on WorldView-3 satellite image (not shown) acquired on December 1, 2021.

week of November 12–18. Minor explosions and small ash emissions took place occasionally during the last two weeks of November 2021, although the volcano was obscured by clouds for much of this period.

From late November through December, the Pavlof Volcano seismic network detected elevated seismicity consisting of episodic, sustained tremor periods and discrete low-frequency events. Many explosions were detected in seismic and infrasound data—these may have produced localized ballistic ejecta fallout around the active vent, as indicated by satellite data acquired on December 1, 2021 (fig. 28). On December 4, a webcam and a passing aircraft

recorded minor ash emissions that rose from the summit of the volcano to an altitude of ~10,000 ft (~3,000 m) ASL. Satellite data from this period also commonly indicated moderately to strongly elevated surface temperatures. High-resolution satellite imagery collected during clear weather commonly showed lava effusion on the upper southeast flank of the volcano, as well as continued interaction with snow and ice that subsequently produced small lahars downslope from the lava flows. For instance, satellite images obtained on December 19, 2021, showed both an ~600-m-long lava flow and minor lahar deposits that extended ~1,300 m beyond the flow front (fig. 29).

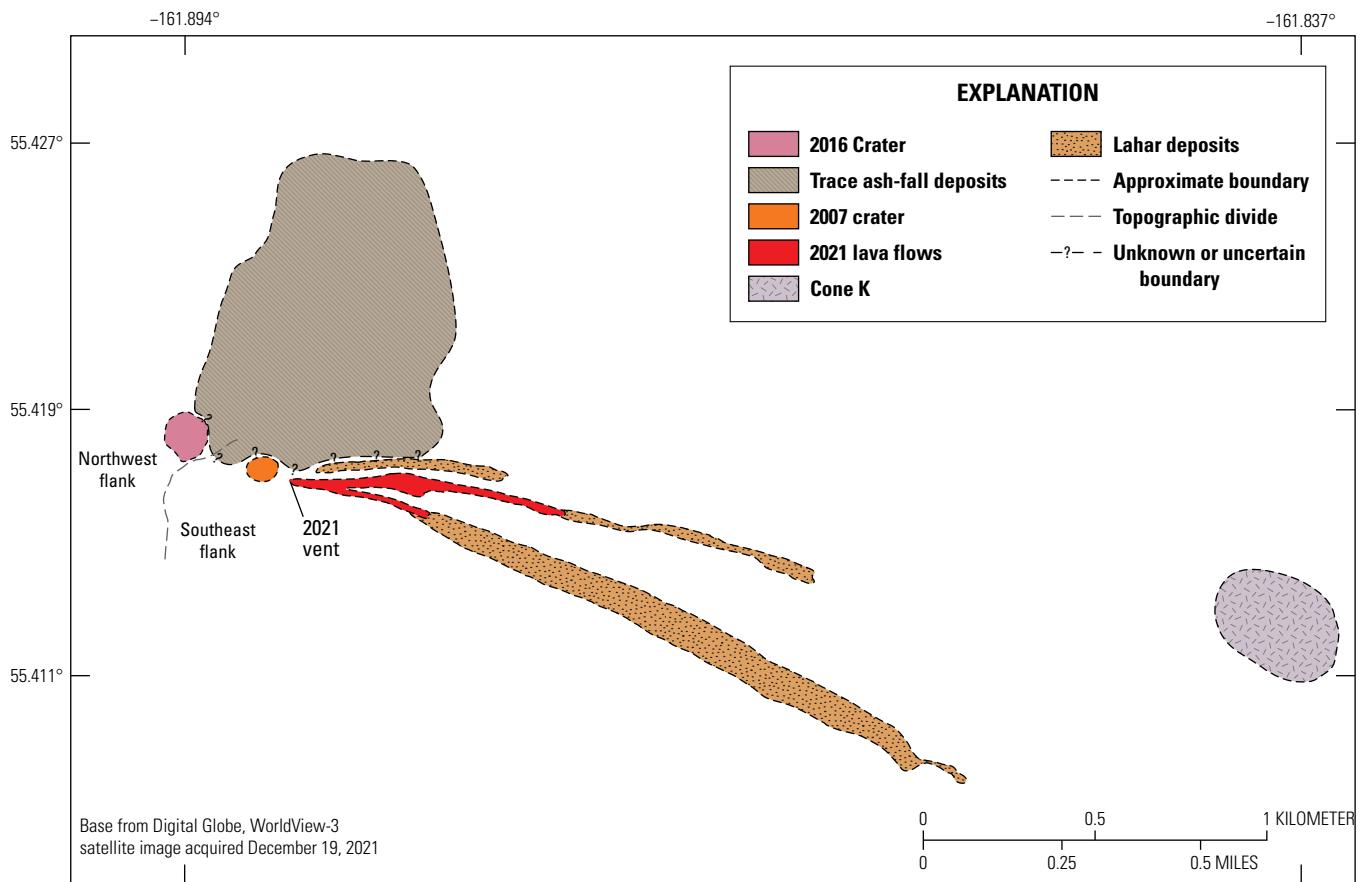


Figure 29. Annotated map of features and deposits on the southeast flank of Pavlof Volcano, Alaska. Annotations drawn on WorldView-3 satellite image (not shown) acquired on December 19, 2021.

Mount Okmok

GVP# 311290

53.419°, -168.132°

1,088 m

Umnak Island, Fox Islands, Aleutian Islands



CONTINUED LONG-TERM INFLATION

Mount Okmok, a volcano defined primarily by a 10-km-wide caldera that contains intracaldera cones and lava flows, occupies most of the east end of Umnak Island in the eastern Aleutian Islands (fig. 30). The volcano is ~115 km southwest of the City of Unalaska and ~1,400 km southwest of Anchorage (fig. 1). Mount Okmok is built on a base of Tertiary volcanic rocks and consists of three rock series: (1) older flows and pyroclastic beds of a pre-caldera shield complex, (2) pyroclastic deposits of two major caldera-forming eruptions, and (3) a post-caldera field of small, young cones and lava flows (Byers, 1959; Larsen and others, 2007). Mount Okmok has had 14 historical eruptions, which produced ash plumes that reached altitudes as high as ~49,000 ft (~15,000 m) ASL. Lava flows were emplaced on the caldera floor during only three eruptions in the last 70 years: those in 1945, 1958, and 1997 (Begét and others, 2005). The most recent eruption took place during the summer of 2008 and was phreatomagmatic, building a new intracaldera cone informally named Ahmanilix

(fig. 30) (Neal and others, 2011). Thermal springs and fumaroles occur within the caldera and at Hot Springs Cove, located between Mount Okmok and Mount Recheshnoi (20 km to the southwest).

In 2021, Mount Okmok continued the long-term deformation trend that began immediately after its 2008 eruption. This deformation takes place as discrete inflationary pulses superimposed onto a lower-rate, steady background inflation (fig. 31) and is consistent with ongoing accumulation of melt at shallow levels. One such pulse was recorded in 2021, appearing on the time-series plots for GNSS stations OKCE (fig. 32), OKNC, and OKSO. The total displacements of the 2021 pulse were similar to the totals of 2019 but larger than those of 2020 (see, for instance, the OKCE time series in figure 31), with amplitudes of 4–5 cm in the horizontal and ~5 cm in the vertical components. This inflation is roughly half that of 2018, when the volcano underwent ~10 cm of horizontal displacement and as many as 12 cm of vertical displacement (Cameron and others, 2023).

From roughly the beginning of October through November 2021, Mount Okmok departed from its common deformation pattern by producing an additional inflationary pulse, prompting AVO to release an Information Statement. This pulse, which was observed at stations OKCE and OKNC (fig. 31), was consistent with a pressure increase at less than 1 km depth that had a source located near Cone D, south of Ahmanilix. Past analyses of GNSS and InSAR geodetic data suggest a shallow magma reservoir exists underneath the caldera floor of Mount Okmok (for example, Freymueller and Kaufman, 2010; Lu and Dzurisin, 2014).

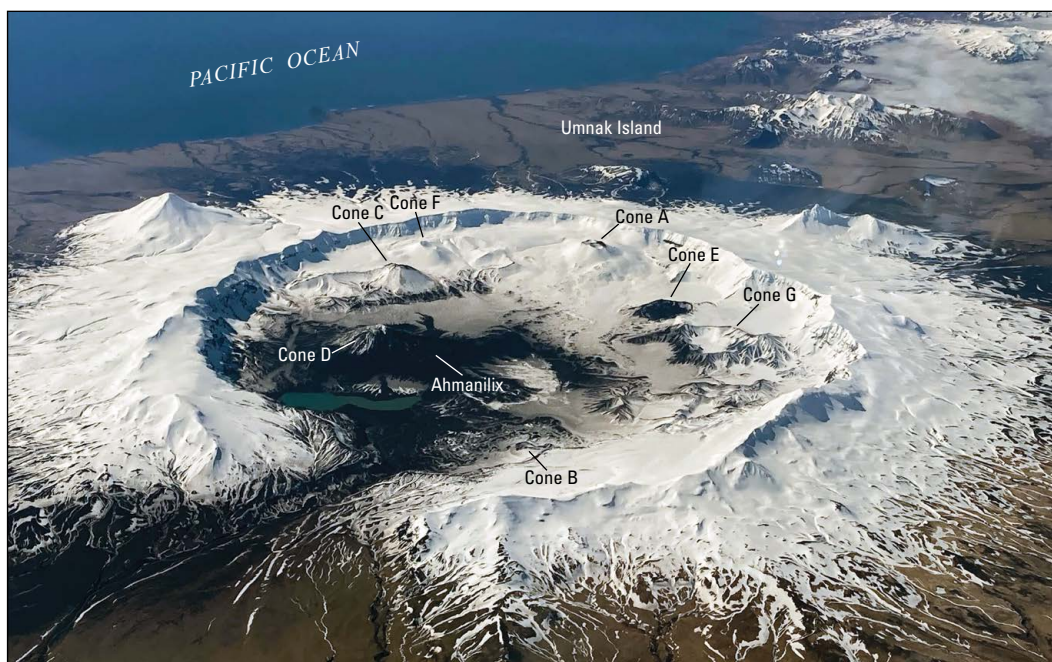


Figure 30. Oblique aerial photograph of Mount Okmok on April 28, 2021, looking southwest. Copyrighted by B. Mees, (2021); used with permission.

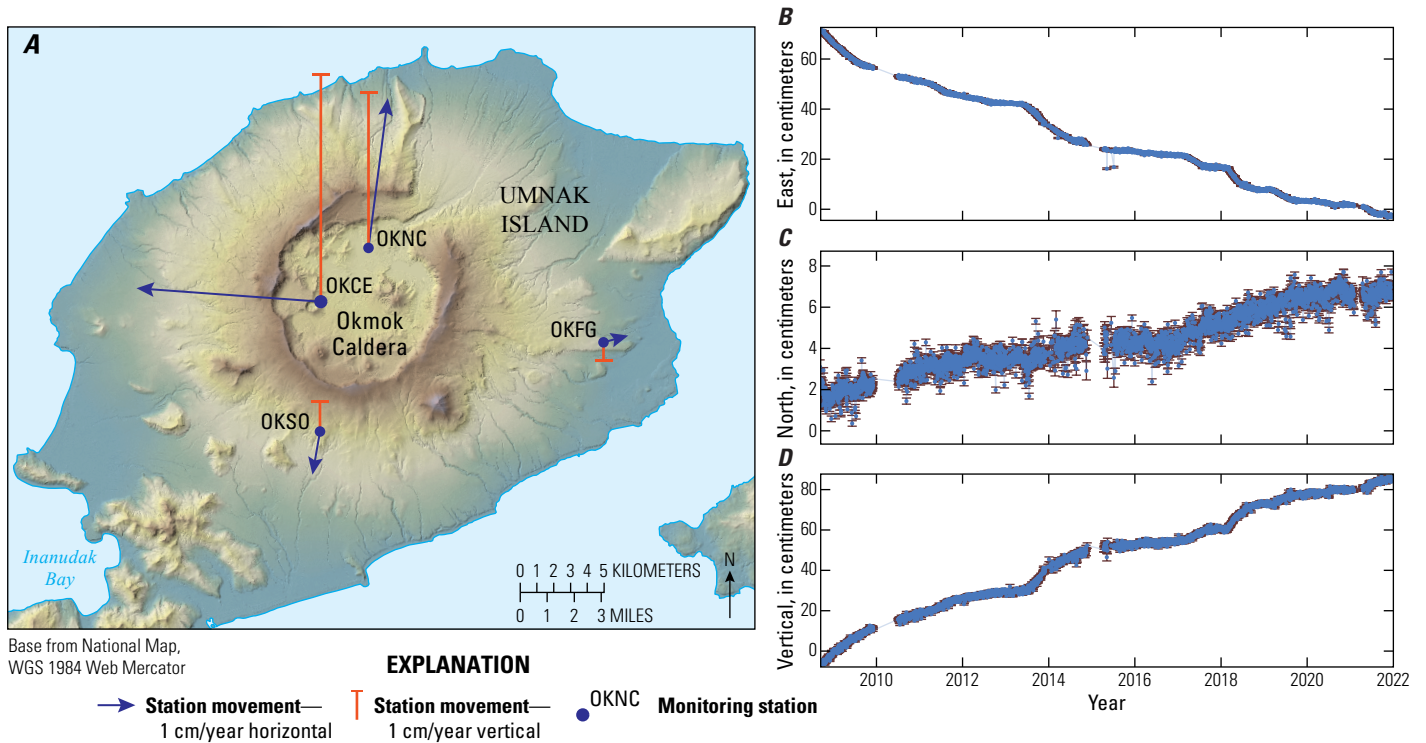


Figure 31. Global Positioning System velocity map (A) and displacement time series with 68 percent confidence levels showing movement of monitoring station OKCE (B–D) from September 2008 through December 2021 at Mount Okmok, Alaska. The map vectors, which show velocity relative to station AV09 (near Dutch Harbor, Alaska), indicate radial outward and upward deformation consistent with long-term inflation. The time-series plots show eastward, northward, and vertical motion relative to station AV09. Inflation at the volcano occurs in steps modulated onto a long-term inflation trend.

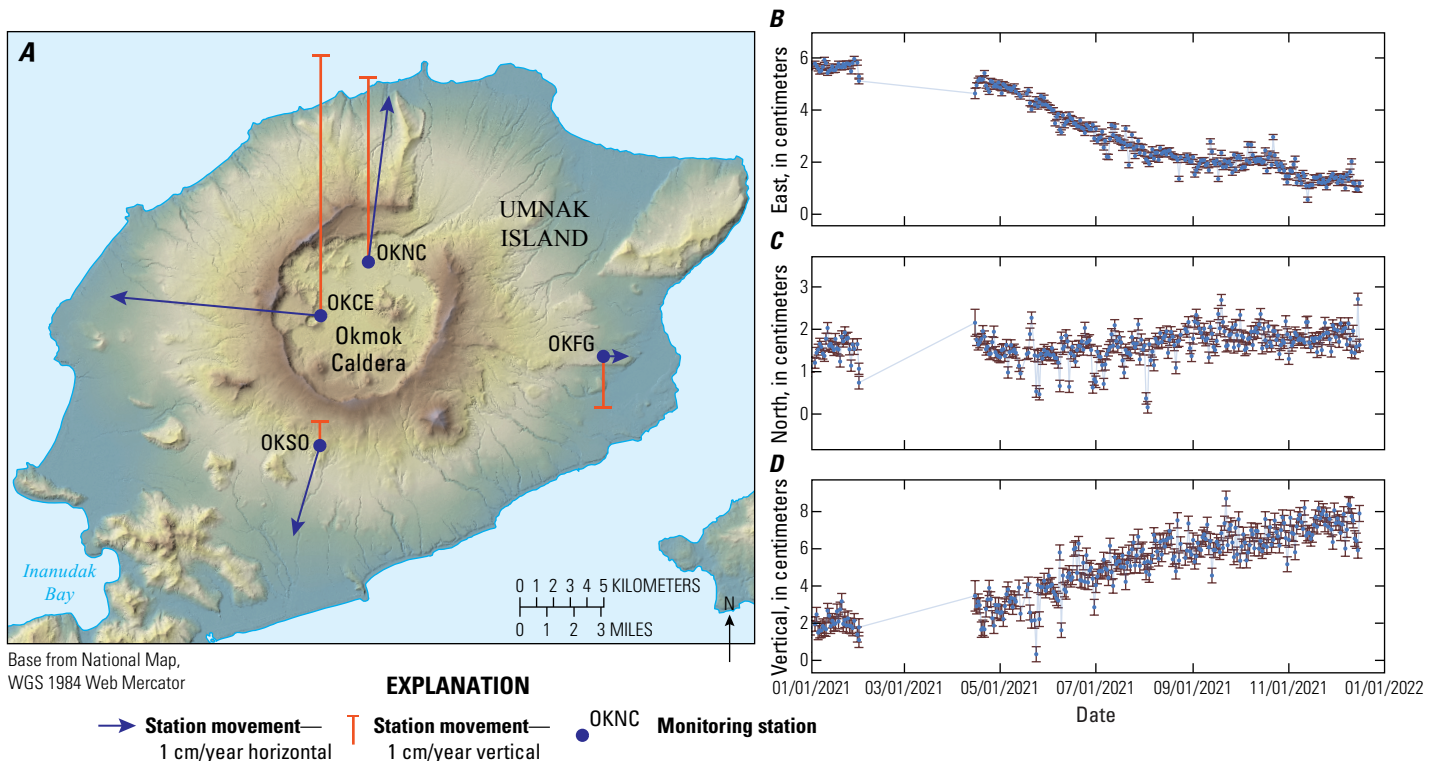


Figure 32. Global Positioning System velocity map (A) and displacement time series with 68 percent confidence levels showing movement of monitoring station OKCE (B–D) from January through December 2021 at Mount Okmok, Alaska. A, Shaded relief map of Mount Okmok showing deformation velocities (red: vertical, black: horizontal) for the period January 1–December 31, 2021. The time-series plots show eastward (B), northward (C), and vertical (D) motion at station OKCE relative to AV09 near Dutch Harbor over the same period. Dates shown as month/day/year.

Mount Cleveland

GVP# 311240
 52.822°, -169.945°
 1,745 m
 Chuginadak Island, Islands of Four Mountains, Aleutian Islands

ELEVATED SURFACE TEMPERATURES AND GAS EMISSIONS



not warrant a **GREEN/NORMAL** status. On March 10, however, an earthquake large enough to be detected 100 km away on Umnak Island took place near Mount Cleveland. This earthquake, combined with the detection of weak thermal anomalies and SO₂ emissions (figs. 34, 35) starting the following week, suggested an increased potential for an eruption. In response, AVO raised the Aviation Color Code and

Mount Cleveland forms the west side of the uninhabited Chuginadak Island, part of the Islands of Four Mountains group in the east-central Aleutian Islands (figs. 1, 33). Mount Cleveland is ~75 km west of the community of Nikolski and ~1,525 km southwest of Anchorage. Its historical eruptions have been characterized by short-lived ash explosions, lava fountaining, lava flows, and pyroclastic flows. In February 2001, after 6 years of quiescence, Mount Cleveland had three explosive events that sent ash to altitudes as high as ~30,000 ft (~9,100 m) ASL, produced a pyroclastic flow that reached the ocean, and erupted a lava flow (Dean and others, 2004; McGimsey and others, 2005). Intermittent explosive eruptions took place every year from 2001 to 2020.

Early 2021 was quiet at Mount Cleveland, so the volcano remained at **UNASSIGNED**—the monitoring network was insufficient to locate earthquakes, so the volcano did



Figure 33. Sentinel-2 satellite image of Mount Cleveland, within the Islands of Four Mountains group, which also includes Carlisle volcano, Herbert volcano, and Tanaʻ Angunaʻ volcano. Blue dot indicates geophysical stations used to monitor activity at Mount Cleveland. Image acquired on August 23, 2020.

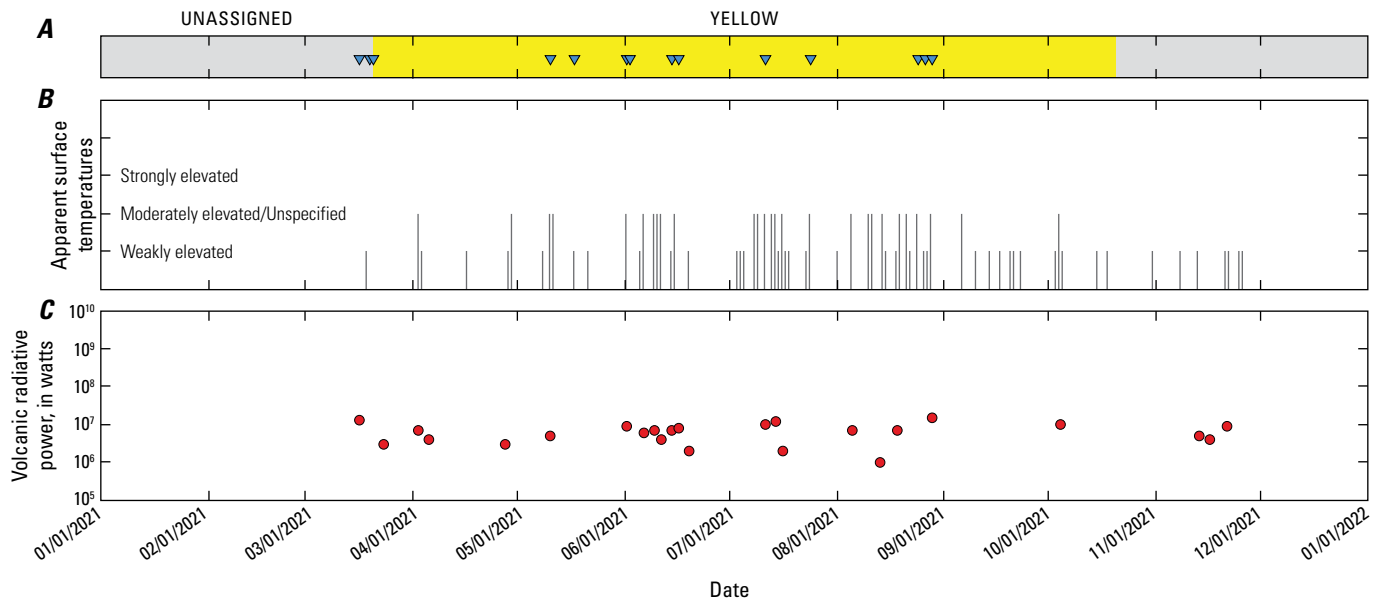


Figure 34. Time-series plots and graph of activity at Mount Cleveland, Alaska, in 2021. *A*, Time-series plot showing timing of Aviation Color Code changes and sulfur dioxide detections (triangles). *B*, Time-series plot of elevated surface temperature observations. Black bars indicate thermal anomaly detections and their subjective strength as recorded in the Alaska Volcano Observatory internal remote-sensing database. *C*, Graph of volcanic radiative power at the volcano. Data from University of Turin and University of Florence (2022), derived from Sentinel-2 thermal imagery (Massimetti and others, 2020). Dates shown as month/day/year.

Volcano Alert Level to **YELLOW** and **ADVISORY** (fig. 34) on March 20. Soon afterward (March 26), an earthquake of local magnitude (M_L) 4.3 took place near Mount Cleveland.

High-resolution synthetic aperture radar (SAR) data spanning March 9 to March 20 recorded slight subsidence within the crater, which seemed to correlate with the appearance of elevated surface temperatures and gas emissions there. The crater was previously floored by cold rubble, so subsidence above the conduit may have formed openings that allowed heat and gases to escape more readily. Near-infrared temperatures in the crater rose above 600 °C, indicating magma near the surface.

Detections of thermal anomalies, SO₂ emissions, a summit plume, and crater floor subsidence continued with little change over the next several months (fig. 34). However, by late summer, signs of unrest had declined: the volcano had quieted seismically, subsidence had ceased, gas emissions were no longer being detected, and thermal anomalies had declined in both strength and frequency. In response to this dwindling activity, AVO changed the Aviation Color Code and Volcano Alert Level to **UNASSIGNED** on October 20. Detections of elevated surface temperatures continued occasionally through the end of the year, but activity at the volcano overall remained low.

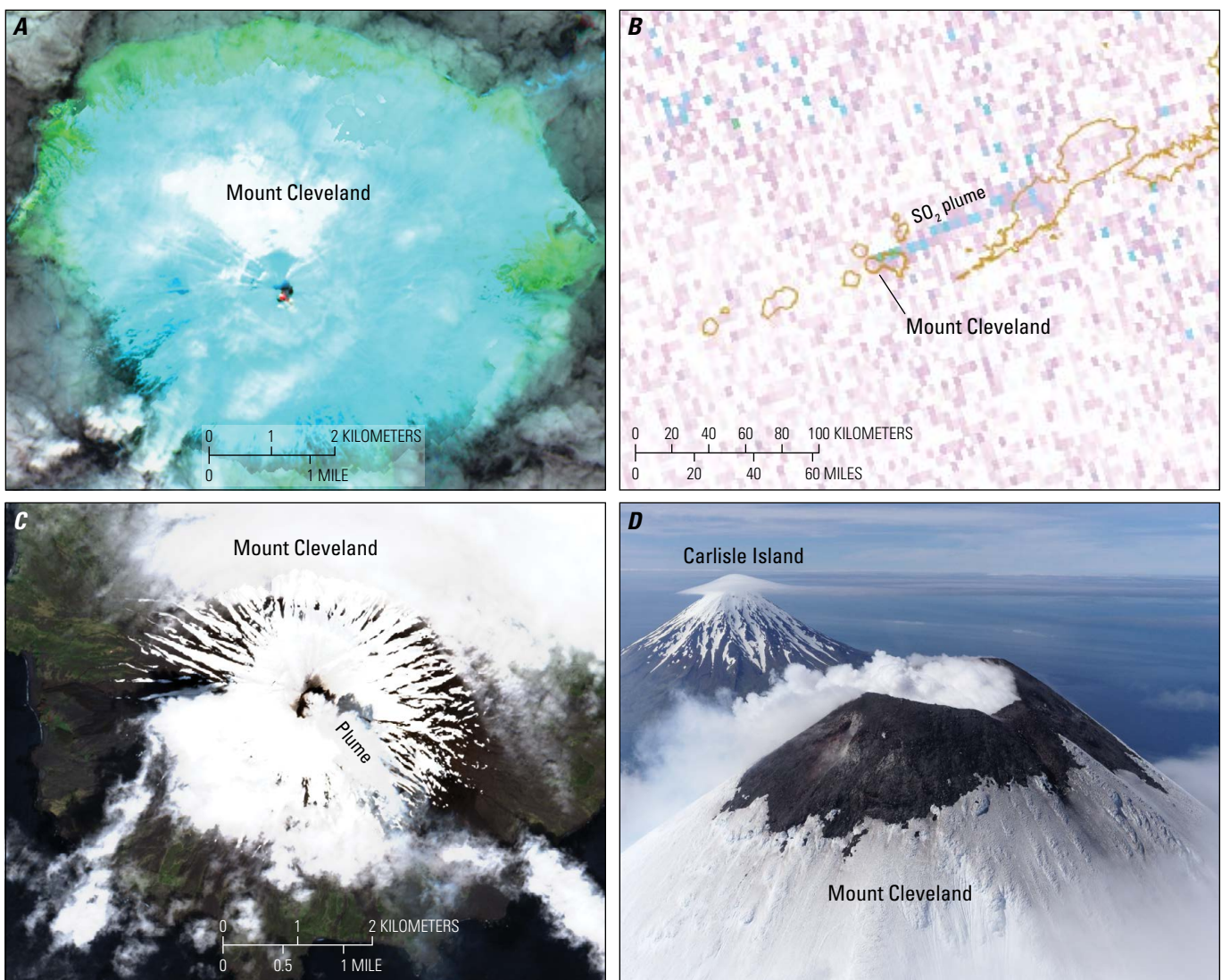



Figure 35. Satellite and oblique aerial images of Mount Cleveland, Alaska, in 2021. *A*, Sentinel-2 satellite image from March 16, 2021, showing a short-wave infrared anomaly at the summit. *B*, TROPospheric Monitoring Instrument satellite image from March 19, 2021, showing a sulfur dioxide (SO₂) plume drifting east-northeastward from Mount Cleveland. *C*, Sentinel-2 satellite image of Mount Cleveland from June 16, 2021, showing a summit plume. *D*, Oblique aerial photograph of Mount Cleveland from June 18, 2021, showing a summit plume. Photograph *D* by M. Herstand, Alaska Division of Geological & Geophysical Surveys.

Atka Volcanic Complex



GVP# 311160
 (Mount Kliuchef)
 52.331°, -174.139°
 1,463 m
 Atka Island, Andreanof Islands, Aleutian Islands

GVP# 311161 (Korovin Volcano)
 52.379°, -174.155°
 1,546 m
 Atka Island, Andreanof Islands, Aleutian Islands

EARTHQUAKE SWARM

Atka volcanic complex, which forms the northern part of Atka Island, lies ~15 km north of the City of Atka and ~1,760 km southwest of Anchorage (fig. 1). The complex consists of several peaks, which are the remnants of Pleistocene volcanoes, and several cones that have been active in the Holocene, including Mount Kliuchef and Korovin Volcano (fig. 36). Mount Kliuchef is composed of a series of five vents aligned northeast-southwest. Its two main summit vents appear young—the eastmost was probably the source of an eruption in 1812 attributed to nearby Sarichef Volcano

(Wood and Kienle, 1990). Korovin Volcano, ~6 km north of Mount Kliuchef, is a compound stratovolcano with two summit craters spaced 600 m apart (Miller and others, 1998). The southeast crater, which is the most recently active of the two, is ~1 km wide at the rim, several hundred meters deep, and holds a small lake.

Beginning on August 10, 2021, AVO detected a swarm of earthquakes at Atka volcanic complex that lasted several days before tapering off (fig. 37). In response to this local seismicity, AVO raised the Aviation Color Code and Volcano Alert Level to **YELLOW** and **ADVISORY** on August 11.

AVO analysts located 204 earthquakes between August 10 and 12; these events had epicenters approximately 3–9 km west-southwest of Mount Kliuchef (fig. 36) and typical depths of 2–5 km below sea level. The largest earthquake took place on August 11 and had an M_L of 2.5. Five other earthquakes exceeded M_L 2.0. The rate of earthquakes began to decline after August 12 and returned to background levels by the end of the month. In response, AVO changed the Aviation Color Code and Volcano Alert Level of Atka volcanic complex to **GREEN** and **NORMAL** on August 27. Satellite imagery and infrasound sensors detected no anomalous activity or unrest around the time of the earthquake swarm, in contrast with observations from October 2020, when satellite data showed detectable SO_2 emissions from the volcano in close conjunction with an increase in earthquake activity (Cameron and others, 2023).

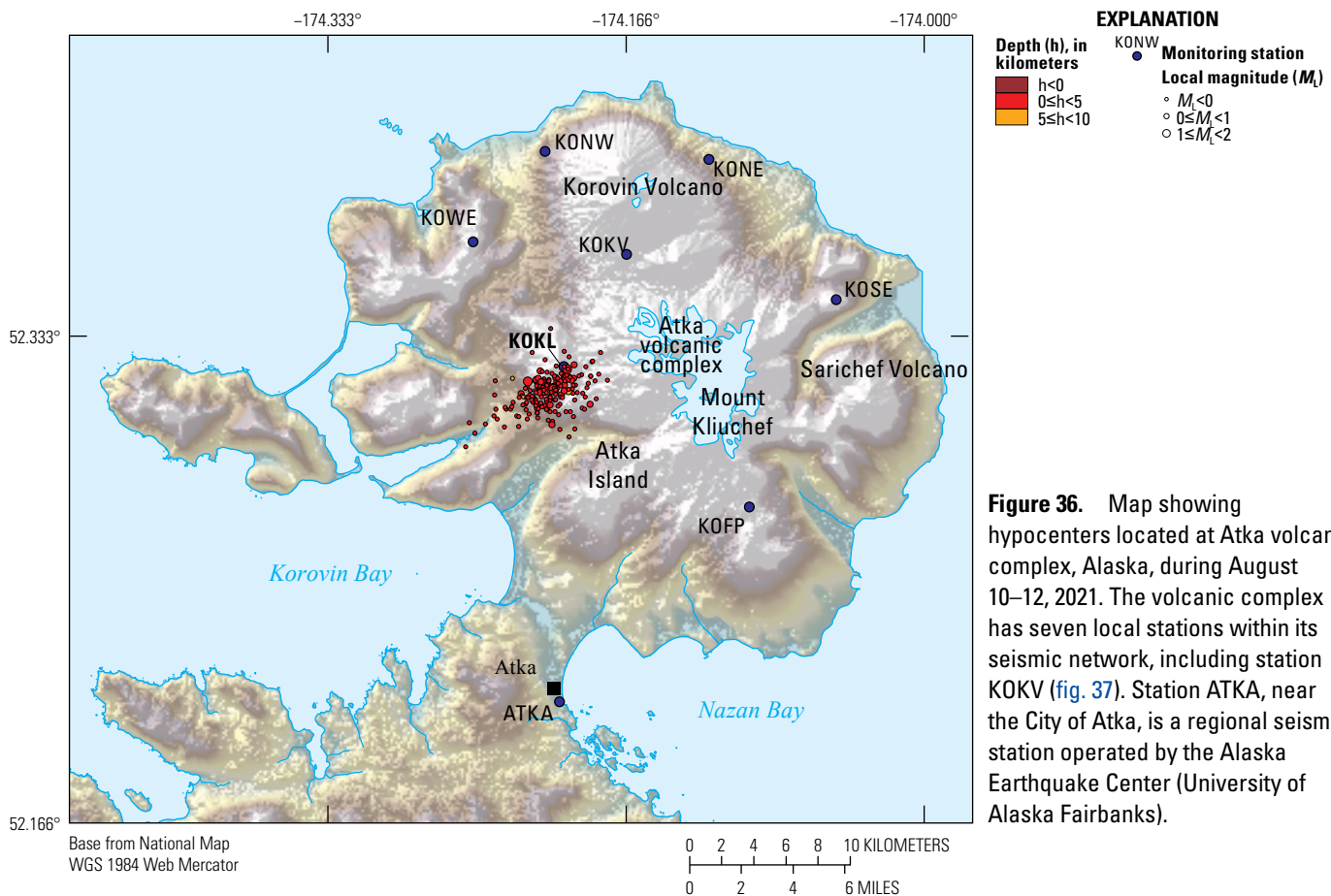


Figure 36. Map showing hypocenters located at Atka volcanic complex, Alaska, during August 10–12, 2021. The volcanic complex has seven local stations within its seismic network, including station KOKV (fig. 37). Station ATKA, near the City of Atka, is a regional seismic station operated by the Alaska Earthquake Center (University of Alaska Fairbanks).

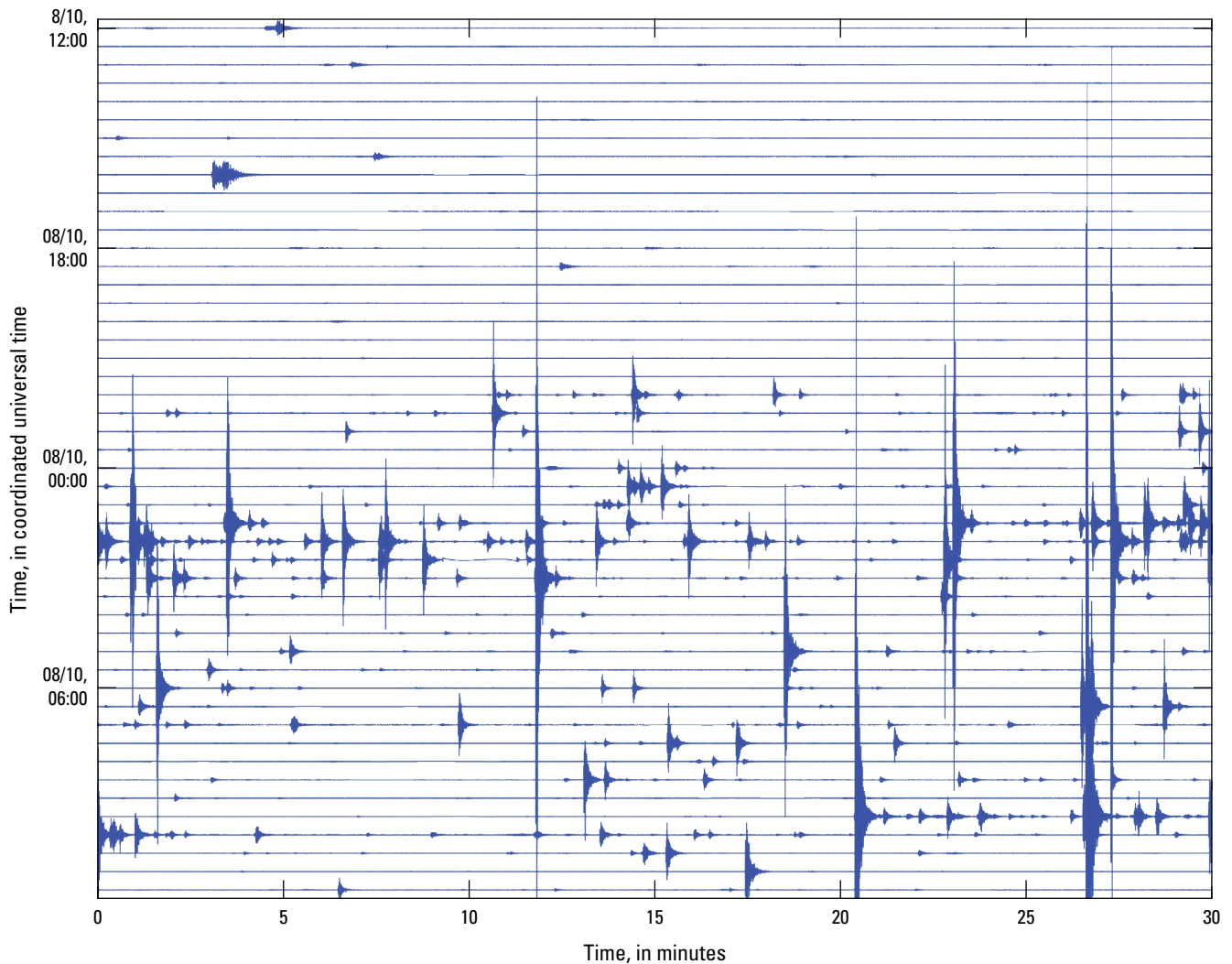



Figure 37. Helicorder plot of seismic data from station KOKV (fig. 36) during August 10–11, 2021 (coordinated universal time), showing an earthquake swarm beneath Atka volcanic complex, Alaska. Dates shown as month/day.

Great Sitkin Volcano

ALASKA



GVP# 311120
 52.077°, -176.111°
 1,743 m
 Great Sitkin Island, Andreanof Islands, Aleutian Islands

EXPLOSIVE ERUPTION AND LAVA FLOW

Great Sitkin Volcano (fig. 38) is a basaltic andesite volcano that composes most of the northern half of Great Sitkin Island, part of the Andreanof Islands group of the central Aleutian Islands. The volcano, which is ~40 km northeast of the City of Adak, Alaska, and ~1,900 km southwest of Anchorage (fig. 1), consists of an older, partly collapsed volcano and a younger resurgent cone with a summit

crater 1.5 km in diameter (fig. 39) (Simons and Mathewson, 1955; Waythomas and others, 2003a). The volcano has erupted several times in the last 250 years (Waythomas and others, 2003b); its most recent eruption prior to 2021 was in 1974, when a steep-sided lava dome formed in the crater and produced at least one ash cloud, which was reported to have reached an estimated altitude of 10,000 ft (~3,000 m) ASL (Associated Press, 1974). A poorly documented eruption in 1945 also formed a lava dome, which was then partially destroyed by the 1974 eruption. Great Sitkin Volcano erupted in 2021 after a period of seismic unrest and minor steam explosions that began in 2016 (for example, Dixon and others, 2020).

Leading up to 2021, activity at Great Sitkin Volcano was characterized by years of precursory seismicity, elevated surface temperatures, and gas emissions. This unrest culminated with a Vulcanian explosion on May 25, 2021, an event successfully forecasted by AVO in the hours prior. An effusive eruption then began in mid-July, gradually filling both

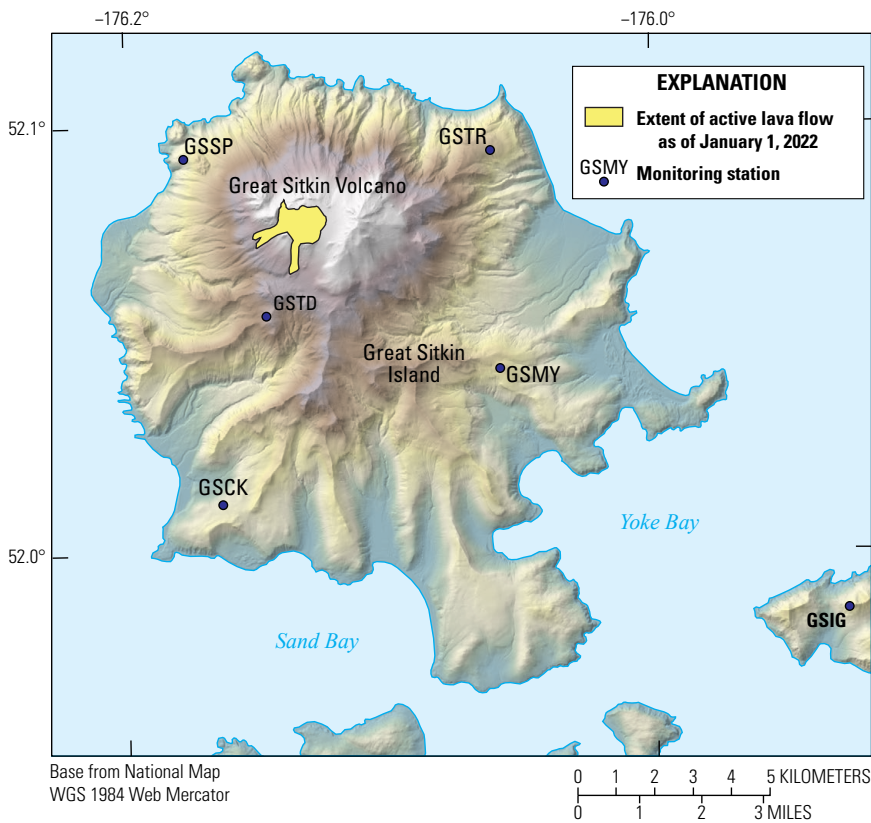


Figure 38. Map showing the extent of active lava flow on Great Sitkin Island, Alaska, as of January 1, 2022.

the 2021 explosion crater and much of the summit crater with lava, which then spilled down the volcano’s flanks. Lava effusion persisted at the volcano throughout the rest of the year. The 2021 eruption followed the pattern of the 1974 eruption: an explosive event followed by lava effusion in the summit crater. AVO crews visited the volcano in June 2021 to sample the explosive eruption deposits and to carry out a gas and airborne imaging survey.

2016–2021 Precursory Unrest

Volcanic unrest began at Great Sitkin Volcano in July 2016 and was characterized by elevated seismicity, anomalous steam emissions from the summit crater, and a few small explosive events. The thousands of small earthquakes detected between 2016 and 2021 were located primarily in the shallow crust (between the surface and ~10 km depth) and had M_L values of less than 3 (for example, Dixon and others, 2020). The elevated seismicity at Great Sitkin Volcano began waning in early 2020 and had declined to background levels before the end of that year, leading AVO to lower the Aviation Color Code and Volcano Alert Level to **GREEN** and **NORMAL** on October 21, 2020.

In January 2021, AVO observed a slight elevation of surface temperatures within the summit crater (fig. 40). More signs of activity began appearing

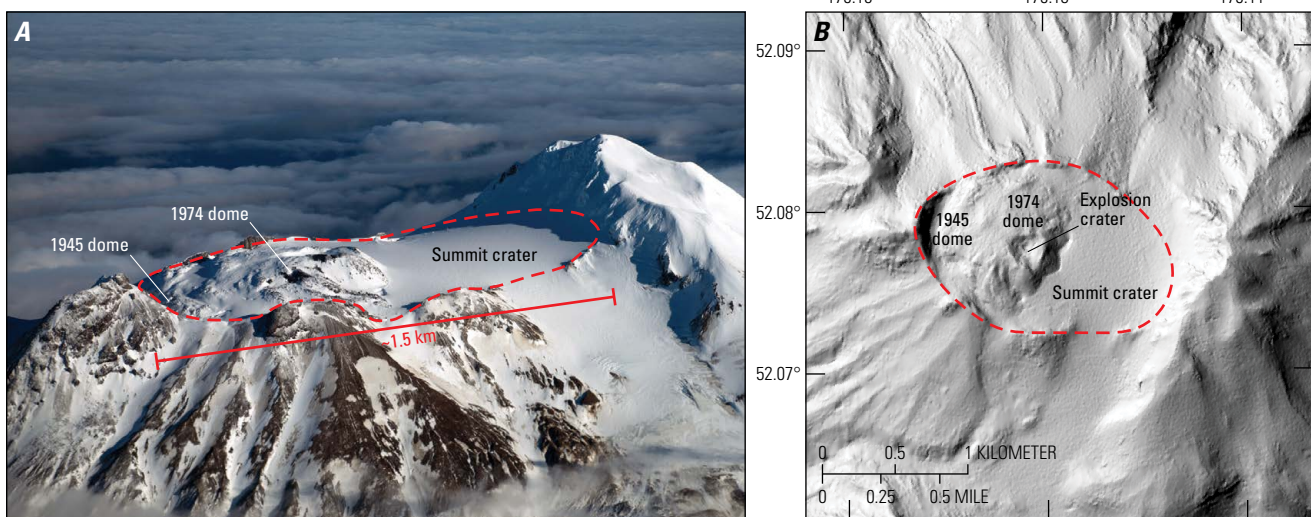


Figure 39. Photograph and Interferometric Synthetic Aperture Radar (InSAR) image of the summit of Great Sitkin Volcano, Alaska. *A*, Oblique aerial photograph of Great Sitkin Volcano in November 2012, looking north, showing the upper edifice, summit crater, and lava domes from 1945 and 1974. Copyrighted by R. Clifford, (2012); used with permission. *B*, Interferometric Synthetic Aperture Radar (InSAR) shaded relief image of the summit crater region in 2019. Dashed lines denote the margins of the summit crater. ~, approximately; km, kilometer.

that spring: earthquakes were recorded at an increasing frequency, satellite observations increasingly showed weakly to moderately elevated surface temperatures, and TROPOMI

sensors began detecting SO₂ emissions. This increasing unrest led AVO to raise the Aviation Color Code and Volcano Alert Level to **YELLOW** and **ADVISORY** on May 12.

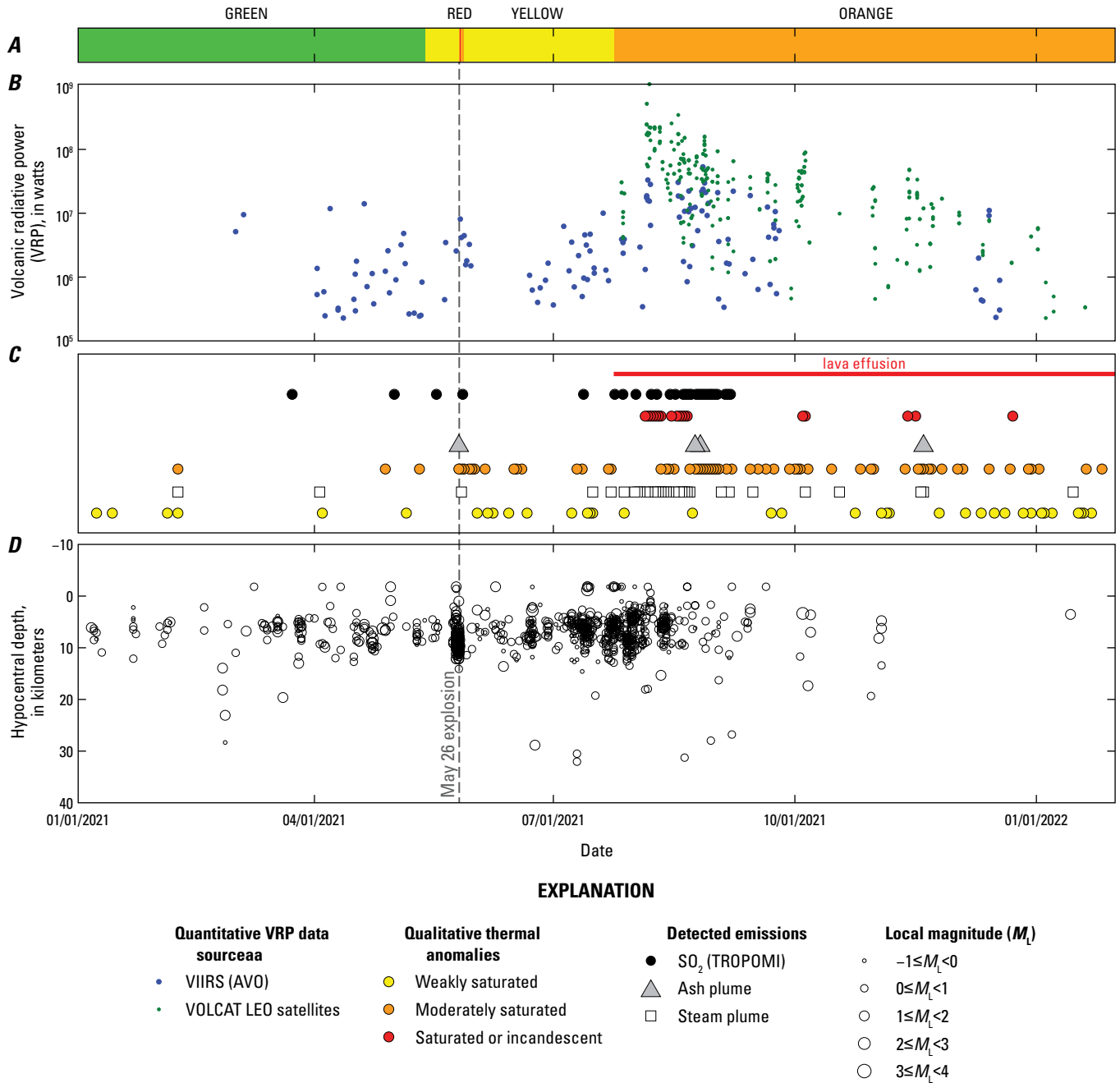


Figure 40. Chronology of the volcanic unrest and eruption at Great Sitkin Volcano, Alaska, in 2021. *A*, Timeline of changes to the Aviation Color Code at Great Sitkin Volcano. *B*, Time-series plot of thermal emissions at Great Sitkin Volcano, as shown in Visible Infrared Imaging Radiometer Suite (VIIRS) imagery (Loewen and others, 2021) and in other low Earth orbit (LEO) satellites through the experimental VOLcanic Cloud Analysis Toolkit (VOLCAT) system of the National Oceanic and Atmospheric Administration and the Cooperative Institute for Meteorological Satellite Studies (Pavolonis and others, 2018; Poland and others, 2020). *C*, Timeline showing elevated surface temperatures and reports of volcanic gas (sulfur dioxide [SO₂]), steam, and ash emissions. SO₂ detections are from the TROPospheric Monitoring Instrument (TROPOMI). *D*, Time-series plot of earthquake magnitudes and depths. The dashed line in *A–D* marks May 26, the date of the explosion (in coordinated universal time). AVO, Alaska Volcano Observatory; volcanic radiative power, VRP.

May 25 Explosion

An earthquake swarm began on May 24, and the earthquake rate steadily increased (fig. 41), which indicated an increased potential for eruptive activity. This led AVO to raise the Aviation Color Code and Volcano Alert Level to **ORANGE** and **WATCH** on May 25. Great Sitkin Volcano produced an explosion one hour and 39 minutes later, at 20:04 HADT on May 25 (05:04 UTC on May 26), sending an ash and gas plume northeastward at an elevation of ~15,000 ft (~4,600 m) ASL. The ~2-minute-long explosion was detected in seismic, infrasound, and satellite data, as well as by local

observers (fig. 42). The eruption and resulting ash cloud led AVO to raise the Aviation Color Code and Volcano Alert Level to **RED** and **WARNING** at 20:30 HADT on May 25 (05:30 UTC on May 26). After a decline in seismic activity and cessation of ash emissions, AVO lowered the Aviation Color Code and Volcano Alert Level to **ORANGE** and **WATCH** at 07:31 HADT (16:31 UTC) on May 26. A continued lack of eruptive activity accompanied by a decrease in seismicity, surface temperatures, and steam emissions led AVO to further reduce the Aviation Color Code and Volcano Alert Level to **YELLOW** and **ADVISORY** on May 27.

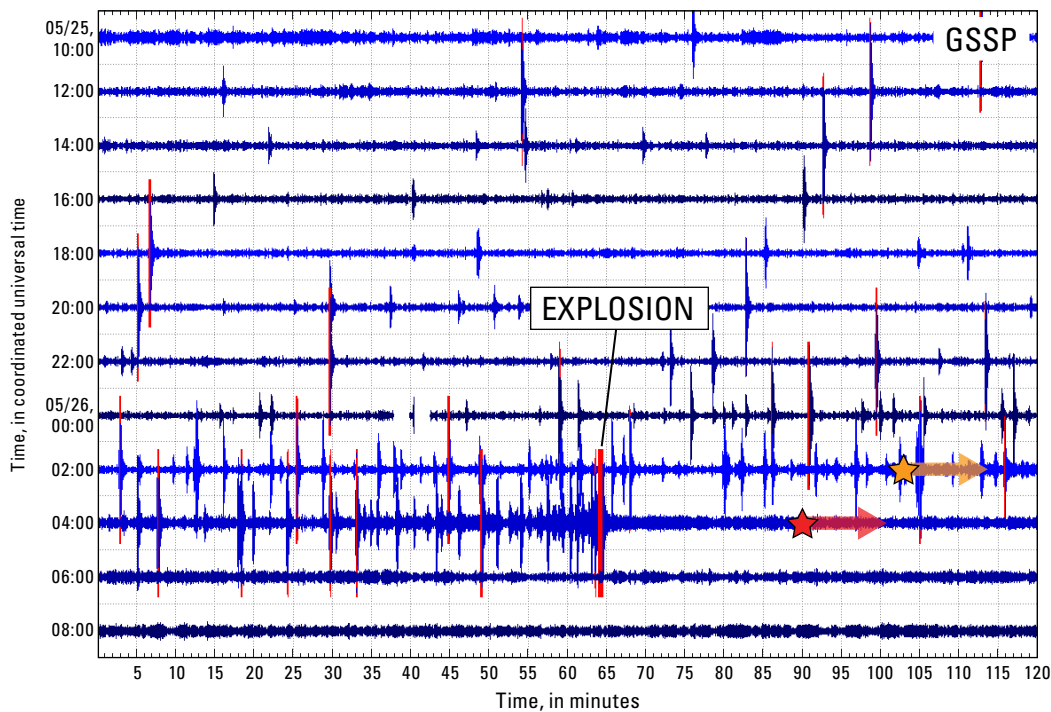


Figure 41. Helicorder plot (24-hour) of seismic data from station GSSP, on the west side of Great Sitkin Island, Alaska (fig. 38), showing the swarm of long-period events that immediately preceded a small explosion that took place on May 26, 2021, at 05:04 coordinated universal time (May 25 at 20:04 Hawaii-Aleutian daylight time). Orange and red stars with arrows indicate when the Aviation Color Code was elevated to **ORANGE** and **RED**.



Figure 42. Photographs of the May 25, 2021, explosion of Great Sitkin Volcano, Alaska, taken at 20:04 Hawaii-Aleutian daylight time (HADT) (05:04 coordinated universal time [UTC] on May 26) (A) and B, 20:06 HADT (05:06 UTC on May 26) (B) from aboard the passing research vessel Tiglax, operated by the U.S. Fish and Wildlife Service (USFWS). The volcano summit elevation is 1,740 meters for scale. View is to the south. Photographs by L. Flynn, USFWS.

Characterization of the May 25 Eruption

Analysis of geophysical, geological, and remote sensing data suggest that the May 25 explosion of Great Sitkin Volcano was a Vulcanian eruption. The event produced high-amplitude infrasound (~190 pascals at 6 km distance) and was preceded by a slow pressure rise (fig. 43), a phenomenon that

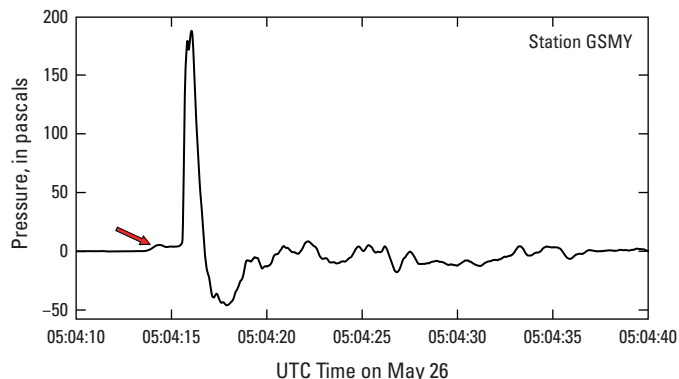


Figure 43. Time-series plot showing infrasound bracketing the explosion of Great Sitkin Volcano, Alaska, on May 25, 2021 (May 26 coordinated universal time[UTC]), as recorded at station GSMY. The signal consists of a slow rise in pressure (red arrow) before the main pressure pulse. This is consistent with dome distension prior to the explosion.

is consistent with other Vulcanian explosions and is caused by pre-explosion inflation of a dome or plug feature (for example, Yokoo and others, 2009; Iezzi and others, 2020). The explosion infrasound signal also showed two peaks in pressure that were likely related to a multi-part failure of the dome. After the main explosion, lower-amplitude infrasound emissions were recorded for tens of seconds. The explosion produced an ash cloud (fig. 42) that quickly detached and drifted northeastward before dispersing. The next day, TROPOMI data showed an SO₂ plume over the Bering Sea consistent with the eruptive cloud’s trajectory. The explosion also widened the pre-existing explosion crater in the 1974 dome (fig. 39B), blasting large blocks (wider than 2 m) of old, altered lavas into a radial ballistic field ~1.5 km in diameter (fig. 44). Some likely landed warm because they were found in deep melt pits (fig. 44B) when observed later by AVO geologists. Other eruptive deposits were a trace tephra deposit extending 5 km east-southeast, dark pyroclastic surge deposits ~1 km long, and a lahar that extended 2 km downslope to the south (fig. 44). Extending between the lahar starting point at the southeast crater rim and the vent within the crater was a 600-m-long, pyroclastic flow deposit made of large, altered blocks, some more than 3 m in diameter. The deposits of the May 25 explosion were mapped with high-resolution optical and thermal imagery and sampled by an AVO field team on June 11.

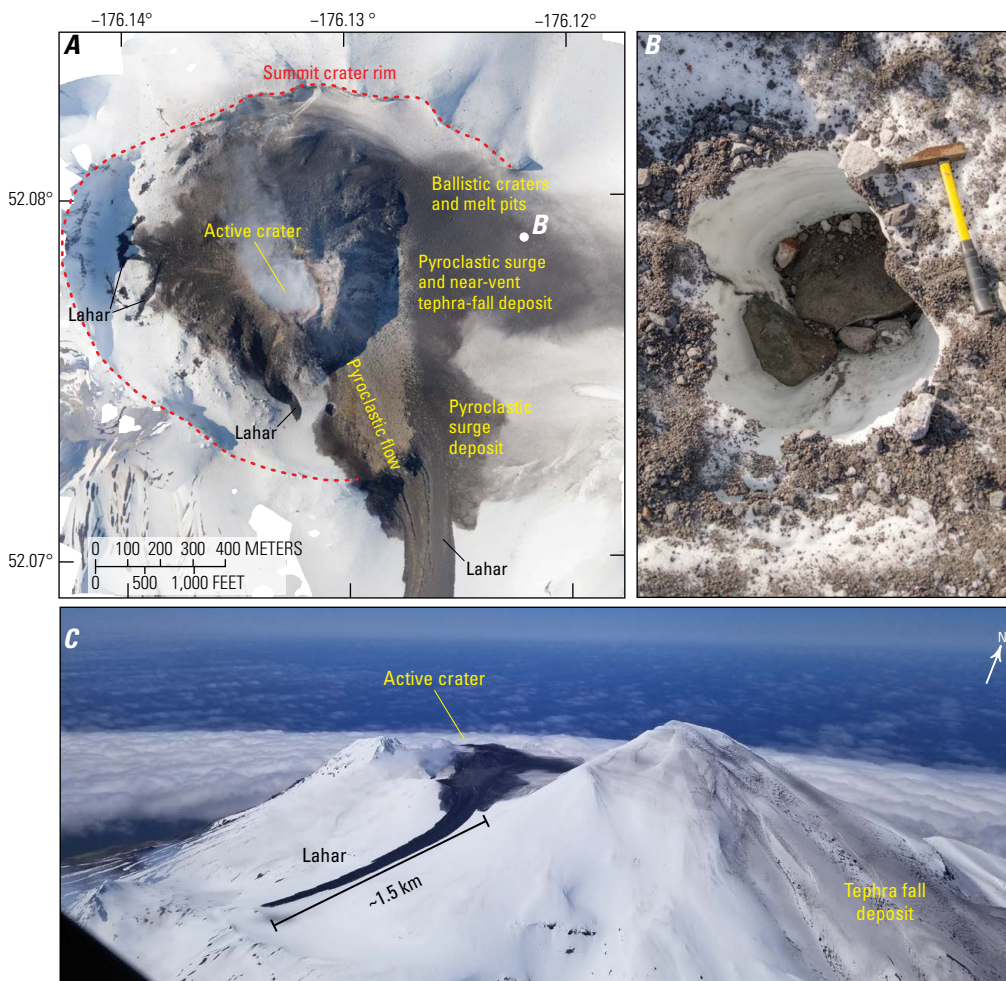


Figure 44. Images of deposits associated with the May 25, 2021, explosion at Great Sitkin Volcano, Alaska. A, Orthoimage of the summit derived from airborne imagery (using structure-from-motion photogrammetric methods with the program Agisoft Metashape). Circle east of crater marks location of image B. B, Field photograph of ballistic deposits, including a small pit made as warm blocks melted the ice. Hammer is 41 centimeters long for scale. Photograph by M. Loewen, U.S. Geological Survey, June 11, 2021. C, Annotated oblique aerial image of the May 25 explosion deposits at Great Sitkin Volcano, looking northwest, on May 30, 2021. Copyrighted by S. Rhodes, (2012); used with permission.~, approximately; km, kilometer.

The eruption samples showed that the tephra deposit was primarily lithic and coarse-grained with rare juvenile breadcrust bombs (less than 1 percent of the deposit) (fig. 45). The breadcrust bombs have a bulk andesite composition comprising a matrix of high-silica (rhyolitic?) glass and phenocrysts of highly zoned plagioclase, clinopyroxene, orthopyroxene, magnetite, and apatite (fig. 46). The high

crystallinity, presence of both apatite and a silica groundmass phase, and evolved interstitial melt composition all suggest that the erupted magma was a shallow, low-pressure, and near-solidus magma plug. The coarse-grained, poorly sorted, and lithic-rich deposit characteristics also support a Vulcanian eruption mechanism, which is consistent with geophysical observations and photographs of the eruption event.

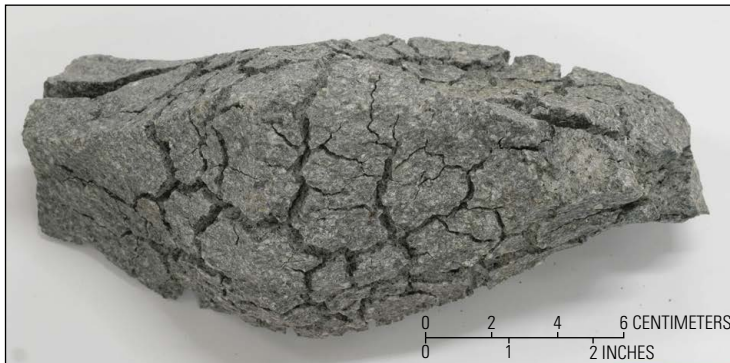


Figure 45. Example of a juvenile breadcrust bomb collected from deposits of the May 26, 2021, explosion at Great Sitkin Volcano, Alaska. Photograph by M. Loewen, U.S. Geological Survey.

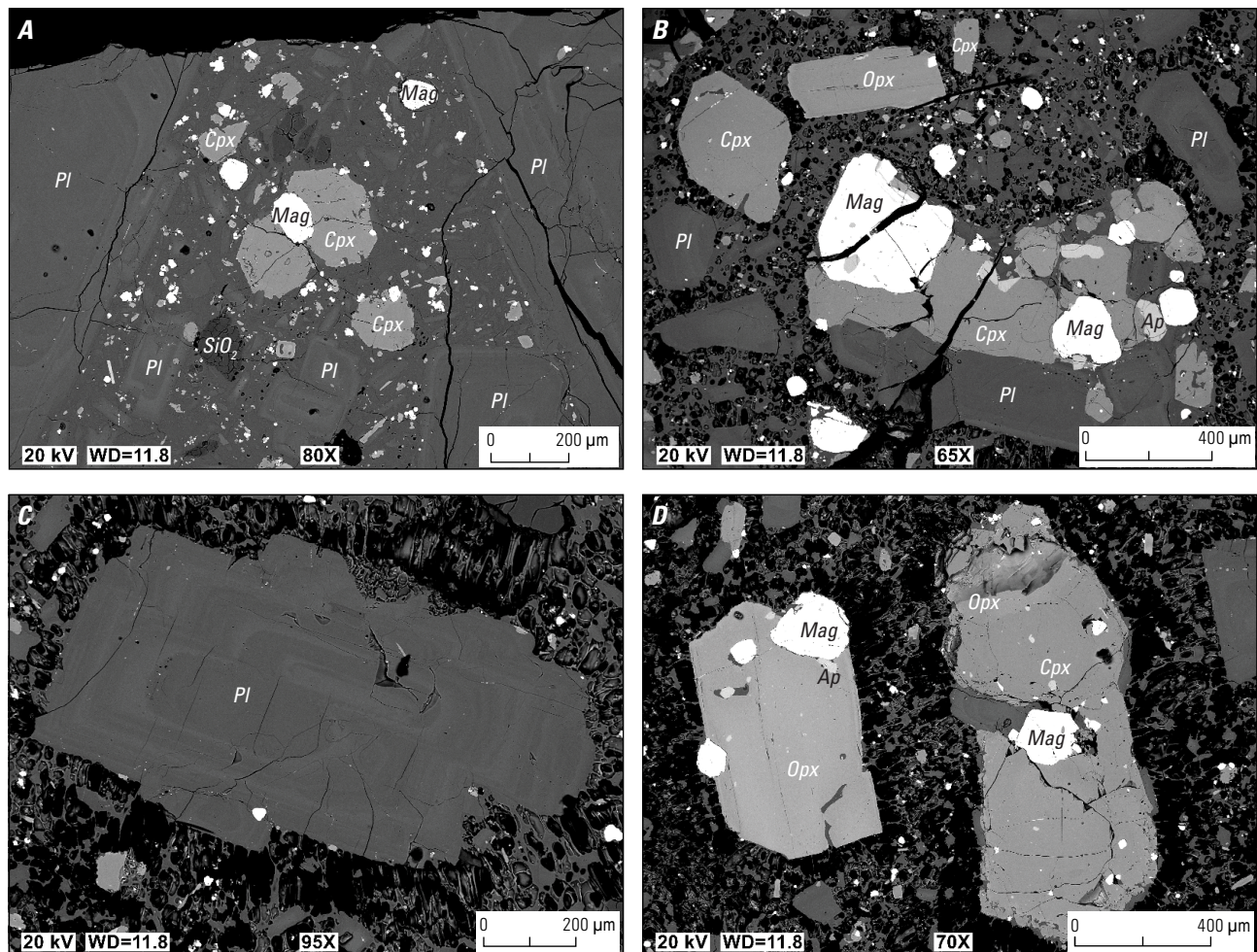


Figure 46. Backscatter electron images of polished breadcrust bomb samples from the May 25, 2021, explosion of Great Sitkin Volcano, Alaska. *A*, Dense outermost rind of a breadcrust bomb showing large phenocrysts of plagioclase (Pl); smaller clinopyroxene (Cpx) and magnetite (Mag); and a groundmass silica (SiO_2) phase. *B*, Vesicular interior of a breadcrust bomb showing a Pl-Cpx-Mag-apatite (Ap) crystal clot and loose Cpx and orthopyroxene (Opx) phenocrysts. *C*, Oscillatory-zoned Pl. *D*, Pair of pyroxene crystals. Opx mantles part of the Cpx crystal on the right. Images taken with a JEOL 6510LV scanning electron microscope. kV, kilovolt; WD, working distance, μm , micrometer.

2021 Effusive Phase

After the May 25 explosion, seismicity and elevated surface temperatures were regularly recorded at the volcano (fig. 40), consistent with post-explosion fumarolic activity observed in a thermal survey on June 11 (fig. 47). Steaming, elevated surface temperatures, and SO₂ emissions were observed through mid-July. On July 23, high-resolution TerraSAR-X spotlight SAR imagery showed a small, new lava dome in the center of the explosion crater (fig. 48). No lava was present in previous imagery from July 14, so lava effusion began sometime during the period of July 14–23. In response to the onset of effusion, AVO raised the Aviation Color Code and Volcano Alert Level to **ORANGE** and **WATCH** on July 23.

Lava overflowed the explosion crater by August 4, spreading radially over the 1974 and 1945 lava domes and onto the ice that filled the east part of the summit crater. The lava effusion in July and August was accompanied by steam

and SO₂ emissions; incandescence; saturated SWIR and mid-infrared satellite data; and elevated seismicity (fig. 40). Lava effusion rates were 3–7 cubic meters per second (m³/s) in August as estimated by mapping the flow extent and thickness. This mapping was produced using high-resolution optical and radar satellite imagery, as well as the thermal radiative power measured by the Moderate Resolution Imaging Spectroradiometer and Visible Infrared Imaging Radiometer Suite (satellite sensors). The effusion rate declined after August, dropping to ~2 m³/s in September and falling below 1 m³/s in November (fig. 49). Seismicity and SO₂ emissions also waned when effusion rates declined in September.

Lava began to overflow the summit crater in September, eventually forming three flow lobes that advanced down the steep flanks of the volcano: a west lobe that started by September 19, a south lobe that started by September 29, and a north lobe that started by November 12. The flow fronts had minor rockfall activity, depositing blocks as far as ~50 m

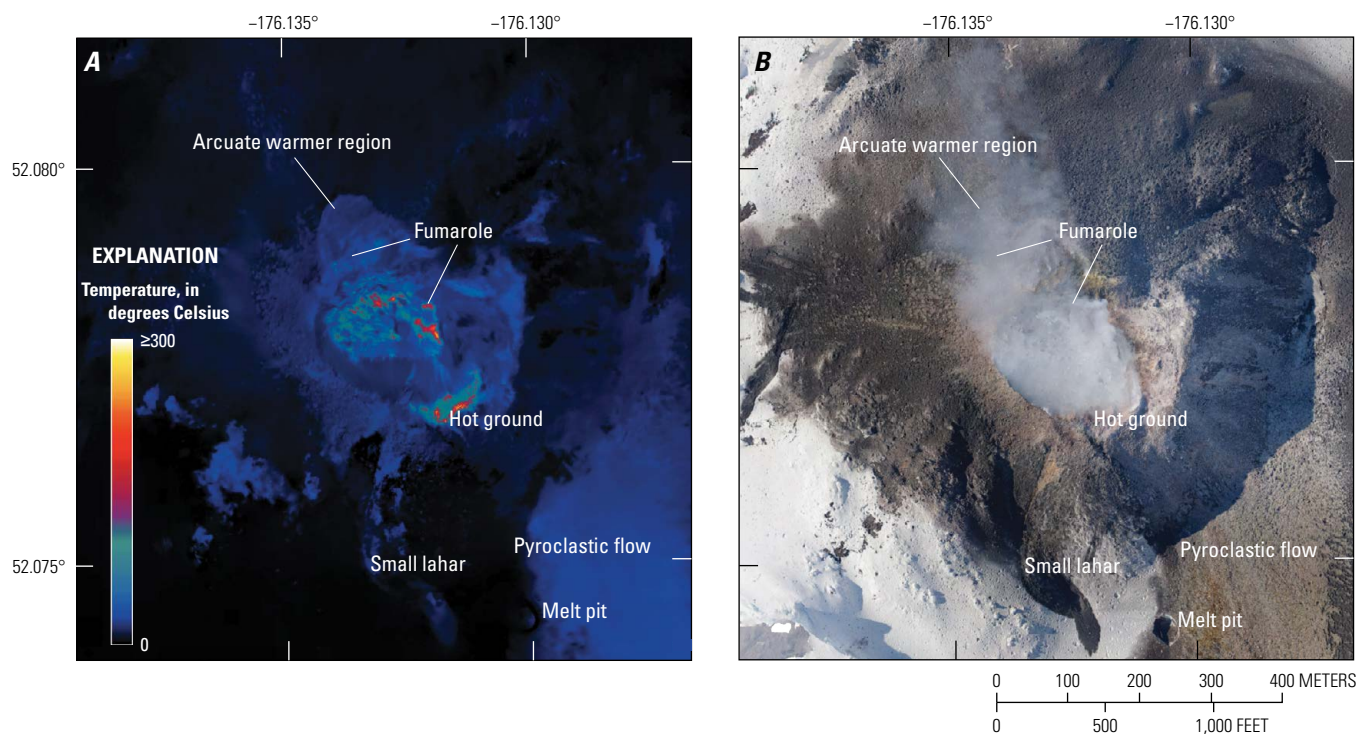
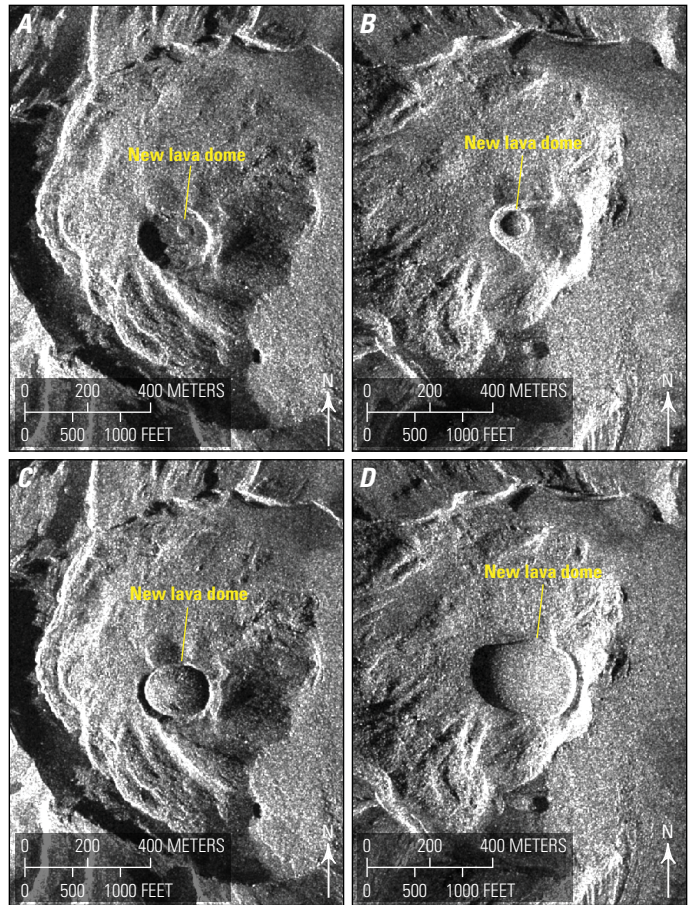


Figure 47. Orthoimages of Great Sitkin Volcano, Alaska, on June 11, 2021. *A*, Thermal image of the summit of Great Sitkin Volcano, derived from airborne thermal forward-looking infrared imagery (using structure-from-motion photogrammetric methods with the program Agisoft Metashape). *B*, Image of the summit, also derived from airborne imagery using structure-from-motion photogrammetric methods with Agisoft Metashape.

below the flow front. The east flow margin advanced onto the ice, melting it and causing fracturing and collapse of the ice near the flow front, but only producing minor steaming. By the end of 2021, the lava flow covered 1.3 square kilometers and had an estimated total volume of 0.031 km³. The dome within the summit crater was ~1,230 m wide (in its east-west direction), whereas the west, south, and north flow lobes were ~830, ~865, and ~180 m long, respectively. Slow effusion continued into 2022.

During 2021, AVO located 966 earthquakes near Great Sitkin Volcano (fig. 50), ranging in M_L from -1.1 to 2.1 and in depth from -1.8 to 32.04 km below sea level (negative depths reflect height above sea level). Most hypocenters clustered between 0 and 10 km depth beneath the Great Sitkin Volcano edifice (fig. 50). The most notable seismicity during 2021 was a ~24-hour-long swarm of LP earthquakes that immediately preceded the explosive eruption on May 25 (fig. 41).



Base images from German Aerospace Center and courtesy of Simon Plank, copyright 2021.

Figure 48. High-resolution satellite synthetic aperture radar amplitude spotlight imagery of the summit of Great Sitkin Volcano, Alaska, on July 23, 2021, at 5:32 coordinated universal time (UTC) (A), July 25, 2021, at 17:56 UTC (B), August 3, 2021, at 5:32 UTC (C), and August 5, 2021, at 17:56 UTC (D). Images show the new lava dome inside of and eventually overtopping the active crater of Great Sitkin Volcano. Images are not terrain-corrected, so geolocation and scale bar are approximate. Images acquired by satellites TerraSAR-X and TanDEM-X; courtesy of Simon Plank, German Aerospace Center.

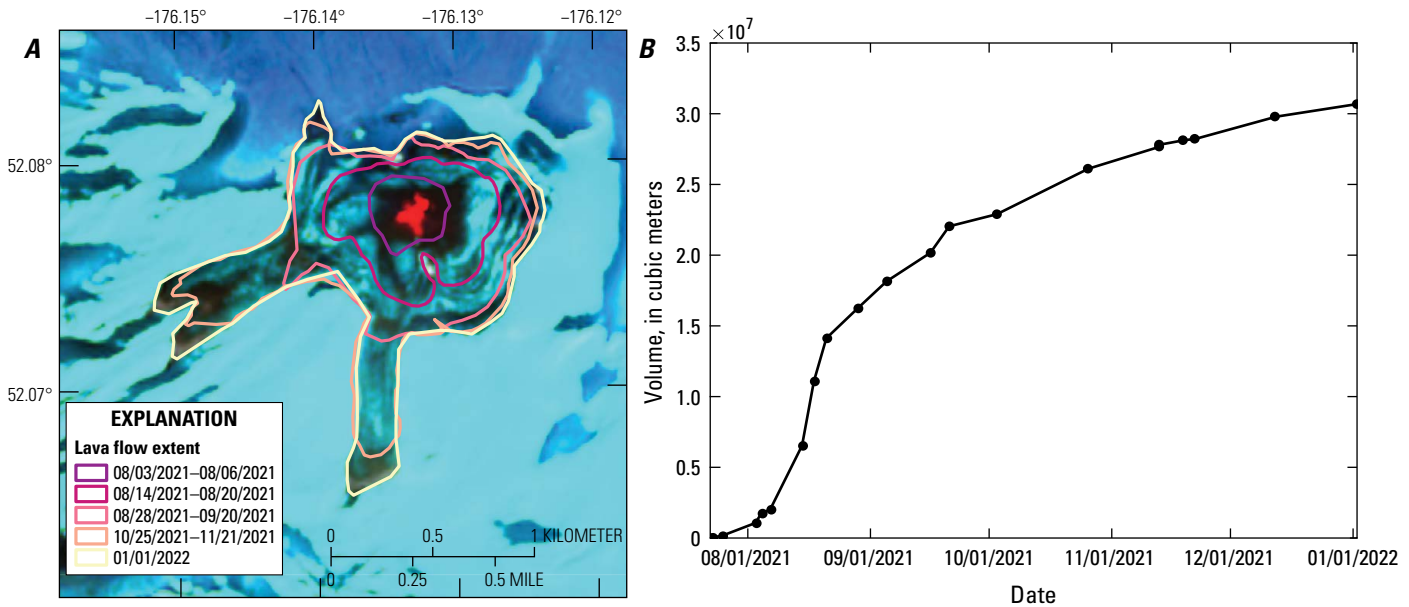


Figure 49. Growth over time of the lava flow at Great Sitkin Volcano, Alaska. A, Lava flow extents over time (mapped from cloud-free satellite imagery) overlaid on a Sentinel-2 short-wave infrared satellite image from January 1, 2022, at 23:01 coordinated universal time. B, Plot showing approximate lava volume erupted over time, as calculated from satellite imagery. Dates shown as month/day/year.

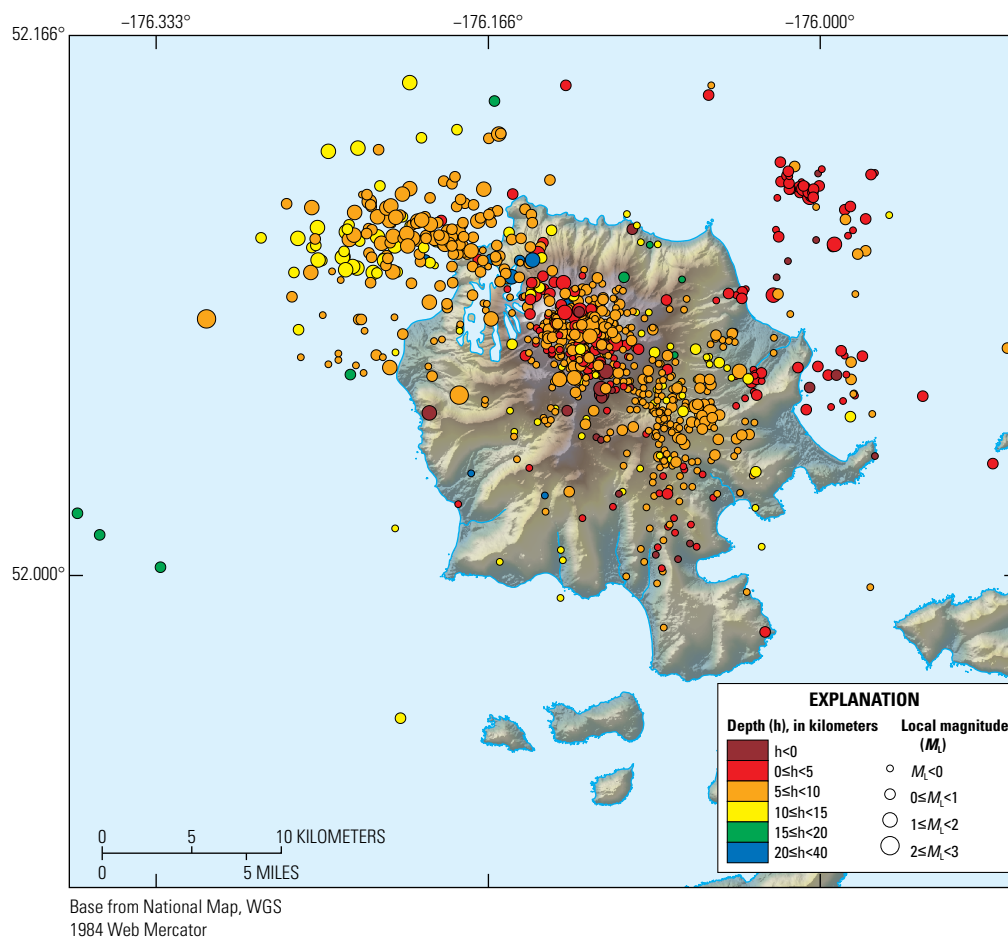


Figure 50. Map showing earthquake hypocenters located at Great Sitkin Volcano, Alaska, during 2021.

Mount Gareloi

GVP# 311070
 51.789°, -178.794°
 1,550 m
 Gareloi Island, Andreanof Islands, Aleutian Islands

ELEVATED SEISMICITY

Mount Gareloi, which makes up Gareloi Island, is a prominent stratovolcano located in the western Aleutian Islands, ~150 km west of Adak and ~2,000 km southwest of Anchorage (fig. 1). Mount Gareloi has had 16 reports of eruptive activity since 1760, making it one of the most active volcanoes in the Aleutian Islands since the 1740s. The uninhabited volcano has two summit peaks (Miller and others, 1998), spaced ~500 m apart and separated by a narrow saddle, which have both been active historically (Coombs and others, 2012). The slightly higher north peak has an ~300-m-wide crater containing a small lake. The south peak

has a crater that is open to the south and that hosts several active fumaroles on its west rim, often forming a conspicuous plume (fig. 51). Thirteen younger craters with diameters of 80–1,600 m are aligned on a fissure that extends south-southeastward from the southern summit to the coast (Coats, 1959). These craters formed during an explosive eruption in 1929 that also produced four blocky lava flows and deposited a blanket of glassy andesitic tuff over an area of 2.5×5 km on the volcano's southeast flank (Coats, 1959). Mount Gareloi commonly shows low-energy, LP seismic activity sourced beneath its edifice, suggesting the presence of shallow magma interacting with a hydrothermal system (Harris and others, 2021). The volcano is currently monitored by a local seismic and infrasound network, satellite data, a webcam, and regional infrasound and lightning-detection networks.

Beginning on May 18, 2021, anomalous seismicity was recorded at the Mount Gareloi. In particular, the low-energy LP events commonly observed at the volcano overlapped with a harmonic tremor recorded on every station on the island. The dominant tremor frequencies peaked at ~3.4 hertz (Hz), ~6.4 Hz, ~8.3 Hz, and ~10.7 Hz. These harmonic signals, which were intermittent during at least the previous day, became conspicuous after a regional M_L 5.0 earthquake at



Figure 51. Photographs of Mount Gareloi, Alaska. *A*, Photograph of Mount Gareloi from Ogliuga Island showing a gas plume from the volcano's south peak on May 23, 2021. View to the north-northwest; copyrighted by A. McComb, (2021); used with permission. *B*, Oblique aerial photograph of gas emissions from the inner crater wall of the south peak. View to the northeast. Photograph by R. Jackson, Pathfinder Aviation, June 8, 2021.

20:42 HADT on May 17 (05:42 UTC on May 18), though this change might be coincidental. Harmonic tremor took place intermittently until May 27, when highly frequent and highly energetic LP events emerged, sometimes merging into continuous broadband tremor (fig. 52). An ~2-Hz infrasound signal was also recorded locally on June 3, although it was unclear if the signal was of volcanic origin. A monochromatic, ~7 Hz seismic signal lasting 15–20 min was recorded on June 6, while elevated-amplitude seismicity, ongoing since about May 27, continued. Hence, on June 8, AVO raised the Aviation Color Code and Volcano Alert Level to **YELLOW** and **ADVISORY**. The increase in seismic activity likely reflected a change to the magmatic-hydrothermal system interaction. No indications of unrest, however, were observed by an AVO field crew that flew over the summit on May 23.

Over the following two months, the elevated and anomalous seismicity continued intermittently; SO₂ was detected in satellite imagery but was consistent with measurements from the last several years; light steaming was observed in partly cloudy satellite and webcam views of the volcano; and weakly elevated surface temperatures were sometimes observed in satellite data. No eruptive activity was observed in satellite views of the volcano and no activity was detected by local or regional infrasound sensors. Starting in the second week of July, seismic activity gradually diminished and returned to background levels. AVO lowered the Aviation Color Code and Volcano Alert Level to **GREEN** and **NORMAL** on July 28, 2021.

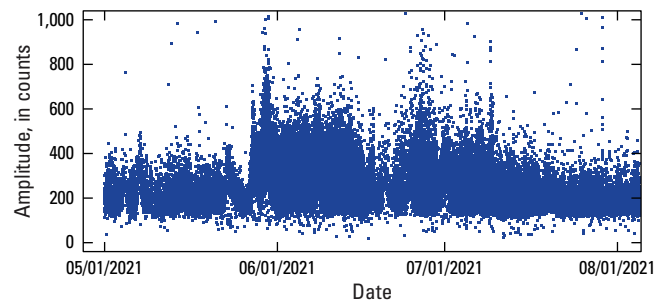


Figure 52. Time-series graph showing the amplitude of long-period (LP) events automatically recorded during the 2021 episode of unrest at Mount Gareloi, Alaska. The seismic amplitude shown is the median of the absolute value of the waveform of the LP events recorded. Results were obtained from the vertical component of station GAEA. Dates shown as month/day/year.

**Semisopchnoi Island
(Mount Young)**

GVP# 311060
51.929°, 179.598°
815 m

Semisopchnoi Island, Rat Islands, Aleutian Islands

**PHREATOMAGMATIC EXPLOSIONS WITH ASH
EMISSIONS**



Semisopchnoi Island is located in the western Aleutian Islands, ~260 km west of Adak and ~2,100 km southwest of Anchorage (fig. 1). The volcano has a caldera 7 km in diameter that formed 6,900–5,000 years ago, as well as several post-caldera cones (fig. 53) (Coombs and others, 2018). Mount Young, a cluster of three cones within the caldera, has erupted repeatedly in the Holocene, producing crystal-rich basaltic andesite lavas and tephtras. The fall deposits associated with Mount Young are consistent with mostly small- to

moderate-sized ash clouds, but some lapilli-size units suggest its eruptions have reached a volcanic explosivity index (VEI) value as high as 3 (Coombs and others, 2018). The north cone of Mount Young (figs. 53, 54) began erupting in 2018 and continued to do so into 2021. Prior to 2018, the last eruption at Semisopchnoi Island was in 1987 on the south side of the island at Sugarloaf Peak. This event produced a 90-km-long plume that was visible in satellite images. Pilots at the time also reported ash on the volcano’s flanks (Reeder, 1990). The most recent noneruptive unrest at Semisopchnoi Island before the 2018–2021 eruption began was a period of increased seismicity and deformation in 2014–2015. Modeling by DeGrandpre and others (2019) explained this unrest as the rapid intrusion of 0.072 km³ of magma (as two batches) into a spheroidal magma storage zone ~8 km beneath the caldera.

Eruptive activity at Semisopchnoi Island, which began in September 2018, was characterized in 2021 by frequent, low-level ash emissions and explosions from the north cone of Mount Young (fig. 54). An equipment failure on Amchitka Island meant that activity observations during the first half of the year were limited to those from satellite imagery and

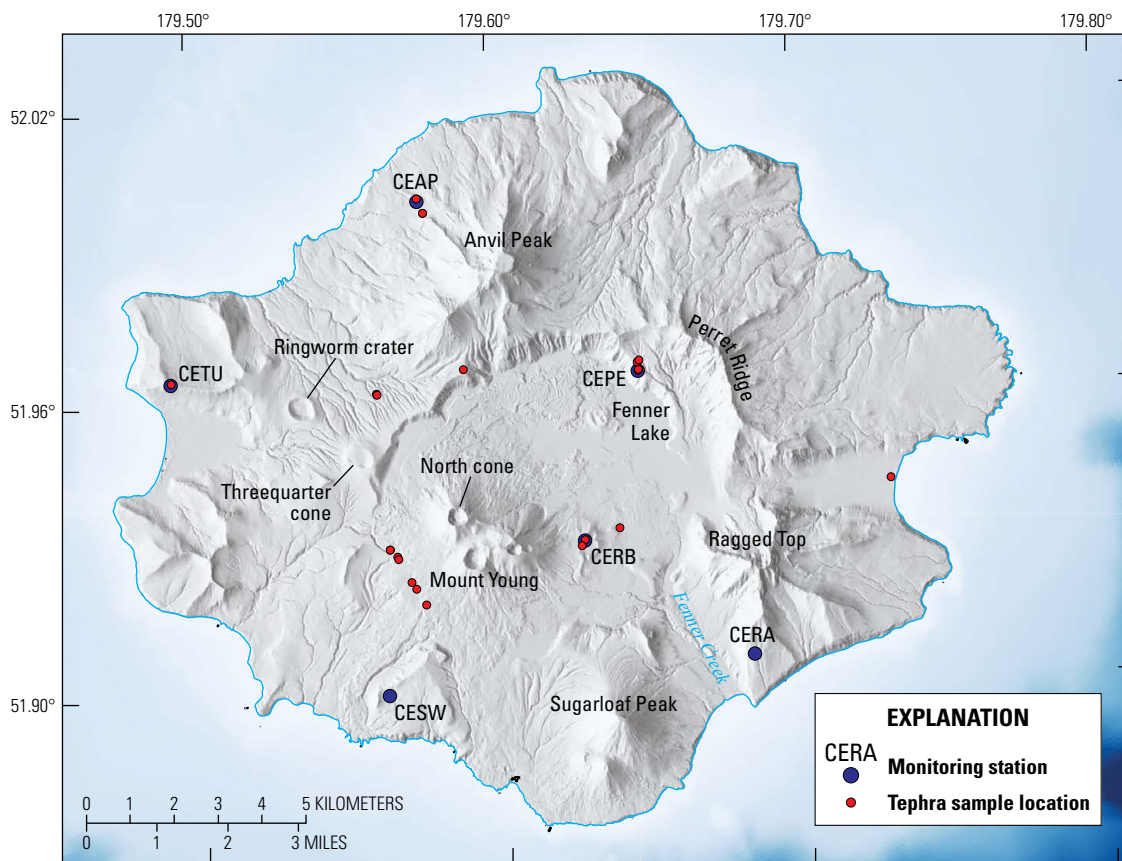


Figure 53. Map of Semisopchnoi Island, Alaska, showing the active north cone of Mount Young and other important geographic features. The monitoring network comprises six stations with three-component broadband seismometers. In addition, three of the stations have broadband infrasound sensors (CERB, CESW, CEPE) and two have webcams (CEPE and CETU).

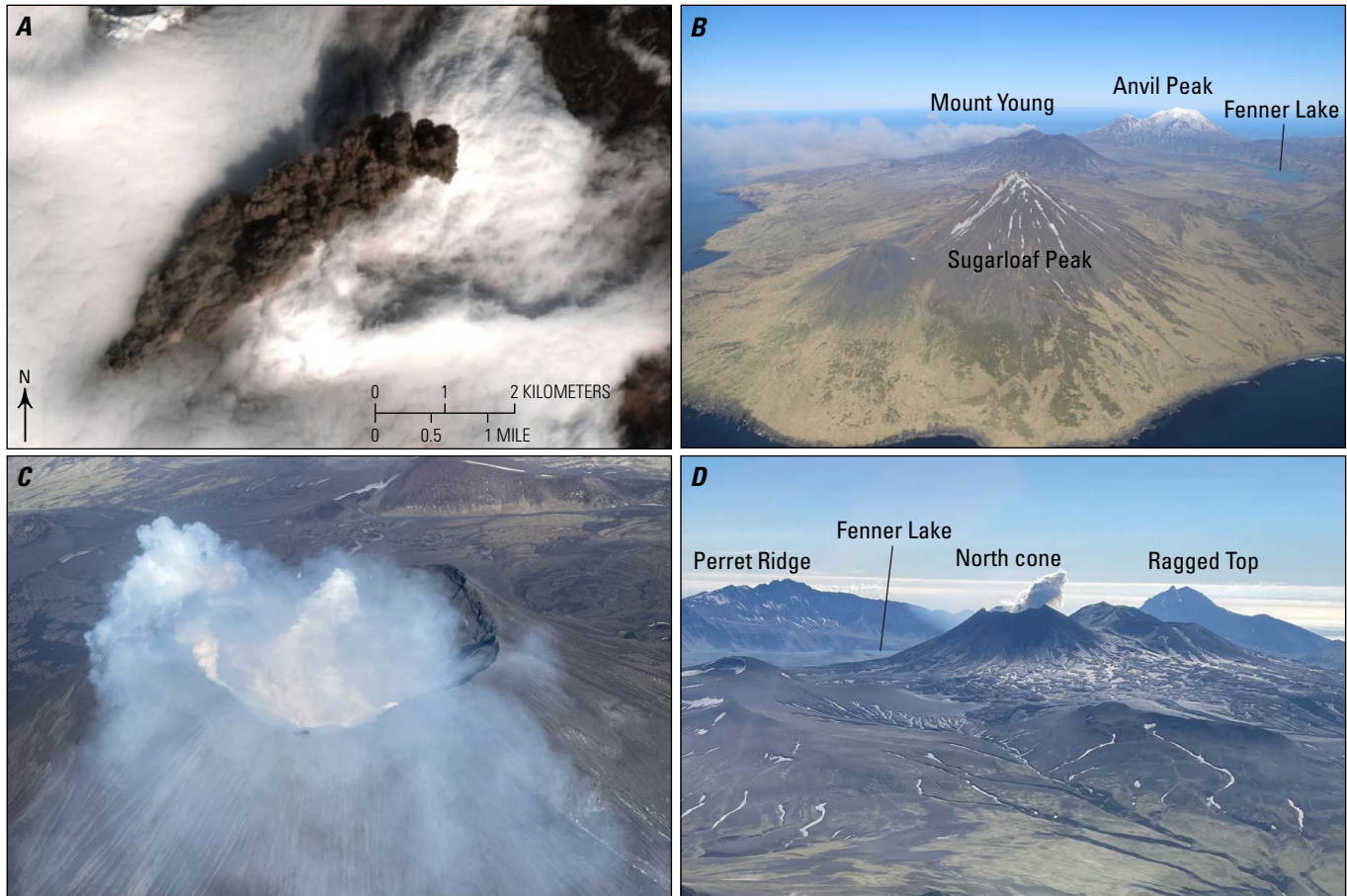


Figure 54. Images of gas emissions from Mount Young, Alaska, in 2021. *A*, Worldview-2 satellite image from April 1, 2021, showing ash emissions from the north cone of Mount Young. Base image from DigitalGlobe NextView License, copyright 2021. *B*, Oblique aerial photograph of low-level ash emissions from Mount Young. Photograph by H. Dieterich, U.S. Geological Survey, May 30, 2021. *C*, Oblique aerial photograph of gas emissions from the north cone of Mount Young. Photograph by A. Lerner, U.S. Geological Survey, June 8, 2021. *D*, Oblique aerial photograph of gas emissions from the north cone. Photograph by A. Lerner, U.S. Geological Survey, June 8, 2021.

regional infrasound and seismic stations. In early June 2021, the equipment on Amchitka Island was repaired and the local network on Semisopchnoi Island was completely upgraded. These upgrades involved a change from analog to digital telemetry; the replacement of short-period vertical-component seismometers with three-component broadband seismometers; the addition of broadband infrasound sensors at stations CERB, CESW, and CEPE; and the addition of webcams at stations CEPE and CETU (fig. 53). A six-element infrasound array was also installed on Amchitka Island in late May 2021 to provide improved regional monitoring.

Seismic activity was low prior to the network outage; thus, the first activity noted in 2021 was a satellite observation of a small ash deposit from the north cone of Mount Young on February 6. In response, AVO raised the Aviation Color Code and Volcano Alert Level from

UNASSIGNED to **YELLOW** and **ADVISORY** the next day. Ash emissions appeared in satellite imagery on February 8, which led AVO to further elevate the volcano to **ORANGE** and **WATCH**.

In the following months, satellites recorded intermittent ash emissions and regional infrasound sensors detected small explosions (table 5; fig. 55). Ash emissions increased considerably on April 16, when an ash cloud as high as ~20,000 ft (~6,100 m) ASL extended more than 350 km from the north cone of Mount Young. This change prompted AVO to raise the Aviation Color Code and Volcano Alert Level from **ORANGE** and **WATCH** to **RED** and **WARNING**. The next day, ash emissions declined and the volcano was lowered back to **ORANGE** and **WATCH**. Satellite imagery and regional infrasound sensors recorded intermittent, small explosions over the next few months.

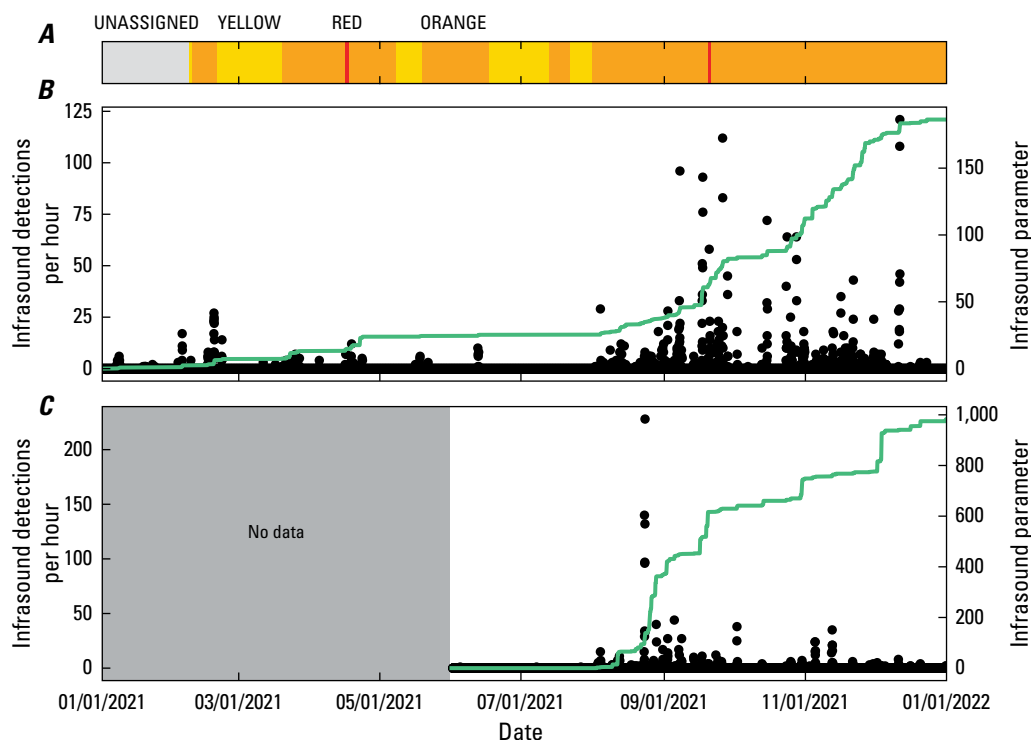


Figure 55. Timeline of Aviation Color Code changes and time-series plots of infrasound detections at Semisopchnoi Island, Alaska, in 2021. *A*, Timeline of Aviation Color Code changes. *B*, Time-series plot of the regional infrasound detection rate and cumulative infrasound parameter at the ADKI array, on Adak Island. *C*, Time-series plot of the regional infrasound detection rate and cumulative infrasound parameter at the AMKA array (installed in late May 2021), on Amchitka Island. Each infrasound detection window is 15 seconds long. The infrasound parameter is the number of detections per hour multiplied by the median infrasound pressure. Dates shown as month/day/year.

Table 5. Summary of activity and observations at Mount Young, Alaska, in 2021. Dates shown as month/day/year.

Aviation Color Code/Volcano Alert Level	Date of change	Observation description
UNASSIGNED	01/01/2021	Low seismicity prior to network outage
YELLOW/ADVISORY	02/07/2021	Small ash deposit from tin satellite image
ORANGE/WATCH	02/08/2021	Ongoing, intermittent low-level ash emissions in satellite images
YELLOW/ADVISORY	02/19/2021	No activity observed in satellite or regional infrasound
ORANGE/WATCH	03/19/2021	Small explosions detected in regional infrasound data
RED/WARNING	04/16/2021	Sustained ash eruption with plume extending +350 km at ~20,000' ASL
ORANGE/WATCH	04/17/2021	Decline in ash emissions
YELLOW/ADVISORY	05/07/2021	No eruptive activity in satellite or regional geophysical data since 26 April
ORANGE/WATCH	05/19/2021	Small explosions in regional infrasound and ash emissions in satellite data
YELLOW/ADVISORY	06/16/2021	Local network repaired; seismicity low but satellite sulfur dioxide observed
ORANGE/WATCH	07/13/2021	Seismic tremor and low-level ash emissions
YELLOW/ADVISORY	07/22/2021	Decline in seismicity and no ash emissions observed
ORANGE/WATCH	07/31/2021	Increase in seismic activity
RED/WARNING	09/20/2021	Increased ash emissions
ORANGE/WATCH	09/21/2021	Ash emissions continue but at decreased rate

Seismicity was initially low after the local geophysical sensors were restored in June, but both seismicity and the number of discrete explosions increased into July and August. Seismic activity remained elevated, although variably so, for the rest of the year, during which time tremor and explosion signals dominated the data (fig. 56). On September 20, increased ash emissions observed in satellite imagery (fig. 57A) again prompted AVO to raise the Aviation Color Code and Volcano Alert Level from **ORANGE** and **WATCH** to **RED** and **WARNING**. A large SO₂ cloud associated with this increase in activity appeared in TROPOMI satellite data (fig. 57B). The following day, ash emissions declined, and Semisopchnoi Island was lowered to **ORANGE** and

WATCH. The activity at the volcano for the rest of the year consisted of low-level ash emissions, seismic tremor, phreatomagmatic explosions, and many satellite SO₂ detections (fig. 58).

In combination with carrying out geophysical maintenance, AVO geologists sampled ash deposits on Semisopchnoi Island on May 30 and June 1. Tephra samples were collected across all parts of the island (fig. 53), but the samples most proximal to Mount Young, taken from a 4-cm-thick deposit, were from 1.6 km southwest of the center of the north cone. The tephra was fine-grained, easily remobilized, and present over the entire island except along the north coast. The coarsest grains in the samples were less

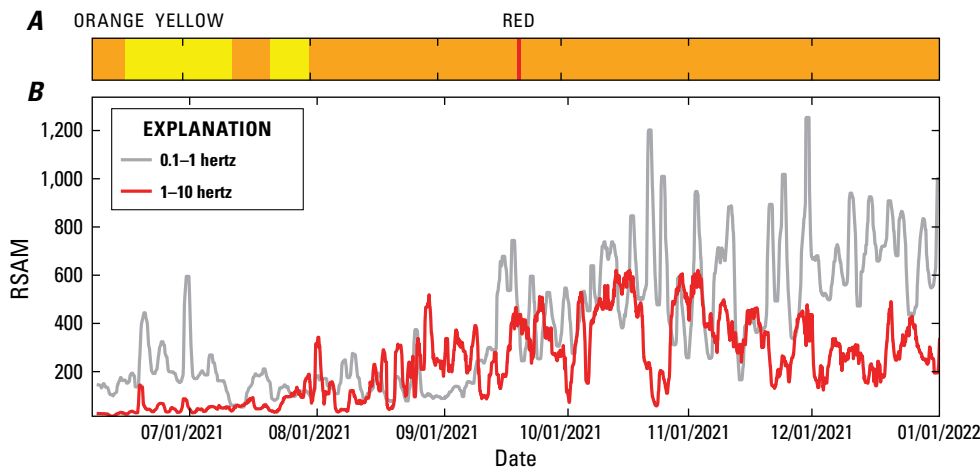


Figure 56. Timeline of Aviation Color Code changes (A) and time-series plot of real-time seismic amplitude measurement (RSAM) values at station CERB (fig. 53) (B), on Semisopchnoi Island, Alaska. No seismic data were recorded prior to June 2021 owing to a prolonged data outage following an equipment failure. Dates shown as month/day/year.

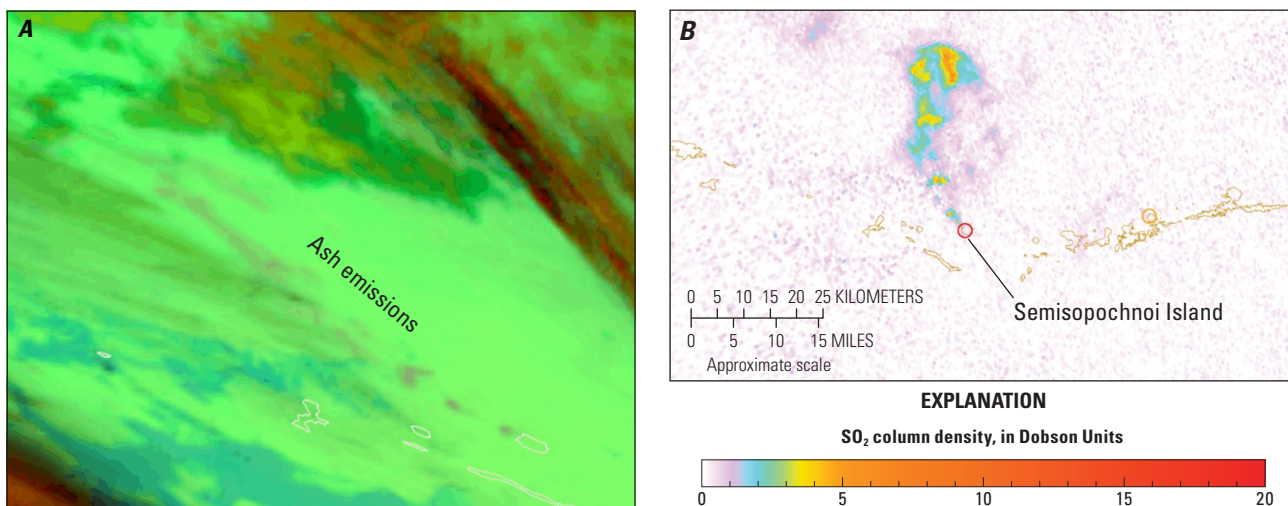


Figure 57. Satellite imagery of ash and sulfur emissions from Semisopchnoi Island (Mount Young), Alaska, in September 2021. A, Multispectral Himawari-9 image showing an ash plume (gray) extending about 300 kilometers northwestward from Semisopchnoi Island on September 20, 2021. The continuous plume transitions to discrete ash bursts closer to the volcano. B, Sulfur dioxide (SO₂) detection image from the TROPOMI satellite showing a large SO₂ cloud extending northward from Semisopchnoi Island (circled) on September 21, 2021.

than 4 mm in diameter. Approximately 50 percent of the material was less than 50 micrometers in diameter. No larger ballistic particles were observed, including on the flanks of the north cone. The internal structures of deposits were not preserved; thus, the samples represent a bulk aggregate of deposits from throughout the spring of 2021.

A microscopic analysis of the samples showed that they are mostly crystal-lithic grains or loose crystals. A minor proportion of the grains are scoriaceous juvenile material characterized by low vesicularity and microlitic glass (fig. 59A). Microlite phases comprise plagioclase, clinopyroxene (augite and pigeonite), orthopyroxene, and iron-titanium oxides (fig. 59B).

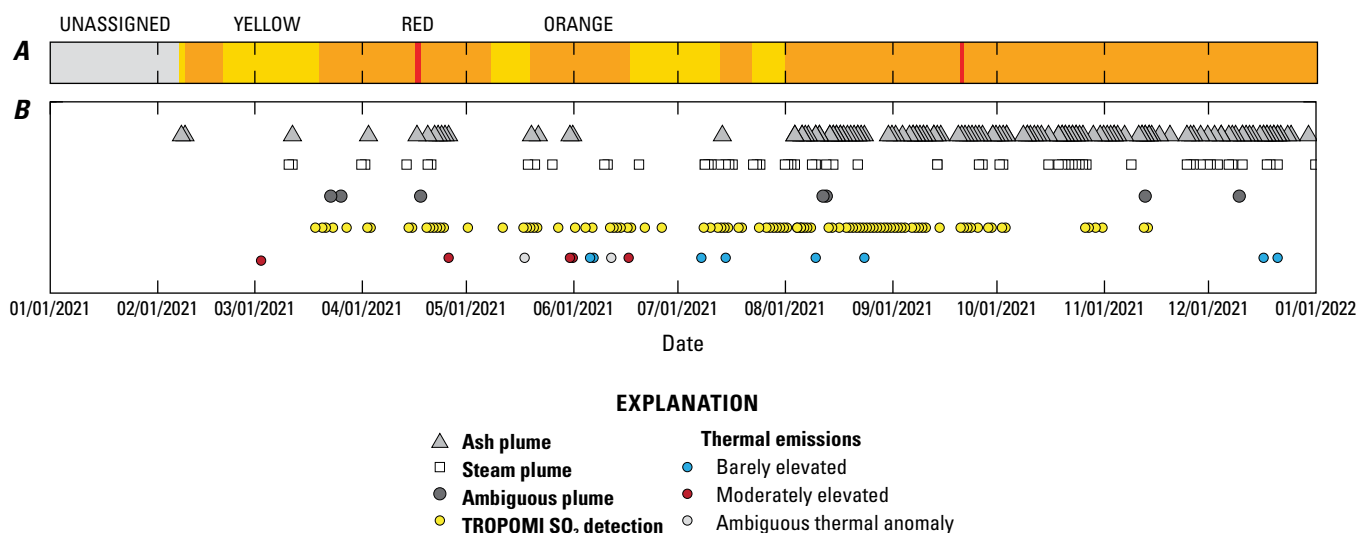


Figure 58. Timeline of Aviation color codes (A) and remote sensing observations (B) at Semisopochnoi Island, Alaska, in 2021. TROPOMI, TROPospheric Monitoring Instrument; SO₂, sulfur dioxide. Dates shown as month/day/year.

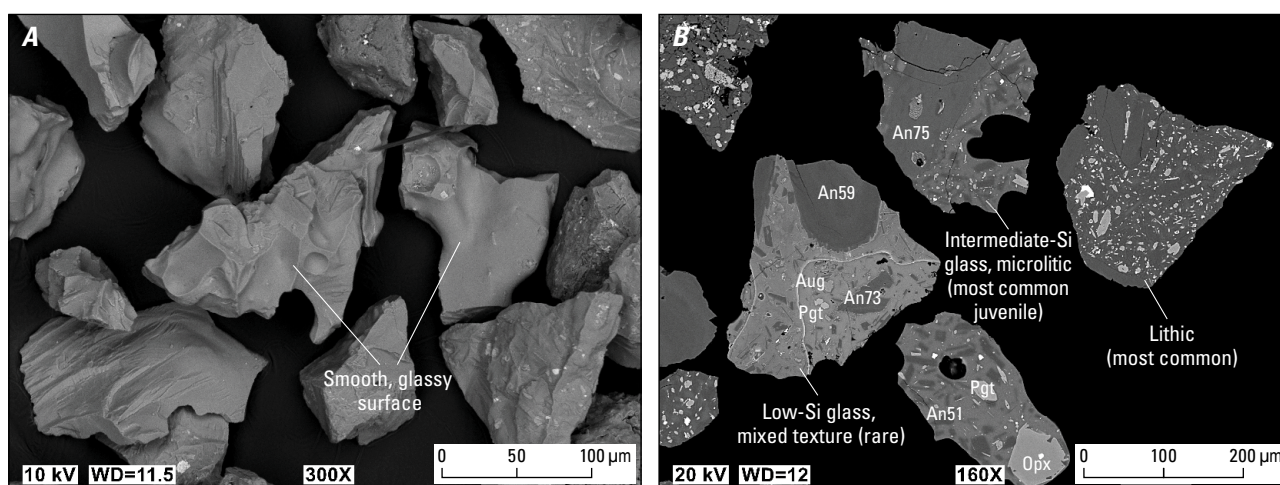


Figure 59. Backscatter electron images of samples collected from Mount Young, Alaska, on May 30 and June 1, 2021. A, Image showing tephra grain morphology (examples of juvenile grains with smooth, glassy surfaces and broken vesicles). B, Polished sample mount showing grain cross-section of typical lithic grains and examples of juvenile grains: augite (Aug), pigeonite (Pgt), orthopyroxene (Opx), and plagioclase (An; number represents the molecular proportion of the anorthite endmember in the albite-anorthite solid solution series of plagioclase feldspars). Images taken with a JEOL 6510LV scanning electron microscope. Si, silicon; kV, kilovolt; WD, working distance, μm , micrometer.

Davidof Volcano

GVP# 311040

51.954°, 178.326°

325 m

Rat Islands (Davidof Island, Khvostof Island, and Pyramid Island), Aleutian Islands

EARTHQUAKE SWARM

Davidof volcano is a mostly submerged stratovolcano in the Rat Islands group of the western Aleutian Islands, ~350 km west of Adak and ~2,200 km west of Anchorage (fig. 1). The subaerial part of the volcano comprises Davidof Island, Khvostof Island, and Pyramid Island, all of which encircle Crater Bay, a caldera 2.5 km in diameter (figs. 60, 61). The islands are composed of interbedded lava flows and explosive deposits, although the volcano itself has been scarcely studied. In 2021, AVO geologists visited Davidof volcano, where they documented the thick sequences of rhyolite-to-andesite pyroclastic flow and fall deposits that represent its most recent explosive eruptions (fig. 62). The ages of these deposits are unknown, but the rhyolite deposit on Davidof Island is older than the overlying soil layer that has been dated to 5,500 years



before present, and the andesite deposit on Kovostof Island is older than the overlying soil layer there that has been dated to 6,100 years before present (Loewen and others, 2023). Davidof volcano has no known historical eruptions.

On December 7, 2021, at 15:33 HAST (December 8 at 01:33 UTC), an earthquake swarm occurred 7.5 km north of Davidof volcano. During the first few days of the swarm,

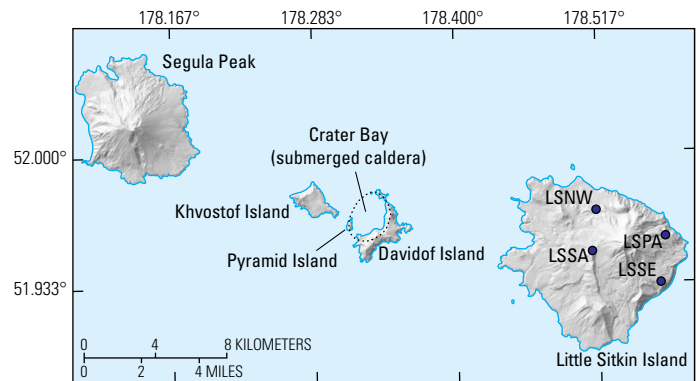


Figure 60. Map of Davidof volcano, an informal name for a volcanic system comprising Davidof Island, Khvostof Island, and Pyramid Island, Alaska. Segula Peak and Little Sitkin Island are also shown for geographic context. The dotted line approximates the partly submerged caldera rim of Davidof volcano. Blue dot indicates monitoring stations on Little Sitkin Island.

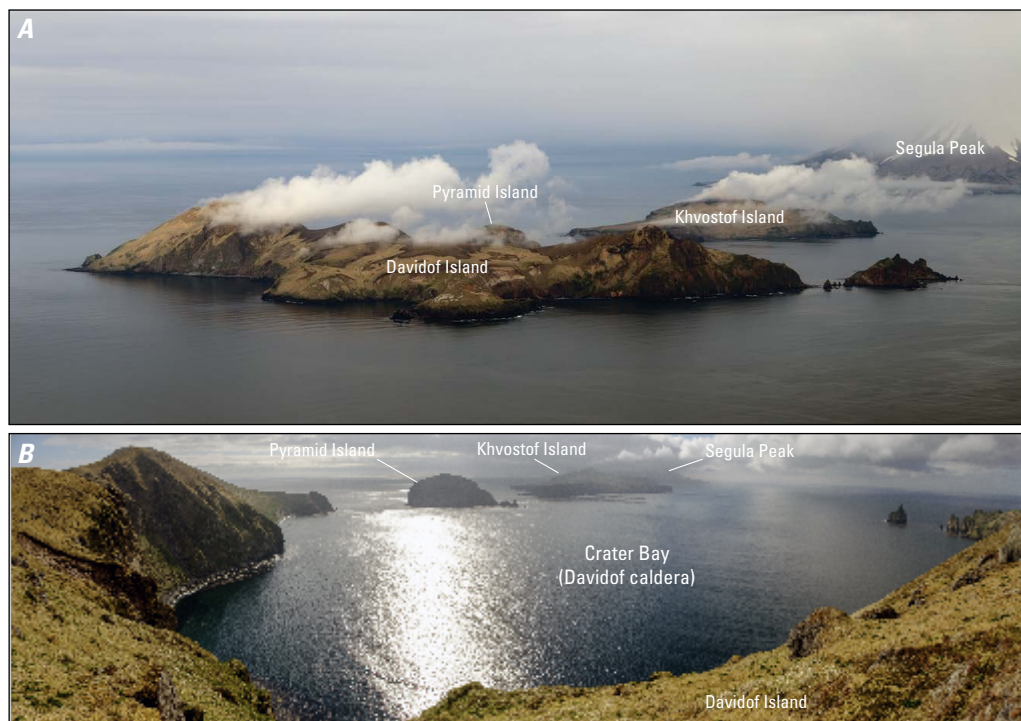


Figure 61. Photographs of Davidof volcano, Alaska. *A*, Oblique aerial photograph of the islands that compose Davidof volcano, looking southwest. Segula Peak is visible in the background. *B*, Ground-level photograph of the islands of Davidof volcano, which partly encircle Davidof caldera, looking west. Photographs *A* and *B* by H. Dieterich and M. Loewen (both U.S. Geological Survey), respectively, May 25, 2021.

several energetic earthquake bursts took place, the largest of which was a M_L 4.2 on December 10. The sudden increase in seismic activity was uncharacteristic of the area, prompting AVO to raise the Aviation Color Code and Volcano Alert Level from **UNASSIGNED** to **YELLOW** and **ADVISORY** on December 10 in anticipation of possible volcanic activity.

Seismicity waned gradually over the next week and the swarm seemingly ceased on December 20. The hypocenters of earthquakes from the swarm formed a northeast-southwest trending lineation north of the volcano (fig. 63A). However, this linear trend is interpreted to be an artifact because the earthquakes were located outside the regional network—the closest seismic stations are the four on Little Sitkin Island, ~12 km east of Davidof volcano. The earthquakes occurred at a variety of depths, the deepest of which was 9.8 km below sea level (fig. 63B). Notably, the swarm produced 2 earthquakes of $M_L > 4$ and 13 earthquakes of $M_L > 3$. On December 29, more than one week after the swarm ended, AVO lowered the Aviation Color Code and Volcano Alert Level of Davidof volcano to **UNASSIGNED**.

Figure 62. Photograph of thick pyroclastic flow and fall deposits on Davidof Island, Alaska. Geologist is 1.6 meters tall. Photograph by M. Loewen, U.S. Geological Survey, May 25, 2021.

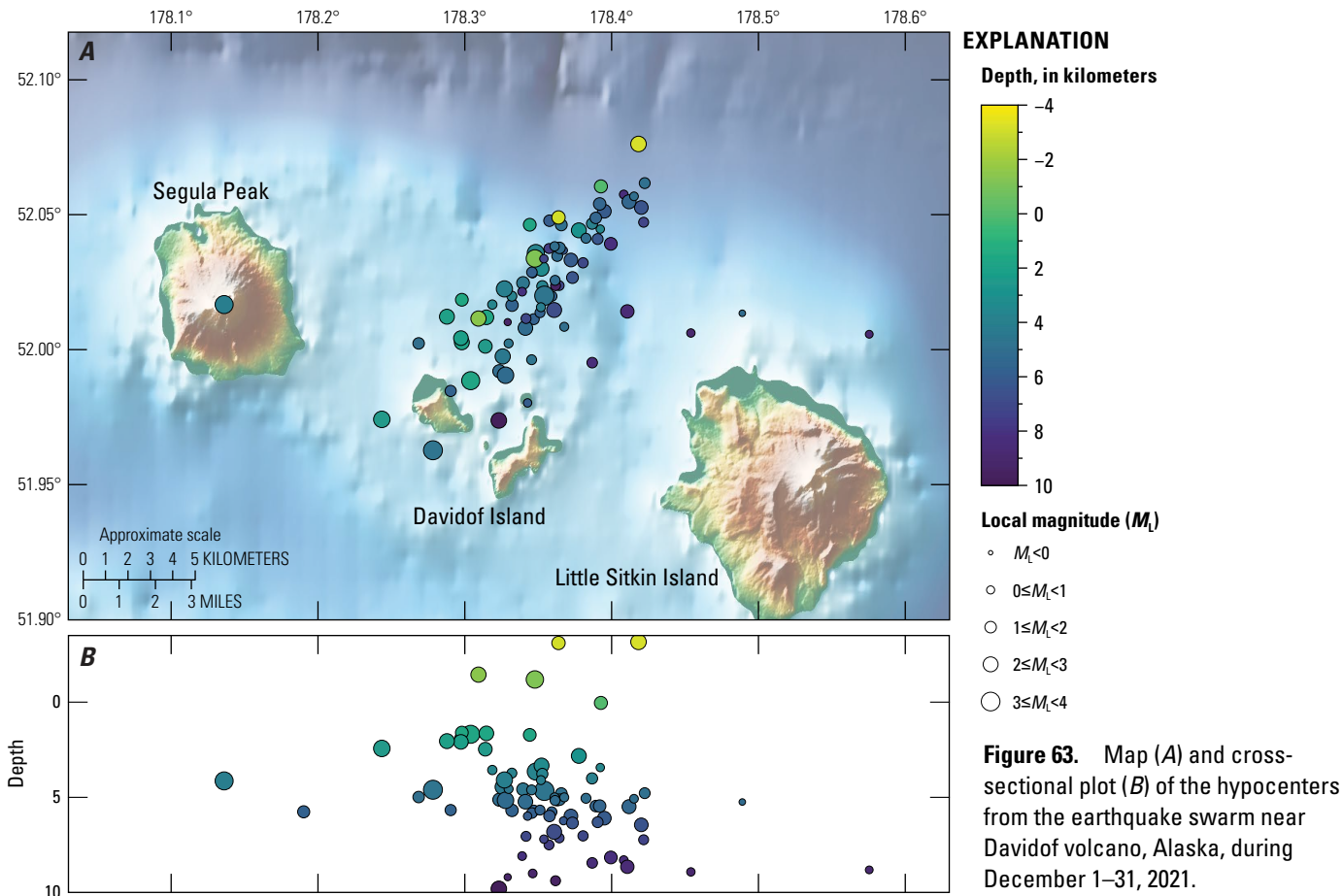
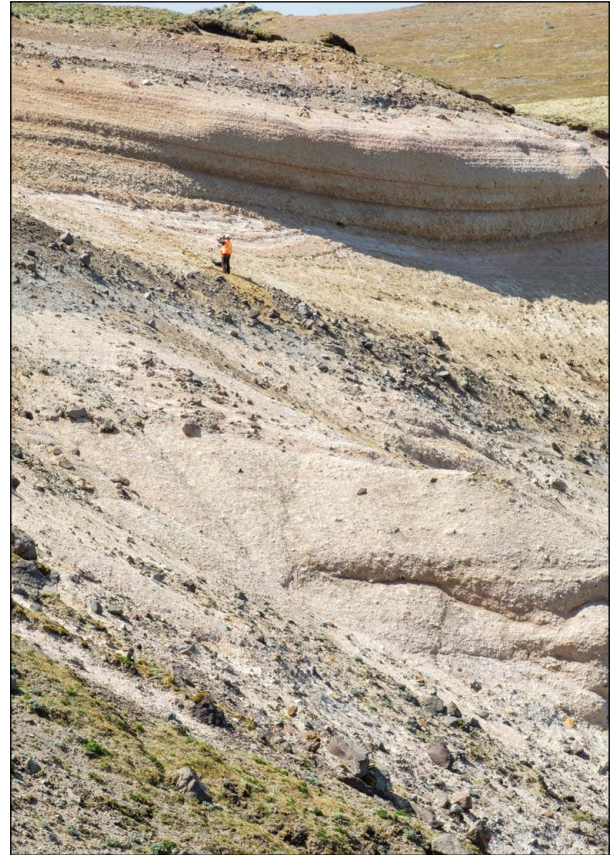



Figure 63. Map (A) and cross-sectional plot (B) of the hypocenters from the earthquake swarm near Davidof volcano, Alaska, during December 1–31, 2021.

Mount Pagan

GVP# 284170
 18.13°, 145.8°
 570 m
 Pagan Island, Commonwealth of the Northern Mariana Islands

EXPLOSIVE ERUPTION WITH ASH EMISSIONS



A small map showing the location of Pagan Island (marked with a red square) and Guam (marked with a black square) in the Northern Mariana Islands.

Mount Pagan is the northern of the two volcanoes, separated by a narrow isthmus, that make up Pagan Island in the CNMI (fig. 64). Mount Pagan is located 500 km north-northeast of the U.S. Territory of Guam and 320 km north of island of Saipan (fig. 1). The volcano, which is nested within an older caldera ~6 km wide, is one of the most historically active volcanoes in the CNMI and may have formed in the past 1,000 years (Trusdell and others, 2006). The last large eruption (VEI 4) of Mount Pagan took place in 1981 (Banks and others, 1984) and preceded four decades of intermittent, weaker activity characterized by vigorous steam plumes and degassing from a shallow magma source. Because Mount Pagan is not monitored with ground-based geophysical instrumentation, the primary sources of information on it come from local observers and satellite image data.

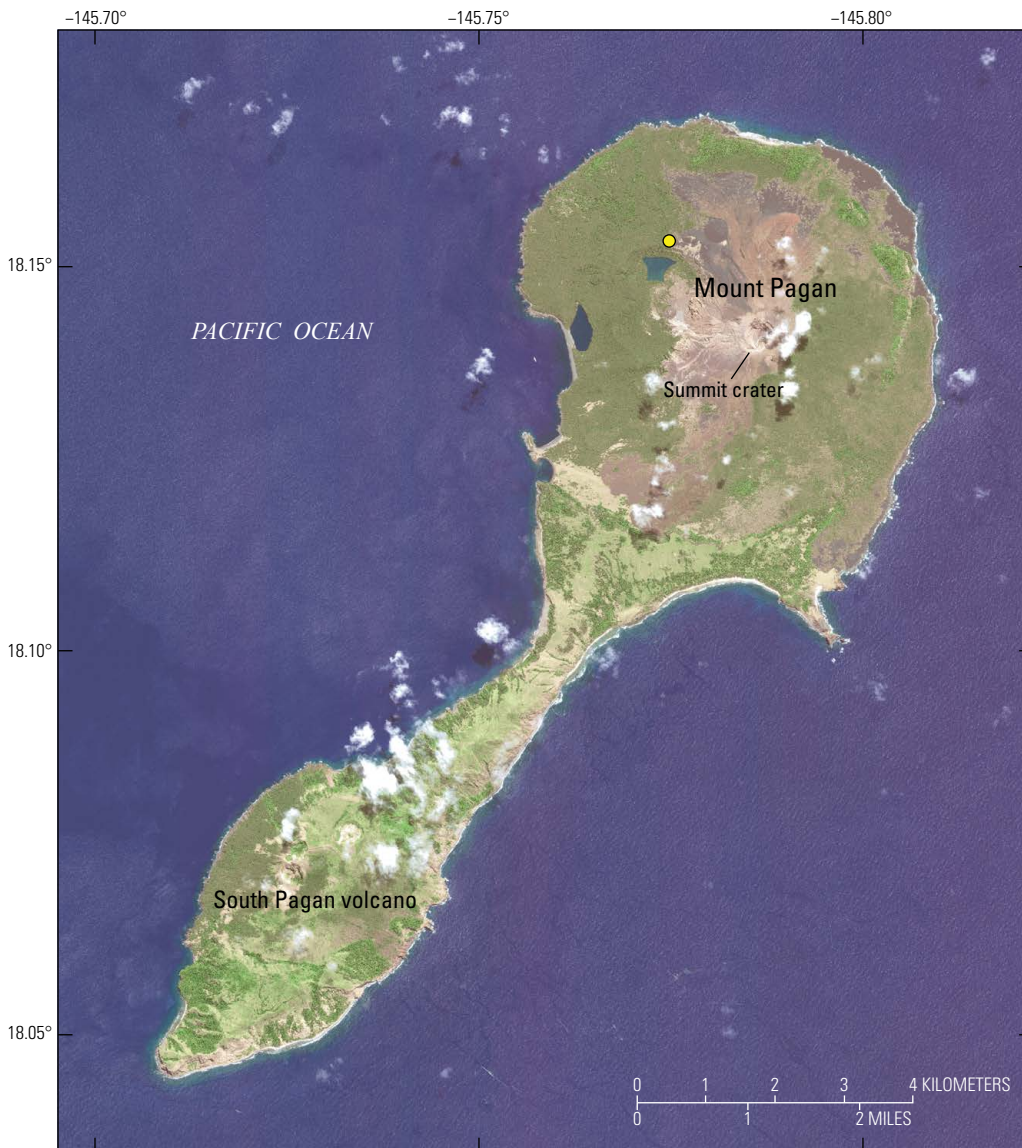


Figure 64. Annotated satellite image of Pagan Island showing Mount Pagan and South Pagan volcano. The yellow dot on Mount Pagan marks the approximate viewpoint of figure 65.

Mount Pagan erupted briefly in 2021. The first indication of its unrest came on the afternoon of July 29, when Pagan Island residents reported felt earthquakes and “light emission” from the crater (fig. 65). Residents stated that the weak gas emissions contained minor amounts of entrained volcanic ash. These observations represented a departure from normal background activity, so the USGS increased the Aviation Color Code and Volcano Alert Level of Mount Pagan from **UNASSIGNED** to **YELLOW** and **ADVISORY** later that day. In response to this heightened activity, the CNMI Office of Homeland Security and Emergency Management and the Department of Public Safety began evacuating the 14 residents of Pagan Island as a precautionary measure.

Throughout the month of August, satellites detected steam emissions and increasing amounts of SO_2 , suggesting that shallow degassing of magma was occurring. Figure 66

Figure 65. Screenshot from a video showing ash emissions from Mount Pagan on July 29, 2021 (Chamorro standard time). View is to the southeast. Video courtesy of the Commonwealth of the Northern Mariana Islands Office of Homeland Security and Emergency Management.

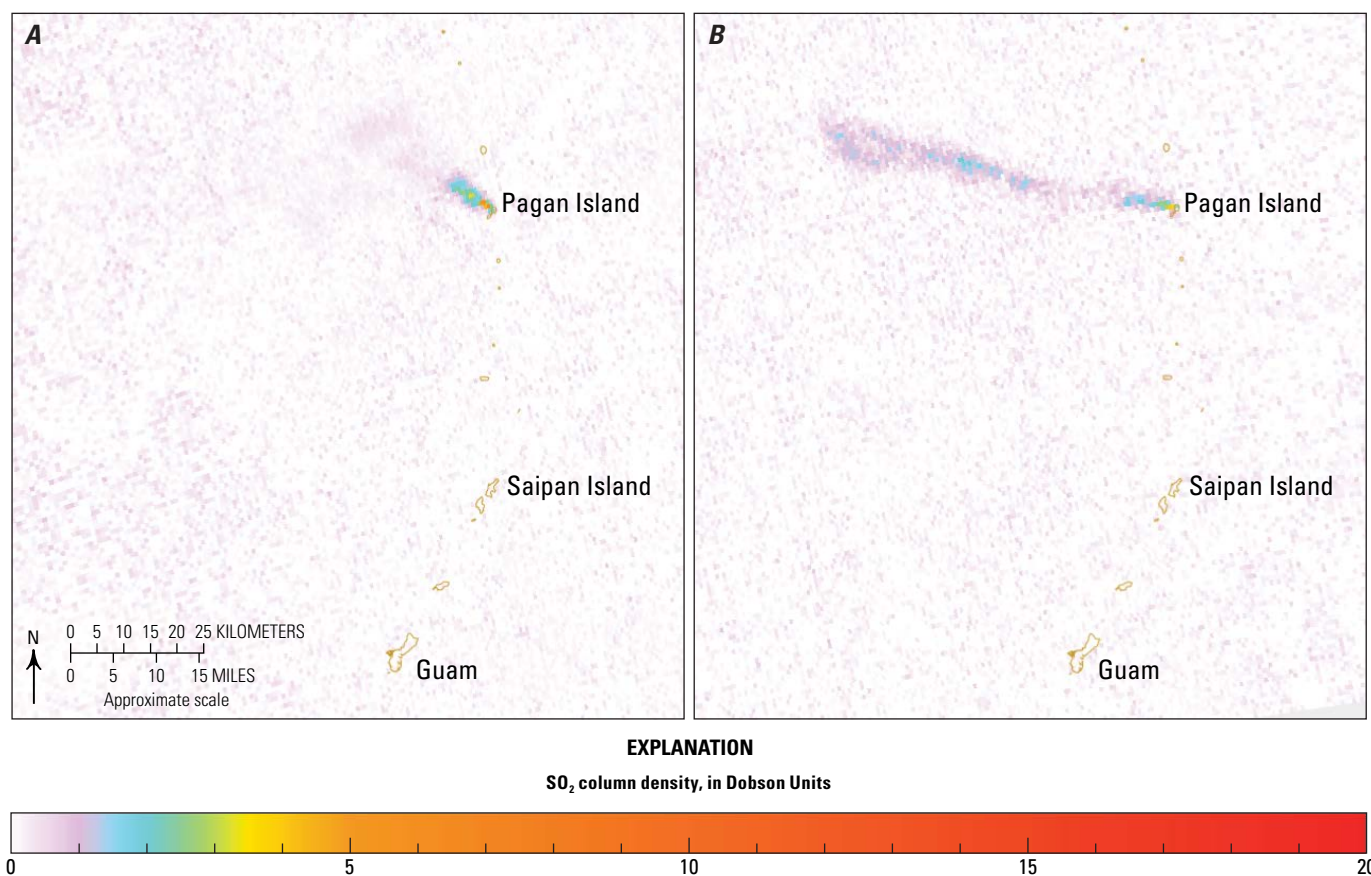


Figure 66. TROPOMI satellite images showing sulfur dioxide (SO_2) gas extending from Mount Pagan, Alaska. *A*, Image from August 15, 2021, at 03:31 coordinated universal time (UTC) (13:31 Chamorro standard time [ChST]), showing an SO_2 plume extending approximately (~) 80 kilometers (km) northwestward from Mount Pagan. *B*, Image from August 25, 2021, at 03:46 UTC (13:46 ChST), showing an SO_2 plume extending ~430 km westward from Mount Pagan.

shows representative TROPOMI satellite images of the SO₂ gas plume from August 15 and 25, which extended ~80 and ~430 km from the volcano, respectively.

Mount Pagan began continuously emitting low-altitude ash on August 31. The precise timing of onset for these emissions is impossible to determine because the eruption cloud was only discernible in daytime visible-wavelength images; although thermal infrared satellite images can detect high-altitude eruption clouds at night (owing to the temperature contrast between the cloud and the surface beneath it), discerning low-altitude eruption clouds can be extremely difficult. Ash first appeared in a Himawari-8 satellite image acquired on September 1 at ~07:00 ChST (August 31 at ~21:00 UTC), by which time the leading edge of the cloud was ~150 km west of Mount Pagan. Subsequent satellite images showed continued ash emissions through ~23:00 ChST (13:00 UTC) on September 1.

The USGS increased the Aviation Color Code and Volcano Alert Level of Mount Pagan to **ORANGE** and **WATCH** on September 2 at 04:44 ChST (September 1 at 18:44

UTC). Although the ash emissions had paused by that time, the alert level was increased on the basis of the potential for the resumption of eruptive activity. The following morning, visible-wavelength satellite data showed that ash emissions had resumed; by 10:26 ChST (00:26 UTC) on September 2, a sinuous ash plume extended more than 500 km westward at an altitude of ~10,000 ft (~3 km) ASL (fig. 67).

Ash and SO₂ emissions continued on a gradually declining trend through at least September 4 when high meteorological cloud cover moved into the region. Without local geophysical monitoring, the timing for the cessation of ash emissions could not be precisely determined. Clear satellite viewing conditions on September 7 showed that ash emissions had ceased, although robust steaming continued to be observed through September 10. With no observations of resumed eruptive activity, the Aviation Color Code and Volcano Alert Level were lowered from **ORANGE** and **WATCH** to **YELLOW** and **ADVISORY** on September 11 and to **UNASSIGNED** on September 25.

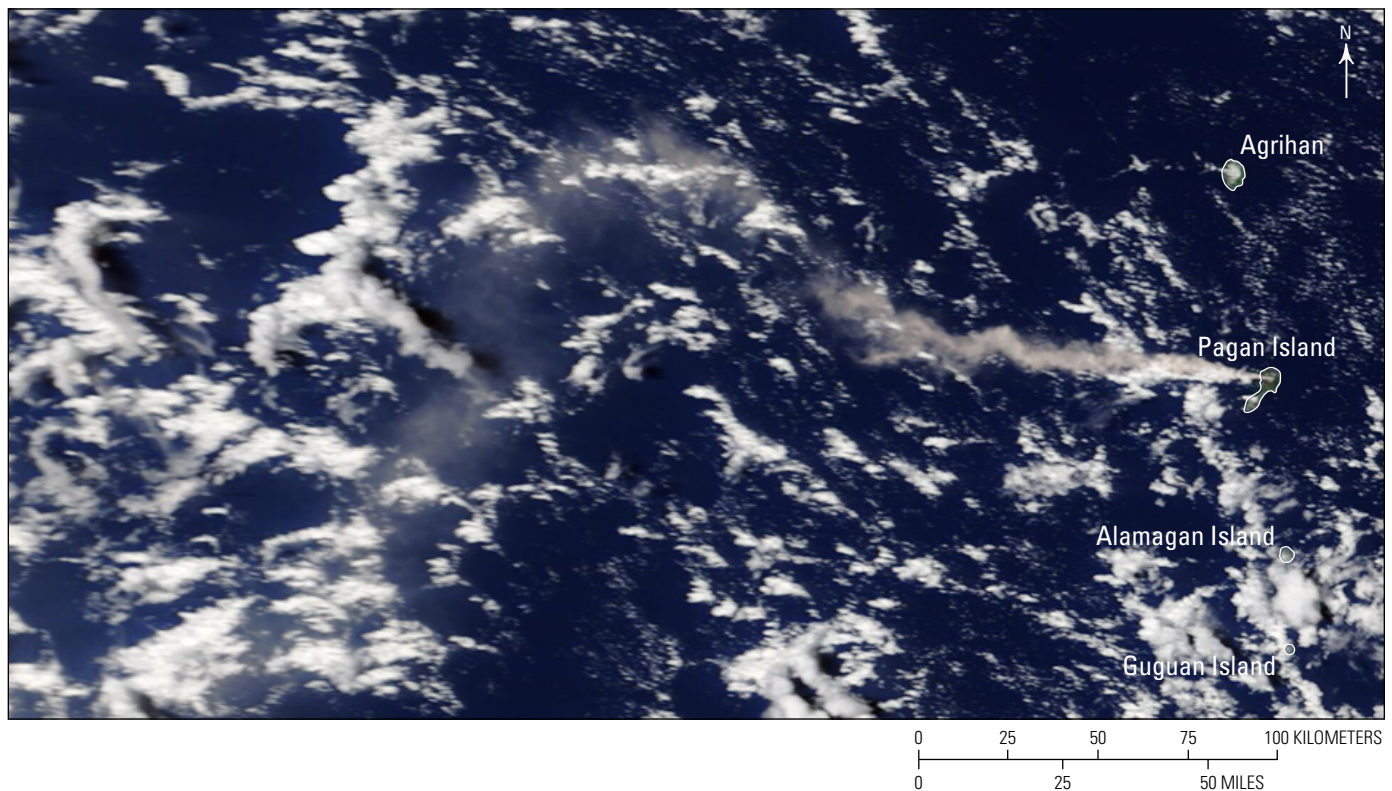


Figure 67. True-color satellite image (from the Moderate Resolution Imaging Spectroradiometer on the Terra satellite) showing a sinuous ash cloud extending more than 500 kilometers (km) westward from Mount Pagan at an altitude of 3 kilometers above sea level. Image acquired on September 2, 2021, at 00:26 coordinated universal time (10:26 Chamorro standard time).

References Cited

- Associated Press, 1974, Sitkin Island volcano puts on bright show: Fairbanks Daily News-Miner, February 21, 1974, p. 1.
- Bacon, C.R., Sisson, T.W., Calvert, A.T., and Nye, C.J., 2009, Geologic map of the 350 km³ basalt-to-dacite Veniaminof Volcano, Aleutian Arc [abs.]: Geological Society of America Abstracts with Programs, v. 41, no. 7, p. 660–661.
- Bacon, C.R., Neal, C.A., Miller, T.P., McGimsey, R.G., and Nye, C.J., 2014, Postglacial eruptive history, geochemistry, and recent seismicity of Aniakchak Volcano, Alaska: U.S. Geological Survey Professional Paper 1810, 74 p., <https://doi.org/10.3133/pp1810>.
- Banks, N.G., Koyanagi, R.Y., Sinton, J.M., and Honma, K.T., 1984, The eruption of Mount Pagan volcano, Mariana Islands, 15 May 1981: Journal of Volcanology and Geothermal Research, v. 22, no. 3–4, p. 225–269, [https://doi.org/10.1016/0377-0273\(84\)90004-0](https://doi.org/10.1016/0377-0273(84)90004-0).
- Begét, J.E., Larsen, J.F., Neal, C.A., Nye, C.J., and Schaefer, J.R., 2005, Preliminary volcano-hazard assessment for Okmok Volcano, Umnak Island, Alaska: Alaska Division of Geological & Geophysical Surveys Report of Investigation 2004-3, 1 sheet, scale 1:150,000, 32-p. pamphlet, <https://doi.org/10.14509/7042>.
- Byers, F.M., Jr., 1959, Geology of Umnak and Bogoslof Islands, Aleutian Islands, Alaska, *in* Investigations of Alaskan volcanoes: U.S. Geological Survey Bulletin 1028-L, p. 267–369, <https://doi.org/10.3133/b1028L>.
- Calvert, A.T., Moore, R.B., and McGimsey, R.G., 2005, Argon geochronology of Late Pleistocene to Holocene Westdahl Volcano, Unimak Island, Alaska, *in* Haeussler, P.J., and Galloway, J.P., eds., Studies by the U.S. Geological Survey in Alaska, 2004: U.S. Geological Survey Professional Paper 1709-D, 16 p., <https://doi.org/10.3133/pp1709D>.
- Cameron, C.E., Crass, S.W., and AVO Staff, eds., 2022, Geologic Database of Information on Volcanoes in Alaska (GeoDIVA): Alaska Division of Geological & Geophysical Surveys Digital Data Series 20, <https://doi.org/10.14509/30901>.
- Cameron, C.E., Schaefer, J.R., and Mulliken, K.M., 2018, Historically active volcanoes of Alaska: Alaska Division of Geological & Geophysical Surveys Miscellaneous Publication 133, v. 3, 2 sheets, <http://doi.org/10.14509/30142>.
- Cameron, C.E., Dixon, J.P., Waythomas, C.F., Iezzi, A.M., Wallace, K.L., McGimsey, R.G., and Bull, K.F., 2020, 2016 Volcanic activity in Alaska—Summary of events and response of the Alaska Volcano Observatory: U.S. Geological Survey Scientific Investigations Report 2020–5125, 63 p., <https://doi.org/10.3133/sir20205125>.
- Cameron, C.E., Orr, T.R., Dixon, J.P., Dietterich, H.R., Waythomas, C.F., Iezzi, A.M., Power, J.A., Searcy, C., Grapenthin, R., Tepp, G., Wallace, K.L., Lopez, T.M., DeGrandpre, K., and Perreault, J.M., 2023, 2018 Volcanic activity in Alaska—Summary of events and response of the Alaska Volcano Observatory: U.S. Geological Survey Scientific Investigations Report 2023–5029, 68 p., <https://doi.org/10.3133/sir20235029>.
- Caplan-Auerbach, J., and Huggel, C., 2007, Precursory seismicity associated with frequent, large ice avalanches on Iliamna volcano, Alaska, USA: Journal of Glaciology, v. 53, no. 180, p. 128–140, <http://doi.org/10.3189/172756507781833866>.
- Coats, R.R., 1959, Geologic reconnaissance of Gareloi Island, Aleutian Islands, Alaska, *in* Investigations of Alaskan volcanoes: U.S. Geological Survey Bulletin 1028-J, p. 249–256, 1 sheet, scale 1:36,000, <https://doi.org/10.3133/b1028J>.
- Coombs, M.L., Neal, C.A., Wessels, R.L., and McGimsey, R.G., 2006, Geothermal disruption of summit glaciers at Mount Spurr Volcano, 2004–6; an unusual manifestation of volcanic unrest: U.S. Geological Survey Professional Paper 1732-B, 33 p., <https://doi.org/10.3133/pp1732B>.
- Coombs, M.L., McGimsey, R.G., and Browne, B.L., 2012, Geologic map of Mount Gareloi, Gareloi Island, Alaska: U.S. Geological Survey Scientific Investigations Map 3145, 1 sheet, scale 1:24,000, 18-p. pamphlet, <https://doi.org/10.3133/sim3145>.
- Coombs, M.L., Larsen, J.F., and Neal, C.A., 2018, Postglacial eruptive history and geochemistry of Semisopochnoi volcano, western Aleutian Islands, Alaska: U.S. Geological Survey Scientific Investigations Report 2017–5150, 33 p., <https://doi.org/10.3133/sir20175150>.
- Dean, K.G., Engle, K., Groves, J., Dehn, J., and Partington, K., 2002, Analysis of surface processes using SAR data; Westdahl Volcano, Alaska: International Journal of Remote Sensing, v. 23, no. 21, p. 4529–4550, <https://doi.org/10.1080/01431160110113953>.
- Dean, K.G., Dehn, J., Papp, K.R., Smith, S., Izbekov, P., Peterson, R., Kearney, C., and Steffke, A., 2004, Integrated satellite observations of the 2001 eruption of Mt. Cleveland, Alaska: Journal of Volcanology and Geothermal Research, v. 135, no. 1–2, p. 51–73, <https://doi.org/10.1016/j.jvolgeores.2003.12.013>.
- DeGrandpre, K.G., Wang, T., Lu, Z., and Freymueller, J.T., 2017, Episodic inflation and complex surface deformation of Akutan volcano, Alaska revealed from GPS time-series: Journal of Volcanology and Geothermal Research, v. 347, p. 337–359, <https://doi.org/10.1016/j.jvolgeores.2017.10.003>.

- DeGrandpre, K.G., Pesicek, J.D., Lu, Zhong, DeShon, H.R., and Roman, D.C., 2019, High rates of inflation during a noneruptive episode of seismic unrest at Semisopchnoi Volcano, Alaska in 2014–2015: *Geochemistry, Geophysics, Geosystems*, v. 20, no. 12, p. 6163–6186, <https://doi.org/10.1029/2019GC008720>.
- Dixon, J.P., Stihler S.D., Haney, M.M., Lyons, J.J., Ketner, D.M., Mulliken, K.M., Parker, T., and Power, J.A., 2019, Catalog of earthquake parameters and description of seismograph and infrasound stations at Alaskan volcanoes—January 1, 2013, through December 31, 2017: U.S. Geological Survey Data Series 1115, 92 p., <https://doi.org/10.3133/ds1115>.
- Dixon, J.P., Cameron, C.E., Iezzi, A.M., Power, J.A., Wallace, K., Waythomas, C.F., 2020, 2017 Volcanic activity in Alaska—Summary of events and response of the Alaska Volcano Observatory: U.S. Geological Survey Scientific Investigations Report 2020–5102, 61 p., <https://doi.org/10.3133/sir20205102>.
- Dreher, S.T., Eichelberger, J.C., and Larsen, J.F., 2005, The petrology and geochemistry of the Aniakchak caldera-forming ignimbrite, Aleutian Arc, Alaska: *Journal of Petrology*, v. 46, no. 9, p. 1747–1768, <https://doi.org/10.1093/petrology/egi032>.
- Fee, D., Haney, M.H., Matoza, R.S., Van Eaton, A.R., Cervelli, P., Schneider, D.J., and Iezzi, A.M., 2017, Volcanic tremor and plume height hysteresis from Pavlof Volcano, Alaska: *Science*, v. 355, no. 6320, p. 45–48, <https://doi.org/10.1126/science.aah6108>.
- Fischer, T.P., Lopez, T.M., Aiuppa, A., Rizzo, A.L., Ilanko, T., Kelley, K. and Cottrell, E., 2021, Gas emissions from the Western Aleutians volcanic arc: *Frontiers in Earth Science*, v. 9, article 786021, 17 p., <https://doi.org/10.3389/feart.2021.786021>.
- Freymueller, J.T., and Kaufman, A.M., 2010, Changes in the magma system during the 2008 eruption of Okmok volcano, Alaska, based on GPS measurements: *Journal of Geophysical Research*, v. 115, no. B12, article B12415, <https://doi.org/10.1029/2010JB007716>.
- Gardner, J.E., Burgisser, A., and Stelling, P., 2007, Eruption and deposition of the Fisher Tuff (Alaska)—Evidence for the evolution of pyroclastic flows: *Journal of Geology*, v. 115, no. 4, p. 417–435, <https://doi.org/10.1086/518050>.
- Gardner, C.A., and Guffanti, M.C., 2006, U.S. Geological Survey’s alert notification system for volcanic activity: U.S. Geological Survey Fact Sheet 2006–3139, 4 p., <https://doi.org/10.3133/fs20063139>.
- Gunawan, H., Caudron, C., Pallister, J., Primulyana, S., Christenson, B., McCausland, W., Van Hinsberg, V., Lewicki, J., Rouwet, D., Kelly, P., Kern, C., Werner, C., Johnson, J.B., Utami, S.B., Syahbana, D.K., Saing, U., Suparjan, Purwanto, B.H., Sealing, C., Cruz, M.M., Maryanto, S., Bani, P., Laurin, A., Schmid, A., Bradley, K., Agung Nandaka, I.G.M., and Hendrasto, M., 2017, New insights into Kawah Ijen’s volcanic system from the wet volcano workshop experiment, *in* Ohba, T., Capaccioni, B., and Caudron, C., eds., *Geochemistry and geophysics of active volcanic lakes*: Geological Society of London, Special Publications, v. 437, p. 35–56, <https://doi.org/10.1144/SP437.7>.
- Hadley, D., Hufford, G.L., and Simpson, J.J., 2004, Resuspension of relic volcanic ash and dust from Katmai—Still an aviation hazard: *Weather and Forecasting*, v. 19, no. 5, p. 829–840, [https://doi.org/10.1175/1520-0434\(2004\)019<0829:RORVAA>2.0.CO;2](https://doi.org/10.1175/1520-0434(2004)019<0829:RORVAA>2.0.CO;2).
- Harris, K., Caplan-Auerbach, J., and Power, J.A., 2021, What counts as unrest? Exceptionally high rates of background seismicity at Gareloi Volcano, Alaska during a period of volcanic quiescence [abs.]: *Eos, Transactions, American Geophysical Union, Fall Meeting Supplement*, abstract V22B-07, accessed January 13, 2023, at <https://ui.adsabs.harvard.edu/abs/2021AGUFM.V22B..07H>.
- Herrick, J.A., Neal, C.A., Cameron, C.E., Dixon, J.P., and McGimsey, R.G., 2014, 2012 Volcanic activity in Alaska—Summary of events and response of the Alaska Volcano Observatory: U.S. Geological Survey Scientific Investigations Report 2014–5160, 92 p., <https://doi.org/10.3133/sir20145160>.
- Hildreth, W., and Fierstein, J., 2000, Katmai volcanic cluster and the great eruption of 1912: *Geological Society of America Bulletin*, v. 112, no. 10, p. 1594–1620, [https://doi.org/10.1130/0016-7606\(2000\)112<1594:KVCATG>2.0.CO;2](https://doi.org/10.1130/0016-7606(2000)112<1594:KVCATG>2.0.CO;2).
- Hildreth, W., and Fierstein, J., 2012, The Novarupta-Katmai eruption of 1912—Largest eruption of the twentieth century; centennial perspectives: U.S. Geological Survey Professional Paper 1791, 259 p., <https://doi.org/10.3133/pp1791>.
- Hilton, D.R., Hammerschmidt, K., Teufel, S. and Friedrichsen, H., 1993, Helium isotope characteristics of Andean geothermal fluids and lavas: *Earth and Planetary Science Letters*, v. 120, no. 3–4, p. 265–282, [https://doi.org/10.1016/0012-821X\(93\)90244-4](https://doi.org/10.1016/0012-821X(93)90244-4).
- Iezzi, A.M., Fee, D., Haney, M.M., and Lyons, J.J., 2020, Seismo-acoustic characterization of Mount Cleveland volcano explosions: *Frontiers in Earth Science*, v. 8, p. 1–19, <https://doi.org/10.3389/feart.2020.573368>.

- Keith, T.E.C., ed., 1995, The 1992 eruptions of Crater Peak Vent, Mount Spurr volcano, Alaska: U.S. Geological Survey Bulletin 2139, 220 p., <https://doi.org/10.3133/b2139>.
- Larsen, J.F., Neal, C., Schaefer, J., Begét, J., and Nye, C., 2007, Late Pleistocene and Holocene caldera-forming eruptions of Okmok Caldera, Aleutian Islands, Alaska, *in* Eichelberger, J., Gordeev, E., Izbekov, P., Kasahara, M., and Lees, J., eds., *Volcanism and subduction—The Kamchatka region*: American Geophysical Union, Geophysical Monograph Series, v. 172, p. 343–364, <https://doi.org/10.1029/172GM24>.
- Lee, C.-W., Lu, Z., Jung, H.-S., Won, J.-S., and Dzurisin, D., 2010, Surface deformation of Augustine Volcano, 1992–2005, from multiple-interferogram processing using a refined small baseline subset (SBAS) interferometric synthetic aperture radar (InSAR) approach, chap. 18 *of* Power, J.A., Coombs, M.L., and Freymueller, J.T., eds., *The 2006 eruption of Augustine Volcano, Alaska*: U.S. Geological Survey Professional Paper 1769, p. 453–465, <https://doi.org/10.3133/pp176918>.
- Loewen, M.W., Dietterich, H.R., Graham, N., and Izbekov, P., 2021, Evolution in eruptive style of the 2018 eruption of Veniaminof volcano, Alaska, reflected in groundmass textures and remote sensing: *Bulletin of Volcanology*, v. 83, no. 72, 19 p., <https://doi.org/10.1007/s00445-021-01489-6>.
- Loewen, M.W., Dietterich, H.R., and Rosenkrans, H.S., 2023, Davidof volcano samples and analyses: Alaska Division of Geological & Geophysical Surveys Raw Data File 2023-22, 4 p., <https://doi.org/10.14509/31084>.
- Lopez, T., Tassi, F., Aiuppa, A., Galle, B., Rizzo, A.L., Fiebig, J., Capecchiacci, F., Giudice, G., Caliro, S., Tamburello, G., 2017, Geochemical constraints on volatile sources and subsurface conditions at Mount Martin, Mount Mageik, and Trident Volcanoes, Katmai Volcanic Cluster, Alaska: *Journal of Volcanology and Geothermal Research*, v. 347, p. 64–81, <https://doi.org/10.1016/j.jvolgeores.2017.09.001>.
- Lu, Z., Wicks, C., Jr., Power, J.A., and Dzurisin, D., 2000, Ground deformation associated with the March 1996 earthquake swarm at Akutan volcano, Alaska, revealed by satellite radar interferometry: *Journal of Geophysical Research*, v. 105, no. B9, p. 21,483–21,496, <https://doi.org/10.1029/2000JB900200>.
- Lu, Z., and Dzurisin, D., 2014, *InSAR imaging of Aleutian volcanoes*: Springer Praxis Books. Springer, Berlin, Heidelberg, 390 p., https://doi.org/10.1007/978-3-642-00348-6_6.
- Mangan, M., Miller, T., Waythomas, C., Trusdell, F., Calvert, A., and Layer, P., 2009, Diverse lavas from closely spaced volcanoes drawing from a common parent: Emmons Lake Volcanic Center, Eastern Aleutian Arc: *Earth and Planetary Science Letters*, v. 287, p. 363–372, <https://doi.org/10.1016/j.epsl.2009.08.018>.
- Massimetti, F., Coppola, D., Laiolo, M., Valade, S., Cigolini, C., and Ripepe, M., 2020, Volcanic hot-spot detection using SENTINEL-2—A comparison with MODIS—MIROVA thermal data series: *Remote Sensing*, v. 12, no. 5, 32 p., <https://doi.org/10.3390/rs12050820>.
- McGimsey, R.G., Neal, C.A., and Doukas, M.P., 1995, 1992 Volcanic activity in Alaska—Summary of events and response of the Alaska Volcano Observatory: U.S. Geological Survey Open-File Report 95–83, 26 p., <https://doi.org/10.3133/ofr9583>.
- McGimsey, R.G., and Neal, C.A., 1996, 1995 Volcanic activity in Alaska and Kamchatka—Summary of events and response of the Alaska Volcano Observatory: U.S. Geological Survey Open-File Report 96-738, 23 p., <https://doi.org/10.3133/ofr96738>.
- McGimsey, R.G., Neal, C.A., and Girina, O., 2005, 2001 Volcanic activity in Alaska and Kamchatka—Summary of events and response of the Alaska Volcano Observatory: U.S. Geological Survey Open-File Report 2004–1453, 57 p., <https://doi.org/10.3133/ofr20041453>.
- McGimsey, R.G., Neal, C.A., Dixon, J.P., and Ushakov, S., 2007, 2005 Volcanic activity in Alaska, Kamchatka, and the Kurile Islands—Summary of events and response of the Alaska Volcano Observatory: U.S. Geological Survey Scientific Investigations Report 2007–5269, 94 p., <https://doi.org/10.3133/sir20075269>.
- Miller, T.P., and Smith, R.L., 1977, Spectacular mobility of ash flows around Aniakchak and Fisher calderas, Alaska: *Geology*, v. 5, no. 3, p. 173–176, [https://doi.org/10.1130/0091-7613\(1977\)5<173:SMOFAFA>2.0.CO;2](https://doi.org/10.1130/0091-7613(1977)5<173:SMOFAFA>2.0.CO;2).
- Miller, T.P., and Smith, R.L., 1987, Late Quaternary caldera-forming eruptions in the eastern Aleutian arc, Alaska: *Geology*, v. 15, no. 5, p. 434–438, [https://doi.org/10.1130/0091-7613\(1987\)15<434:LQCEIT>2.0.CO;2](https://doi.org/10.1130/0091-7613(1987)15<434:LQCEIT>2.0.CO;2).
- Miller, T.P., McGimsey, R.G., Richter, D.H., Riehle, J.R., Nye, C.J., Yount, M.E., and Dumoulin, J.A., 1998, *Catalog of the historically active volcanoes of Alaska*: U.S. Geological Survey Open-File Report 98-582, 104 p., <https://doi.org/10.3133/ofr98582>.
- Motyka, R.J., Poreda, R.J., and Jeffrey, A.W.A., 1989, Geochemistry, isotopic composition, and origin of fluids emanating from mud volcanoes in the Copper River basin, Alaska: *Geochimica et Cosmochimica Acta*, v. 53, no. 1, p. 29–41, [https://doi.org/10.1016/0016-7037\(89\)90270-6](https://doi.org/10.1016/0016-7037(89)90270-6).
- Motyka, R.J., Liss, S.A., Nye, C.J., and Moorman, M.A., 1993, *Geothermal resources of the Aleutian arc*: Alaska Division of Geological & Geophysical Surveys Professional Report 114, 4 sheets, scale 1:1,000,000, 17-p. pamphlet, <https://doi.org/10.14509/2314>.

- Neal, C.A., McGimsey, R.G., Miller, T.P., Riehle, J.R., and Waythomas, C.F., 2000, Preliminary volcano-hazard assessment for Aniakchak Volcano, Alaska: U.S. Geological Survey Open-File Report 00–519, 35 p., <https://doi.org/10.3133/ofr00519>.
- Neal, C.A., McGimsey, R.G., Dixon, J.P., and Melnikov, D., 2005, 2004 Volcanic activity in Alaska and Kamchatka—Summary of events and response of the Alaska Volcano Observatory: U.S. Geological Survey Open-File Report 2005–1308, 71 p., <https://doi.org/10.3133/ofr20051308>.
- Neal, C.A., McGimsey, R.G., Dixon, J.P., Manevich, A., and Rybin, A., 2009, 2006 Volcanic activity in Alaska, Kamchatka, and the Kurile Islands—Summary of events and response of the Alaska Volcano Observatory: U.S. Geological Survey Scientific Investigations Report 2008–5214, 102 p., <https://doi.org/10.3133/sir20085214>.
- Neal, C.A., McGimsey, R.G., Dixon, J.P., Cameron, C.E., Nuzhaev, A.A., and Chibisova, M., 2011, 2008 Volcanic activity in Alaska, Kamchatka, and the Kurile Islands—Summary of events and response of the Alaska Volcano Observatory: U.S. Geological Survey Scientific Investigations Report 2010–5243, 94 p., <https://doi.org/10.3133/sir20105243>.
- Neal, C.A., Herrick, J., Girina, O.A., Chibisova, M., Rybin, A., McGimsey, R.G., and Dixon, J.P., 2014, 2010 Volcanic activity in Alaska, Kamchatka, and the Kurile Islands—Summary of events and response of the Alaska Volcano Observatory: U.S. Geological Survey Scientific Investigations Report 2014–5034, 76 p., <http://doi.org/10.3133/sir20145034>.
- Nichols, D.R. and Yehle, L.A., 1961, Mud volcanoes in the Copper River Basin, Alaska, *in* Raasch, G.O., ed., *Geology of the Arctic—Proceedings of the First International Symposium on Arctic Geology*: Toronto, Canada, University of Toronto Press, 3 v., p. 1063–1087.
- Nicholson, R.S., Gardner, J.E., and Neal, C.A., 2011, Variations in eruption style during the 1931 A.D. eruption of Aniakchak volcano, Alaska: *Journal of Volcanology and Geothermal Research*, v. 207, no. 3–4, p. 69–82, <https://doi.org/10.1016/j.jvolgeores.2011.08.002>.
- Nye, C.J., and Turner, D.L., 1990, Petrology, geochemistry, and age of the Spurr volcanic complex, eastern Aleutian arc: *Bulletin of Volcanology*, v. 52, no. 3, p. 205–226, <https://doi.org/10.1007/BF00334805>.
- Nye, C.J., Keith, T.E.C., Eichelberger, J.C., Miller, T.P., McNutt, S.R., Moran, S., Schneider, D.J., Dehn, J., and Schaefer, J.R., 2002, The 1999 eruption of Shishaldin Volcano, Alaska: monitoring a distant eruption: *Bulletin of Volcanology*, v. 64, no. 8, p. 507–519, <https://doi.org/10.1007/s00445-002-0225-2>.
- Orr, T.R., Cameron, C.E., Dietterich, H.R., Dixon, J.P., Enders, M.L., Grapenthin, R., Iezzi, A.M., Loewen, M.W., Power, J.A., Searcy, C., Tepp, G., Toney, L., Waythomas, C.F., and Wech, A.G., 2023, 2019 Volcanic activity in Alaska—Summary of events and response of the Alaska Volcano Observatory: U.S. Geological Survey Scientific Investigations Report 2023–5039, 64 p., <http://doi.org/10.3133/sir20235039>.
- Pavolonis, M.J., Sieglaff, J., and Cintineo, J., 2018, Automated detection of explosive volcanic eruptions using satellite-derived cloud vertical growth rates: *Earth and Space Science*, v. 5, no. 12, p. 903–928, <https://doi.org/10.1029/2018EA000410>.
- Pesicek, J.D., Wellik, J.J., II, Prejean, S.G., and Ogburn, S.E., 2018, Prevalence of seismic rate anomalies preceding volcanic eruptions in Alaska: *Frontiers in Earth Science*, v. 6, article 100, <https://doi.org/10.3389/feart.2018.00100>.
- Platt, U., and Stutz, J., 2008, *Physics of Earth and space environments—Differential optical absorption spectroscopy—Principles and applications*: Berlin-Heidelberg, Germany, Springer-Verlag, 598 p., <https://doi.org/10.1007/978-3-540-75776-4>.
- Poland, M.P., Lopez, T., Wright, R., and Pavolonis, M.J., 2020, Forecasting, detecting, and tracking volcanic eruptions from space: *Remote Sensing in Earth Systems Sciences*, v. 3, no. 1, p. 55–94, <https://doi.org/10.1007/s41976-020-00034-x>.
- Power, J.A., 2004, Renewed unrest at Mount Spurr volcano, Alaska: *Eos, Transactions, American Geophysical Union*, v. 85, no. 43, p. 434, <https://doi.org/10.1029/2004EO430004>.
- Power, J.A., Stihler, S.D., Dixon, J.P., Moran, S.C., Caplan-Auerbach, J., Prejean, S.G., McGee, K., Doukas, M.P., and Roman, D.C., 2004, Renewed seismic unrest at Mount Spurr Volcano, Alaska in 2004—Evidence for a magmatic intrusion [abs.]: *Eos, Transactions, American Geophysical Union*, v. 85, no. 47, Fall Meeting Supplement, abstract S51A-0143.
- Prejean, S.G., Werner, C.A., Buurman, H., Doukas, M.P., Kelly, P.J., Kern, C., Ketner, D.M., Stihler, S.D., Thurber, C.H., and West, M.E., 2012, Seismic and gas analyses imply magmatic intrusion at Iliamna Volcano, Alaska in 2012 [abs.]: *Eos, Transactions, American Geophysical Union*, v. 93, Fall Meeting Supplement, abstract V53B-2826.
- Reeder, J.W., 1990, Sugarloaf, *in* *Annual report of the world volcanic eruptions in 1987*: *Bulletin of Volcanic Eruptions*, v. 27, p. 36.

- Richter, D.H., Symonds, R.B., Rosenkrans, D.S., McGimsey, R.G., Evans, W.C., and Poreda, R.J., 1998a, Report on the 1997 activity of Shrub mud volcano, Wrangell-St. Elias National Park and Preserve, south central Alaska: U.S. Geological Survey Open-File Report 98-128, 13 p., <https://doi.org/10.3133/ofr98128>.
- Richter, D.H., Waythomas, C.F., McGimsey, R.G., and Stelling, P.L., 1998b, Geology of Akutan Island: U.S. Geological Survey Open-File Report 98-135, 1 sheet, scale 1:48,000, 22-p. pamphlet, <https://doi.org/10.3133/ofr98135>.
- Riehle, J.R., 1985, A reconnaissance of the major Holocene tephra deposits in the upper Cook Inlet region, Alaska: *Journal of Volcanology and Geothermal Research*, v. 26, no. 1–2, p. 37–74, [https://doi.org/10.1016/0377-0273\(85\)90046-0](https://doi.org/10.1016/0377-0273(85)90046-0).
- Roman, D.C., Power, J.A., Moran, S.C., Cashman, K.V., Doukas, M.P., Neal, C.A., and Gerlach, T.M., 2004, Evidence for dike emplacement beneath Iliamna Volcano, Alaska in 1996: *Journal of Volcanology and Geothermal Research*, v. 130, no. 3–4, p. 265–284, [https://doi.org/10.1016/S0377-0273\(03\)00302-0](https://doi.org/10.1016/S0377-0273(03)00302-0).
- Schneider, D., Bartelt, P., Caplan-Auerbach, J., Christen, M., Huggel, C., and McArdell, B.W., 2010, Insights into rock-ice avalanche dynamics by combined analysis of seismic recordings and a numerical avalanche model: *Journal of Geophysical Research*, v. 115, no. F4, article F04026, 20 p., <https://doi.org/10.1029/2010JF001734>.
- Siebert, L., Simkin, T., and Kimberly, P., 2010, *Volcanoes of the World* (3d ed.): Berkley, Calif., University of California Press, 568 p.
- Simons, F.S., and Mathewson, D.E., 1955, Geology of Great Sitkin Island, Alaska, *in* *Investigations of Alaskan volcanoes*: U.S. Geological Survey Bulletin 1028-B, <https://doi.org/10.3133/b1028B>.
- Snyder, G.L., 1959, Geology of Little Sitkin Island, Alaska, *in* *Investigations of Alaskan volcanoes*: U.S. Geological Survey Bulletin 1028-H, p. 169–210, <https://doi.org/10.3133/b1028H>.
- Stelling, P., Gardner, J.E., and Begét, J., 2005, Eruptive history of Fisher Caldera, Alaska, USA: *Journal of Volcanology and Geothermal Research*, v. 139, no. 3–4, p. 163–183, <https://doi.org/10.1016/j.jvolgeores.2004.08.006>.
- Symonds, R.B., Poreda, R.J., Evans, W.C., Janik, C.J., and Ritchie, B.E., 2003, Mantle and crustal sources of carbon, nitrogen, and noble gases in Cascade-Range and Aleutian-Arc volcanic gases: U.S. Geological Survey Open-File Report 2003–436, 26 p., <https://doi.org/10.3133/ofr03436>.
- Toney, L., Fee, D., Allstadt, K.E., Haney, M.M., and Matoza, R.S., 2021, Reconstructing the dynamics of the highly similar May 2016 and June 2019 Iliamna Volcano (Alaska) ice–rock avalanches from seismoacoustic data: *Earth Surface Dynamics*, v. 9, no. 2, p. 271–293, <https://doi.org/10.5194/esurf-9-271-2021>.
- Trusdell, F.A., Moore, R.B., and Sako, M.K., 2006, Preliminary geologic map of Mount Pagan Volcano, Pagan Island, Commonwealth of the Northern Mariana Islands: U.S. Geological Survey Open-File Report 2006-1386, 32 p., <https://doi.org/10.3133/ofr20061386>.
- University of Turin and University of Florence, 2022, Middle Infrared Observations of Volcanic Activity [database]: MIROVA website, accessed August 29, 2022, at <https://www.mirovaweb.it>.
- Wallace, K.L., and Schwaiger, H.F., 2019, Volcanic ash resuspension from the Katmai region: *Alaska Park Science*, v. 18, no. 1, p. 63–70. [Also available at <https://www.nps.gov/articles/aps-18-1-download.htm>.]
- Waythomas, C.F., and Miller, T.P., 1999, Preliminary volcano-hazard assessment for Iliamna Volcano, Alaska: U.S. Geological Survey Open-File Report 99-373, 31 p., <https://doi.org/10.3133/ofr99373>.
- Waythomas, C.F., Power, J.A., Richter, D.H., and McGimsey, R.G., 1998, Preliminary volcano-hazard assessment for Akutan Volcano, east-central Aleutian Islands, Alaska: U.S. Geological Survey Open-File Report 98-360, 36 p., <https://doi.org/10.3133/ofr98360>.
- Waythomas, C.F., Miller, T.P., and Begét, J.E., 2000, Record of Late Holocene debris avalanches and lahars at Iliamna Volcano, Alaska: *Journal of Volcanology and Geothermal Research*, v. 104, no. 1–4, p. 97–130, [https://doi.org/10.1016/S0377-0273\(00\)00202-X](https://doi.org/10.1016/S0377-0273(00)00202-X).
- Waythomas, C.F., Miller, T.P., and Nye, C.J., 2003a, Preliminary geologic map of Great Sitkin Volcano, Alaska, U.S. Geological Survey Open-File Report 2003–36, <https://doi.org/10.3133/ofr0336>.
- Waythomas, C.F., Miller, T.P., and Nye, C.J., 2003b, Preliminary volcano-hazard assessment for Great Sitkin Volcano, Alaska: U.S. Geological Survey Open-File Report 2003–112, 32 p., <https://doi.org/10.3133/ofr03112>.
- Waythomas, C.F., Miller, T.P., and Mangan, M.T., 2006, Preliminary Volcano Hazard Assessment for the Emmons Lake volcanic center, Alaska: U.S. Geological Survey Scientific Investigations Report 2006–5248, 41 p., <https://doi.org/10.3133/sir20065248>.

- Waythomas, C.F., Haney, M.M., Wallace, K.L., Cameron, C.E., and Schneider, D.J., 2017, The 2014 eruptions of Pavlof Volcano, Alaska: U.S. Geological Survey Scientific Investigations Report 2017–5129, 27 p., <https://doi.org/10.3133/sir20175129>.
- Waythomas, C., 2021, Simultaneous effusive and explosive cinder cone eruptions at Veniaminof Volcano, Alaska: *Volcanica*, v. 4, no. 2, p. 295–307, <https://doi.org/10.30909/vol.04.02.295307>.
- Werner, C.A., Doukas, M.P., and Kelly, P.J., 2011, Gas emission from failed and actual eruptions from Cook Inlet volcanoes, Alaska, 1989–2006: *Bulletin of Volcanology*, v. 73, no. 2, p. 155–173, <https://doi.org/10.1007/s00445-011-0453-4>.
- Werner, C., Kern, C., Coppola, D., Lyons, J.J., Kelly, P.J., Wallace, K.L., Schneider, D.J., Wessels, R.L., 2017, Magmatic degassing, lava dome extrusion, and explosions from Mount Cleveland volcano, Alaska, 2011–2015—Insight into the continuous nature of volcanic activity over multi-year timescales: *Journal of Volcanology and Geothermal Research*, v. 337, p. 98–110, <https://doi.org/10.1016/j.jvolgeores.2017.03.001>.
- Werner, C., Power, J.A., Kelly, P.J., Prejean, S., Kern, C., 2022, Characterizing unrest—A retrospective look at 20 years of gas emissions and seismicity at Iliamna Volcano, Alaska: *Journal of Volcanology and Geothermal Research*, v. 422, article 107448, <https://doi.org/10.1016/j.jvolgeores.2021.107448>.
- Wood, C.A., and Kienle, J., 1990, *Volcanoes of North America*: New York, Cambridge University Press, 354 p.
- Yokoo, A., Tameguri, T., and Iguchi, M., 2009, Swelling of a lava plug associated with a Vulcanian eruption at Sakurajima Volcano, Japan, as revealed by infrasound record: case study of the eruption on January 2, 2007: *Bulletin of Volcanology*, v. 71, no. 6, p. 619–630, <https://doi.org/10.1007/s00445-008-0247-5>.

Glossary of Selected Terms and Acronyms

A

andesite Volcanic rock composed of about 57–63 weight percent silica (SiO₂).

ash Fine fragments (less than 2 millimeters across) of rock formed in an explosive volcanic eruption.

B

basaltic andesite Volcanic rock composed of about 52–57 weight percent SiO₂.

breadcrust bomb Volcanic bomb (pyroclast >6.4 cm) with a cracked and checkered surface, sometimes resembling the surface of a loaf of bread.

C

caldera Large, roughly circular depression usually caused by volcanic collapse or explosion.

D

dacite Volcanic rock composed of about 63–69 weight percent SiO₂.

Dobson Unit (DU) The standard unit used to depict the amount of sulfur dioxide (SO₂) gas present. Equivalent to 2.69 × 10²⁰ molecules (0.0285 grams) per square meter.

F

fallout General term for debris, which falls to the Earth from an eruption cloud.

fumarole Small opening or vent from which hot gases are emitted.

H

Holocene Geologic epoch that extends from the present to 11,700 years ago.

I

infrasound Low-frequency sound waves, below the threshold of human hearing.

intracaldera Adjective referring to within the caldera.

J

juvenile Adjective describing volcanic material created from magma reaching the surface.

L

lahar Flow of a mixture of pyroclastic material and water.

lava Molten rock that has reached the Earth's surface.

long-period earthquake Earthquake with dominant frequency content between 1 and 5 hertz. Used interchangeably with low-frequency earthquake.

M

magma Molten rock below the surface of the Earth.

multicomponent gas analyzer system (multi-GAS) Instrument that simultaneously measures abundances of water vapor (H₂O), carbon dioxide (CO₂), SO₂, and hydrogen sulfide (H₂S) gases within a volcanic plume via miniature gas sensors integrated into a single field-portable package for ground-based and airborne applications. This technique is commonly used to measure the major-species composition of volcanic emissions and to derive diagnostic gas ratios (Gunawan and others, 2017; Werner and others, 2017).

P

phreatic activity Steam-driven explosive eruption caused by the sudden heating of groundwater as it encounters hot volcanic rock or magma in which only non-juvenile particles are ejected.

phreatomagmatic activity Steam-driven explosive eruption caused by the sudden heating of groundwater as it encounters hot volcanic rock or magma in which both non-juvenile and juvenile particles are ejected.

Pleistocene A geologic epoch that

extends from about 11,700 to 2.6 million years ago.

pyroclast Individual particle ejected during a volcanic eruption; commonly classified by size (for example, ash, lapilli).

pyroclastic Pertaining to or composed of pyroclasts.

R

real-time seismic-amplitude measurement Amplitude of ground shaking caused by earthquakes and volcanic tremor averaged over 10-minute intervals.

S

satellite vent A subsidiary volcanic vent located on the flank of a larger volcano.

earthquake swarm Flurry of closely spaced earthquakes or other ground shaking activity; often precedes an eruption.

spatter Fluidal pyroclasts that deform during flight and often land while still molten, fusing together to form welded deposits.

steam emissions Used herein as a general term to indicate visible (partially condensed) degassing of mixed, and typically unquantified, gas compositions from volcanoes and thermal areas.

stratovolcano Steep-sided volcano commonly conical in shape, built of interbedded lava flows and fragmental deposits from explosive eruptions. Also called a stratocone or composite cone.

Strombolian Type of volcanic eruption characterized by intermittent bursts of fluid lava, commonly basalt, from a vent or crater as gas bubbles rise through a conduit and

burst at the surface.

T

tephra The general name for all volcanic material thrown into the air during a volcanic eruption.

Tertiary A geologic epoch that extends from about 2.6 million to 66 million years ago.

tremor Low-amplitude, continuous earthquake activity often associated with magma movement.

V

vent Opening in the earth's surface through which magma erupts or volcanic gases are emitted.

volcanic explosivity index A scale that describes the size of explosive volcanic eruptions on the basis of magnitude and intensity.

volcano-tectonic earthquake An earthquake generated within or near a volcano by brittle rock failure resulting from strain induced by volcanic processes.

Vulcanian A type of volcanic eruption that ejects material to heights less than about 20 kilometers and that lasts on the order of seconds to minutes. They are characterized by discrete, violent explosions, the ballistic ejection of blocks and bombs, atmospheric shock waves, and the emission of tephra.

Moffett Field Publishing Service Center, California
Manuscript approved for publication February 13, 2024
Edited by Claire Ashcraft and Phil Frederick
Cartography and illustration support by Katie Sullivan
Layout and design by Kimber Petersen

